

**Republic of Iraq
Ministry of Higher Education and
Scientific Research
University of Kerbala
Collage of Engineerin**



Studying the Effect of Notch Depth and Position on Fatigue Properties

A Thesis

**Submitted to the College of Engineering / University of Kerbala in
Partial Fulfillment of the Requierments for the Degree of Master of
Science in Mechanical Engineering –Applied Mechanics**

By

Laith Hussain Mohammed

B.Sc. 2008

Supervised By

Asst. Prof. Dr. Luay Sadiq Al-Ansari

Dr. Mohammed Wahhab Al-Jibory

**March
2017**

**جمادي الثاني
1438**

بِسْمِ اللَّهِ الرَّحْمَنِ الرَّحِيمِ

{ نَرْفَعُ دَرَجَاتٍ مَن نَّشَاءُ^{قُلْ} وَفَوْقَ كُلِّ ذِي عِلْمٍ عَلِيمٌ }

صَدَقَ اللَّهُ الْعَلِيِّ الْعَظِيمِ

سورة يوسف

الآية: (٧٦)

Supervisors Certification

We certify that this thesis entitled (**Studying the Effect of Notch Depth and Position on Fatigue Properties**) has been carried out under our supervision at the University of Kerbala / College of Engineering – Mechanical Engineering Department in partial fulfillment of the requirements for the degree of Master of Science in Mechanical Engineering /Applied Mechanics.

Signature:

Name: **Asst. Prof. Dr Luay Sadiq Al-Ansari**

Date: / / 2017

Signature:

Name: **Dr Mohammed Wahhab Al-Jibory**

Date: / / 2017

LANGUAGE CERTIFICATE

I certify that this thesis entitled “**Studying the Effect of Notch Depth and Position on Fatigue Properties**” was prepared by (**Laith Hussain Mohammed**) under my linguistic supervision. It was amended to meet the style of English language.

Signature:

Name: Dr. Ahmed Niameh Mehdy AL-Husseney

(Linguistic advisor)

College of Engineering

University of Kufa

Date: / / 2017

EXAMINING COMMITTEE CERTIFICATION

We certify that we have read this thesis entitled (**Studying the Effect of Notch Depth and Position on Fatigue Properties**) and as an examining committee examined the student (**Laith Hussain Mohammed**) in its content and that in our opinion it meets the standard of a thesis and is adequate for the award of the Degree of Master of Science in Mechanical Engineering /Applied Mechanics.

Signature:

Name: Asst. Prof. Dr. Luay Sadiq Al-Ansari

Date: / 12 / 2017

(Supervisor)

Signature:

Name: Dr. Mohammed Wahhab Al-Jibory

Date: / 12 / 2017

(Supervisor)

Signature:

Name: Dr. ALAA M. H. ALJASSANI

(Assist. Prof. University of Kufa / Faculty of Eng.)

Date: / 12 / 2017

(Member)

Signature:

Name: Dr.Salah Noori Abbood AL-Nomani

Date: / 12 / 2017

(Member)

Signature:

Name: Prof. Dr. H. J. M. Alalkawi

Date: / 12 / 2017

(Chairman)

Approval of Mechanical Engineering
Department

Approval of Deanery of the College of
Engineering / University of Kerbala

Signature:

Name: Dr. Hazim Umran Alwan

(Head of Mechanical Engineering Dept.)

Date: / 12 / 2017

Signature:

Name: Assist. Prof. Dr. Basim Khalil Nile

(Dean of the College of Engineering)

Date: / 12 / 2017

DEDICATION

To My Parents

ACKNOWLEDGMENT

Thanks to Allah for all his blessings, thanks to the Merciful Prophet Mohammad and Ahl-Albait (peace be upon them) for lightning my way.

I would like to gratefully and sincerely thank my supervisors Asst. Prof Dr. **Luay S. Al-Ansari**, and Dr. **Mohammed W. Al-Jibory** for their invaluable help, advice, guidance, understanding, and encouragement during this work. It has been pride to work with them.

I would like to thank the Staff of Mechanical Engineering Department at Kerbala University for their support and encouragement to complete this thesis.

I would like to thank the Mechanical Engineering Department staff at University of Kufa and Assist. Lec. Mr. **Hayder Zuhair Zainy** to whom I would like to express my sincere appreciation for their help, immense knowledge, and guidance throughout the preparation of the work described in this thesis.

I thank my father and mother for their support and allowing me to be as ambitious as I wanted. I hope they always be well and able to get their satisfaction. I appreciate my brothers' support.

Finally, I would like to thank my dear wife, her continuous help, support, and encouragement enabled me to end the thesis.

LAITH

Abstract

The present work investigates the effects of notch depth, location and load magnitude on fatigue life and thermal behavior of a rotating cantilever beam made of low carbon steel (ST37-2) by applying fully reversed load, zero mean stress. During the fatigue test, the temperature variation on the testing specimens was monitored using an IR camera, particularly at two specific points (edge and notch). By the way studying the effects of the above parameters on the area of sudden fracture surface and hardness of two points on fractured surface (point on propagation region and other point on the sudden fracture region) was done. Numerically, finite element simulation for the fatigue test was implemented using ANSYS Workbench 15.0, where the ANSYS input data was based on an experimental S/N curve.

From the results, the notch location can change the fracture position from the notch to the edge position. Furthermore, the fatigue life is increased to its maximum value through shifting the notch by the maximum ratio: experimentally more than (75) % and numerically more than (73) %. On the other hand, the shifting of notch away from the edge position produces a decreasing the area of sudden fracture surface as well as the hardness of the fracture surface till the transforming point. The comparison between the experimental and numerical results shows apparent agreement in behavior, where the ANSYS model based on experimental S/N curve provides a good prediction for fatigue life. Temperature variation at different points on the specimens offers a practical way to predict the fracture position before it happens.

List of Contents

	Contents	Page
Abstract		I
List of Contents		II
Nomenclature		V
List of Tables		VII
List of Figures		VIII

Chapter One

Introduction

1.1	Phenomenon of Fatigue Failure	1
1.2	Fatigue Failure Stages	3
1.2.1	Crack Initiation	3
1.2.2	Crack Propagation	3
1.2.3	Crack Fracture	4
1.3	Stress Concentration	4
1.4	S/N Curve	5
1.4.1	Basquin's Formula	6
1.5	Notch Effects	6
1.6	Plastic Deformation	8
1.7	Thesis Objectives	9

Chapter Two

Literature Review

2.1	Introduction	10
2.2	Summary of Literature Survey	15
2.3	Conclusion Remarks	22

Chapter Three

Theoretical Background

3.1	Theoretical Considerations	23
3.2	Fatigue Methodologies	23
3.3	Fatigue Parameters	24
3.4	Notch	25
3.4.1	Stress Concentration Factor K_t	25
3.4.2	Fatigue Notch Factor K_f	26
3.5	ANSYS Procedure	28
3.6	Fatigue Analysis by ANSYS	28
3.7	Steps for ANSYS Analysis	29

Chapter Four

Experimental Work

4.1	General	34
4.2	Chemical Composition Test	36
4.3	Tensile Test	36
4.4	Fatigue Test	37
4.4.1	Fatigue Testing Specimen	37
4.4.2	Fatigue Testing Machine	39
4.5	Temperature Change Monitoring	41
4.6	Macroscopic Test	42
4.7	Hardness Test	42

Chapter Five

Results and Discussion

5.1	Introduction	43
5.2	Fatigue Test	43

5.3	Macroscopic Test	48
5.4	Hardness Test	49

Chapter Six

Conclusions and Recommendations

6.1	Introduction	75
6.2	Conclusions	75
6.3	Recommendations	75

References		76
-------------------	--	----

Appendix –A

Results Certifications

A.1	Material Grade Certification	A-1
A.2	Chemical Composition Test results Certification	A-2

Appendix –B

Heat Indication

B.1	Heat Indication	B-1
B.2	Heat Indication Results	B-5

Nomenclatures

Symbol	Title	Unit
A	Area of contact	m ²
B	Fatigue strength coefficient	MPa
b	Fatigue strength exponent	---
C	Specific heat	J/Kg. K
D	Dimeter of the specimen's shoulder	mm
d	Dimeter of the specimen	mm
dx	Effective length	mm
F	Applied farce	N
h	Heat convection coefficient	W/(m ² .K)
K	Thermal Conductivity	W/(m.K)
K _f	Fatigue notch factor	---
K _t	Stress concentration factor	---
L	Length of the specimen	mm
l	Notch location	mm
N _f	Fatigue life	Cycles
Nu	Nusselt number	---
Q _{conv.}	Heat Convection	W
Q _{gen.}	Heat generation	W
Q _{rad.}	Heat Radiation	W
Q _{sto}	Heat stored	W
Q _x	Heat input.	W
Q _{x+dx}	Heat output	W
q _{gen}	Heat generation per unit volume	W/m ³
q _{sto.}	Heat stored per unit volume	W/m ³
R	Stress ratio	----
Re	Reynold number	---

$T_{amb.}$	Ambient temperature	K
T_s	Surface temperature	K
t	Notch depth	mm
V	Notch shape	---
M_b	Bending moment	N.mm
W_b	Section modulus of specimen	m^3
ν	Kinematic viscosity	m^2/s
ρ	Material density	kg/m^3
σ	Stefan boltzman constant	$W/(m^2.K^4)$
σ_a	Amplitude Stress	MPa
σ_e	endurance limit	MPa
σ_f	Fatigue limit	MPa
σ_m	Mean stress	MPa
σ_{N_f}	Fatigue strength	MPa
σ_{ult}	Ultimate stress	MPa
ΔV	Volume	m^3
$\Delta\sigma$	Range stress	MPa
α	Notch angle	0
ω	Angular velocity	rpm

List of Tables

Table No.	Title	Page No.
2-1	Summary of Literature Review	16
4-1	Chemical Composition	36
4-2	Mechanical Properties	37
4-3	Specification of IR Camera	41
5-1	Cases of Experimental and ANSYS Fatigue Test of 0.5 mm Depth	50
5-2	Cases of Experimental and ANSYS Fatigue Test of 1mm Depth	۵۱
5-3	Cases of Experimental and ANSYS Fatigue Test of 1.5 mm Depth	۵۲
5-4	Cases of Experimental and ANSYS Fatigue Test of 2 mm Depth	۵۳

List of Figures

No.	Title	Page No.
1-1	S-N Diagram of Annealed Steel 4340	2
1-2	Fatigue Fracture Surface	3
1-3	Stress Concentration Phenomenon	4
1-4	S/N Curve of Annealed 4340 Steel	5
1-5	S/N Curve of Aluminum Alloy 7075T-6	5
1-6	S-N Curve for Notched and Free -Notch Specimen of E360 Steel Subjected to bending moment	7
1-7	Flow Stress Around the Notch	7
1-8	Plastic behavior of metals	8
3-1	Fatigue Stress Profile	24
3-2	Stress concentration Due to Two Edge Notches in Tension and Bending	25
3-3	Stress concentration Due to Notches in Shouldered Beam	26
3-4	Chart of Notch sensitivity of steel and UNS A92024-T Wrought Aluminum Alloys under axial and reversed bending load	27
3-5	Stress Concentration Factor of Shouldered Beam Under Bending	27
3-6	Stress Concentration Factor of V-Notched Beam Under Bending	28
3-7	AutoCAD Program Window With a Sample	30
3-8	ANSYS Engineering Data window	30
3-9	Meshed model	31
3-10	Effect of Number of Elements on Fatigue Cycle Results	31
3-11	Model with Applied Load and Fixed Support	32
3-12	Solving Procedure	33

4-1	Experimental Work Strategy	35
4-2	Tensile Specimens (DIN50125)	36
4-3	Schematic of Fatigue Test Strategy with No. of Samples	38
4-4	Fatigue Test Sample	39
4-5	Notched Specimen Showed the Notch Position	39
4-6	Schematic of Applied Load on The Testing Specimen	40
4-7	Fracture Surface of The Rotating Bending Fatigue Testing Specimen	42
5-1	Experimental S/N Curve	54
5-2	Experimental and ANSYS Fatigue Life Change Along the Notch Position When the Notch Depth is (0.5) mm and the Applied Load is 100N	55
5-3	Experimental and ANSYS Fatigue Life Change Along the Notch Position When the Notch Depth is (1) mm and the Applied Load is 100N	55
5-4	Experimental and ANSYS Fatigue Life Change Along the Notch Position When the Notch Depth is (1.5) mm and the Applied Load is 100N	56
5-5	Experimental and ANSYS Fatigue Life Change Along the Notch Position When the Notch Depth is (2) mm and the Applied Load is 100N	56
5-6	Experimental and ANSYS Fatigue Life Change Along the Notch Position When the Notch Depth is (.5) mm and the Applied Load is 150N	57
5-7	Experimental and ANSYS Fatigue Life Change Along the Notch Position When the Notch Depth is (1) mm and the Applied Load is 150N	57
5-8	Experimental and ANSYS Fatigue Life Change Along the Notch Position When the Notch Depth is (1.5) mm and the Applied Load is 150N	58

5-9	Experimental and ANSYS Fatigue Life Change Along the Notch Position When the Notch Depth is (2) mm and the Applied Load is 150N	58
5-10	Comparison Among Experimental Fatigue Life for Different Notch Positions When the Applied Load is 100N	59
5-11	Comparison Among Experimental Fatigue Life for Different Notch Positions When the Applied Load is 150N	59
5-12	Comparison Among ANSYS Fatigue Life for Different Notch Positions When the Applied Load is 100N	60
5-13	Comparison Among ANSYS Fatigue Life for Different Notch Positions When the Applied Load is 150N	60
5-14	Comparison Between Experimental and ANSYS Stresses When the Notch Depth is (0.5) mm and the Applied Load is 100N	61
5-15	Comparison Between Experimental and ANSYS Stresses When the Notch Depth is (1) mm and the Applied Load is 100N	61
5-16	Comparison Between Experimental and ANSYS Stresses When the Notch Depth is (1.5) mm and the Applied Load is 100N	62
5-17	Comparison Between Experimental and ANSYS Stresses When the Notch Depth is (2) mm and the Applied Load is 100N	62
5-18	Comparison Between Experimental and ANSYS Stresses When the Notch Depth is (0.5) mm and the Applied Load is 150N	63
5-19	Comparison Between Experimental and ANSYS Stresses When the Notch Depth is (1) mm and the Applied Load is 150N	63
5-20	Comparison Between Experimental and ANSYS Stresses When the Notch Depth is (1.5) mm and the Applied Load is 150N	64
5-21	Comparison Between Experimental and ANSYS Stresses When the Notch Depth is (2) mm and the Applied Load is 150N	64

5-22	Comparison Among Experimental Stresses for Different Notch Depth When the Applied Load is 100N	65
5-23	Comparison Among Experimental Stresses for Different Notch Depth When the Applied Load is 150N	65
5-24	Comparison Among ANSYS Stresses for Different Notch Depth When the Applied Load is 100N	66
5-25	Comparison Among ANSYS Stresses for Different Notch Depth When the Applied Load is 150N	66
5-26	Equivalent Second Moment of Area and Stress Due to Equivalent Second Moment of Area When the Depth of Notch is (0.5) mm	67
5-27	Equivalent Second Moment of Area and Stress Due to Equivalent Second Moment of Area When the Depth of Notch is (1) mm	68
5-28	Equivalent Second Moment of Area and Stress Due to Equivalent Second Moment of Area When the Depth of Notch is (1.5) mm	69
5-29	Equivalent Second Moment of Area and Stress Due to Equivalent Second Moment of Area When the Depth of Notch is (2) mm	70
5-30	Fracture Surface Test	71
5-31	Sudden Fracture Area Changing Due to Notch Position for Different Applied Load When the Notch Depth is (0.5mm)	71
5-32	Sudden Fracture Area Changing Due to Notch Position for Different Applied Load When the Notch Depth is (1mm)	72
5-33	Sudden Fracture Area Changing Due to Notch Position for Different Applied Load When the Notch Depth is (1.5mm)	72
5-34	Sudden Fracture Area Changing Due to Notch Position for Different Applied Load When the Notch Depth is (2mm)	73
5-35	Hardness Test for Fracture Surface	73
5-36	Hardness of Fracture Areas Due to Notch Position When the Notch Depth is (0.5) mm and the Applied Load is 100 N	74

5-37	Hardness of Fracture Areas Due to Notch Position When the Notch Depth is (0.5) mm and the Applied Load is 150 N	74
5-38	Hardness of Fracture Areas Due to Notch Position When the Notch Depth is (1) mm and the Applied Load is 100 N	74
5-39	Hardness of Fracture Areas Due to Notch Position When the Notch Depth is (1) mm and the Applied Load is 150 N	74
5-40	Hardness of Fracture Areas Due to Notch Position When the Notch Depth is (1.5) mm and the Applied Load is 100 N	74
5-41	Hardness of Fracture Areas Due to Notch Position When the Notch Depth is (1.5) mm and the Applied Load is 150 N	74
5-42	Hardness of Fracture Areas Due to Notch Position When the Notch Depth is (2) mm and the Applied Load is 100 N	74
5-43	Hardness of Fracture Areas Due to Notch Position When the Notch Depth is (2) mm and the Applied Load is 150 N	74
B-1	Control Volume of Deformed Region	B1
B-2	Temperature Varying With Time at Edge (Position of Fracture) During Fatigue Test	B4
B-3	Temperature Distribution Measured by IR. Camera Consequently During Fatigue Test of V1-20-150N	B6
B-4	Temperature Distribution Measured by IR. Camera During Fatigue Test of V1.5—20-100N and V1.5-20-150N	B7
B-5	Temperature Increasing of Notch and Edge Points During Fatigue Test on V1-100N	B9
B-6	Temperature Increasing of Notch and Edge Points During Fatigue Test on V1.5-100N	B10
B-7	Temperature Increasing of Notch and Edge Points During Fatigue Test on V1-150N	B11
B-8	Temperature Increasing of Notch and Edge Points During Fatigue Test on V1.5-150N	B12



CHAPTER ONE
INTRODUCTION

Chapter One

Introduction

1.1 Phenomenon of Fatigue Failure

Fatigue knowledge has been developed step by step until this moment. In the 1840s, people in railway industry noticed that railroad axles failed at its shoulders, which was the first major impact of failures due to repeated load. The expression "fatigue" has been used during the 1840s and 1850s to explain failures due to repeated stresses. From 1850 to 1860, Wöhler executed many experimental testing on fatigue, when the concept of the S/N curve was introduced for the first time. After that, a lot of researchers worked in this field to develop theories enriching the knowledge on fatigue as we currently know it [1].

Now, fatigue is defined as "a form of failure caused by fluctuating or cyclic loads over a short or prolong period of time". On the other hand, it is attributed to an ultimate stress less than the static yield strength of a certain metal [2]. Fatigue behavior can be divided into two regions. The first one is when applying high loads resulting in two types of strain, elastic and plastic for each single cycle. The fatigue life in this region is a bit less than 10^4 cycle, which is called a low-cycle fatigue (LCF). The other region is known as a high-cycle fatigue (HCF), in which the stress is less than it is in the (LCF). In such a sort of fatigue, the deformations are totally elastic, and hence, longer fatigue life is achieved, i.e. more than 10^4 cycle [3]. This can be demonstrated by having a look at the S-N curve shown in figure (1.1).

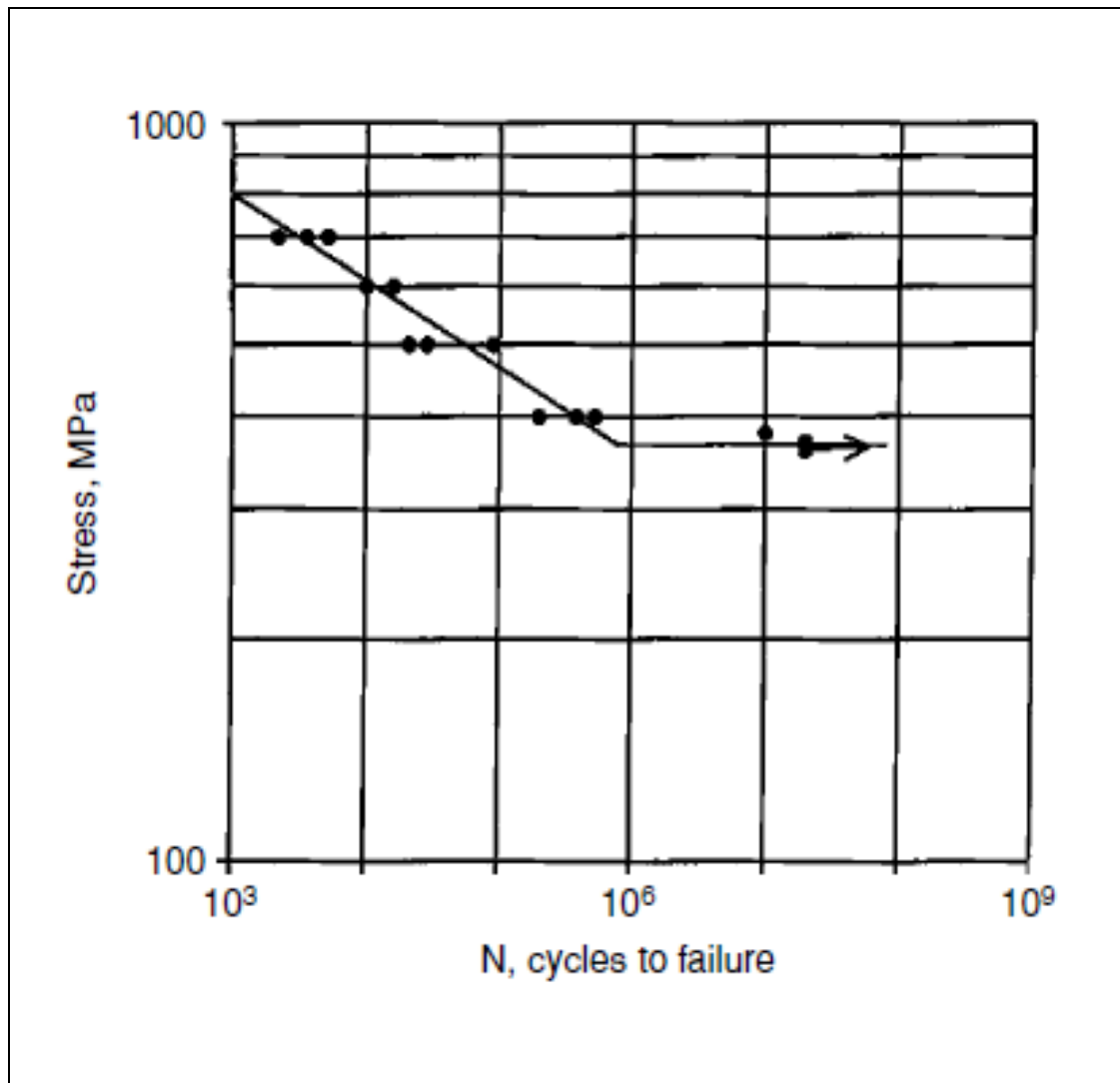


Figure (1.1): S-N Curve of Annealed Steel 4340 [4]

Moreover, this type of failure is known as a progressive failure "due to the crack initiation (stage I), crack growth (stage II), and sudden fracture (stage III)" [2], where these three stages of fatigue life are illustrated in Figure (1.2). These stages require the availability of cyclic stress, tensile stress and plastic strain, where the crack will not initiate if one of them does not exist [5].

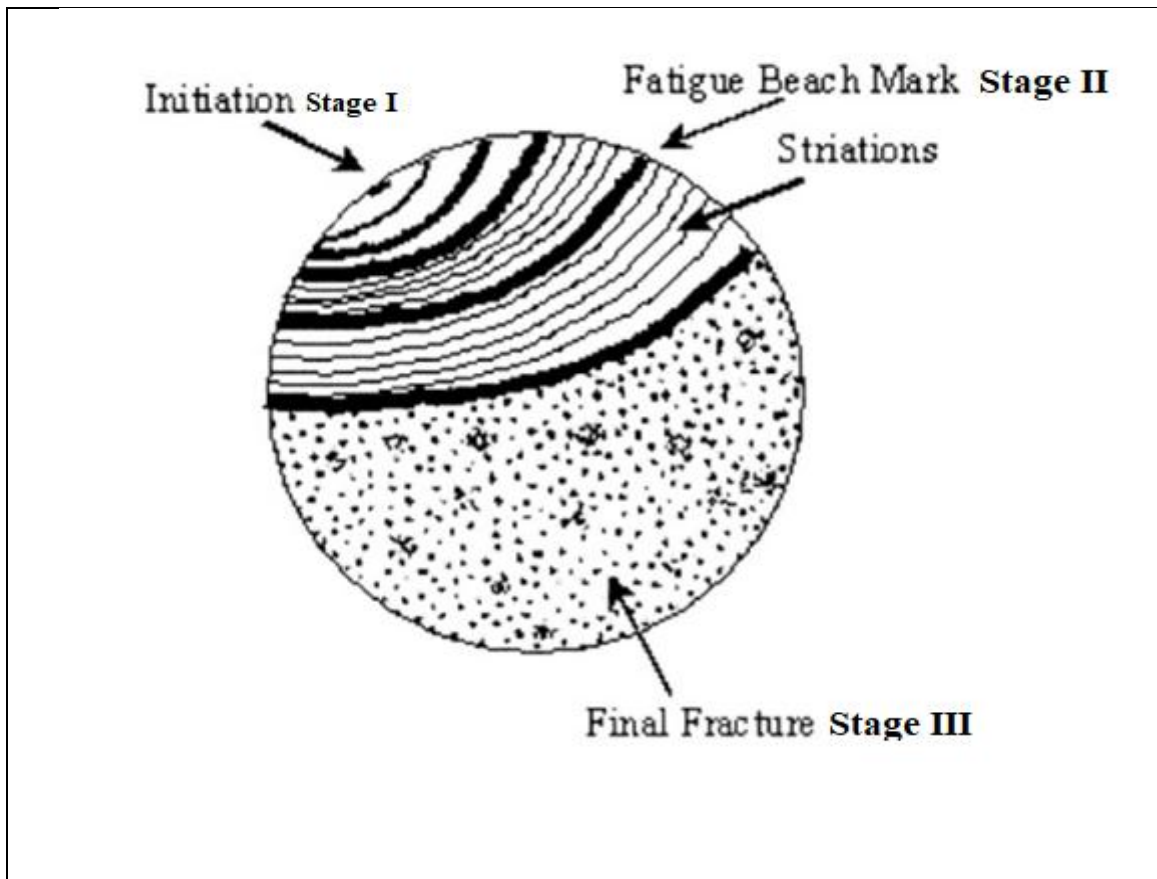


Figure (1.2): Fatigue Fracture Surface [6]

1.2 Fatigue Failure Stages

1.2.1 Crack Initiation

Crack initiation, which is a micro-scale process, begins from the surface toward inside, and meanwhile, propagates starting from a notch or any discontinuity region that has the greatest value of concentrated stress [6].

1.2.2 Crack Propagation

It is macroscopic process moving perpendicularly to the load direction and away from the surface. Stress concentration is higher around the crack tip while every time the load is tensile, the crack size increases a small amount. Hence, the cross section area resisting the applied stress decreases and reaches a critical limit, where it becomes unable to resist the applied load [7].

Furthermore, the peach markets or clamshells are fabricated due to the movement of cracked surface open and close, rubbing together for each cycle depending on the stress magnitude, load frequency and the environment [3].

1.2.3 Crack Fracture

After the crack continues in propagation reaching a critical length, it will grow very quickly without any caution until acquiring the sudden fracture. So, it can be said that the final cycle is done, when the material area is not sufficient to support the applied stress [2].

1.3 Stress Concentration

It is the increment of the maximum stress in small area near cracks, notches, grooves, sharp corners and other change in cross section. It happens due to the force lines being closer to each other causing concentration in stress. This increment, shown in figure (1.3), is calculated in terms of what is known as the stress concentrated factor [8].

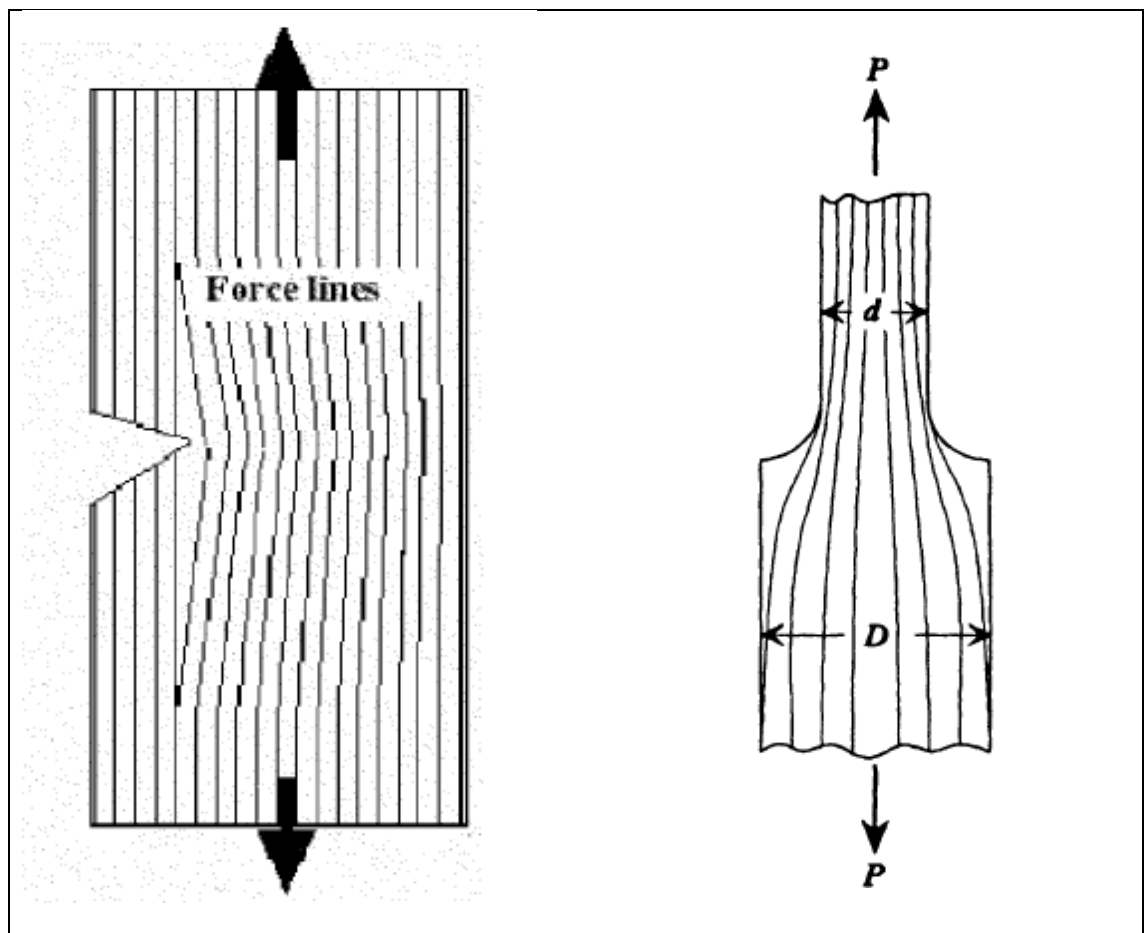
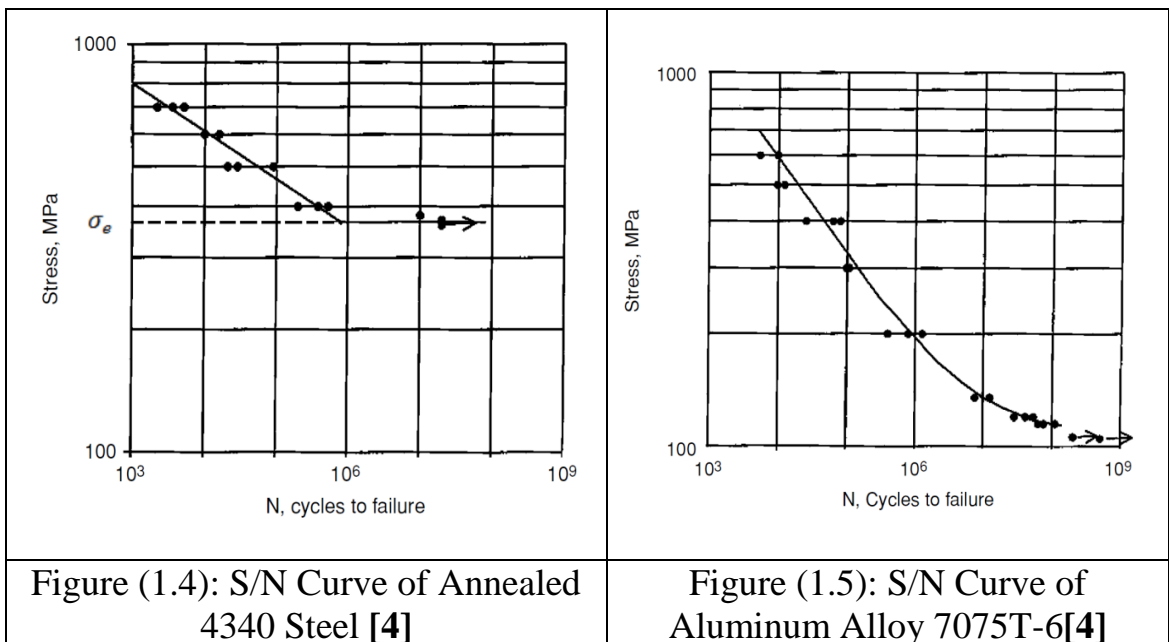


Figure (1.3): Stress Concentration Phenomenon[9]

1.4 S/N Curve

It is a traditional way to describe material behavior under fatigue [10]. Experimentally, the S/N curve has been plotted for different stress amplitude loadings on smooth fatigue specimens. It shows the number of life cycle to failure (N_f) with respect to the stress amplitude (σ_a). There are two types of S/N curve depending on whether the material considered is ferrous or nonferrous, as shown in figures (1.4) and (1.5), respectively [4].



It shows some important characteristics including the fatigue life, fatigue limit and fatigue strength (endurance limit), which are defined as follows:

Fatigue life (N_f): is a number of stress cycles to failure.

Fatigue strength (σ_{N_f}): is the stress value at failure for exactly N_f cycles.

Fatigue limit (σ_f) or endurance limit (σ_e): is the value of applied load applied on a part being safe for infinite number of cycles, or is an applied stress at which S/N curve diagram becomes or remains horizontal. It can be estimated using the following empirical relations [1]:

For cast and wrought steel endurance limit:

$$\sigma_f = 0.5 \sigma_{ult.} \quad \text{For } \sigma_{ult.} \leq 1400 \text{ MPa(200 Kpsi)}$$

$$\sigma_f = 700 \text{ MPa} \quad \text{For } \sigma_{ult.} > 1400 \text{ MPa(200 Kpsi)}$$

For nonferrous materials:

$$\sigma_f \approx (0.35 - 0.5) \sigma_{ult.} \quad (\text{Approximated})$$

There is a number of correction factors added to the above relations to be closest to the experimental results such as surface finishing, size, load, temperature, reliability and miscellaneous effects factors [3].

1.4.1 Basqunis's Formula

It is a relation between fatigue life and applied stress used to make approximate for the S/N curve [1].

$$\sigma_a = BN_f^b \quad \dots (1.1)$$

Where;

σ_a = Stress amplitude (MPa).

N_f = Number of cycle to failure.

B = Fatigue strength coefficient (for most materials $\approx \sigma_f$ fracture strength).

b = Fatigue strength exponent (Basqunis's exponent).

1.5 Notch Effects

Notch can be defined as a discontinuity in shape such as the v- shape, threads, nut-bolt connection, square shape key, scratches and fillets [11]. Although it has two principal effects, the first one is called the "stress riser" because it notch existence concentrates the stress resulting in crack initiation (decreasing the fatigue strength and increasing stress concentration). Thus, it is the main parameter affecting the fatigue strength of structures, as shown in the figure (1.6). Thus, the fatigue limit in the type of smooth (unnotched) structure is higher than the notched one. For this reason, designers always try to avoid using the notches where possible, but mostly it is indispensable to use them due to design requirements [12].

The second effect is the increase in the fatigue strength with reducing the stress concentration.

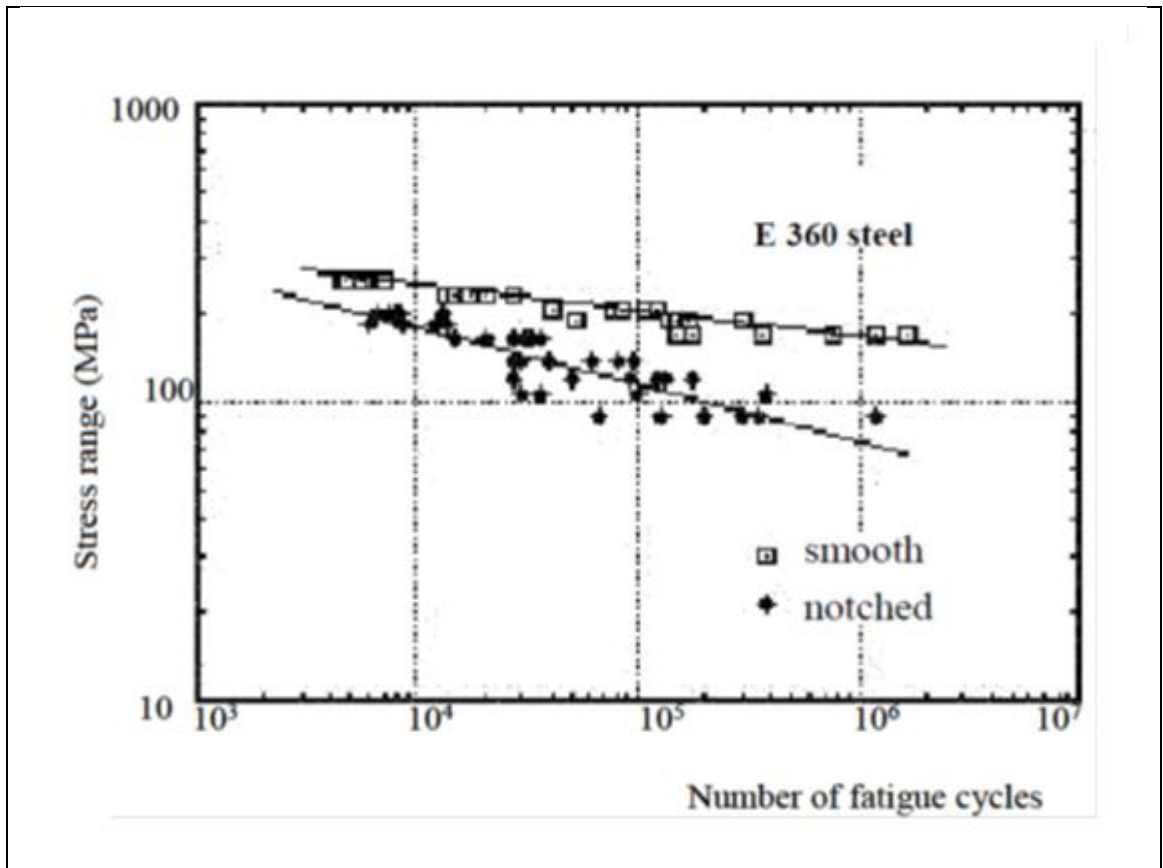


Figure (1.6): S-N Curve for Notched and Free -Notch Specimen of E360 Steel Subjected to bending moment [9]

The latest effect can be demonstrated through what is called the removing material technique, as illustrated in figure (1.7). This technique is based on transition flow to improve it and reducing stress concentration by cut off material from low-stress area, this will transfer the high stress out of the region of stress concentration toward the low-stress region, which decreasing the stress in the high stress area [8].

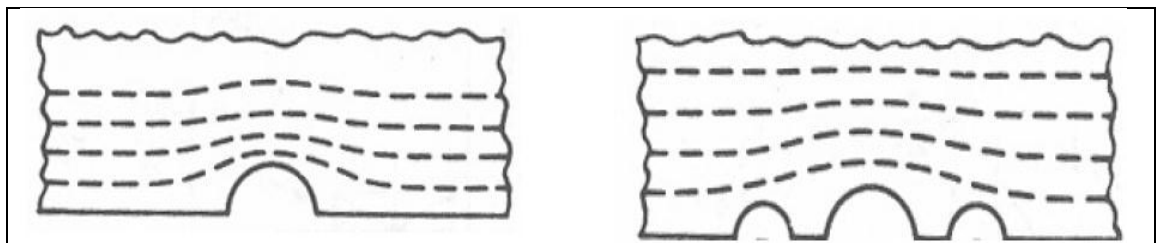


Figure (1.7): Flow Stress Around the Notch [8]

1.6 Plastic Deformation

When a material is stressed, the response sequence will be usually as: elastic deformation, plastic deformation and fracture. Plastic deformation is an irreversible process coming from breaking and reforming atomic bonds. So, the material will stay in deformed shape after releasing the stress [10], as illustrated in figure (1.8). On the other hand, when the plastic deformation occurs, a significant heat will generate particularly when deformation is concentrated due to dislocation of material crystalline. The amount of heat generation depends on the strain rate and deformation [13].

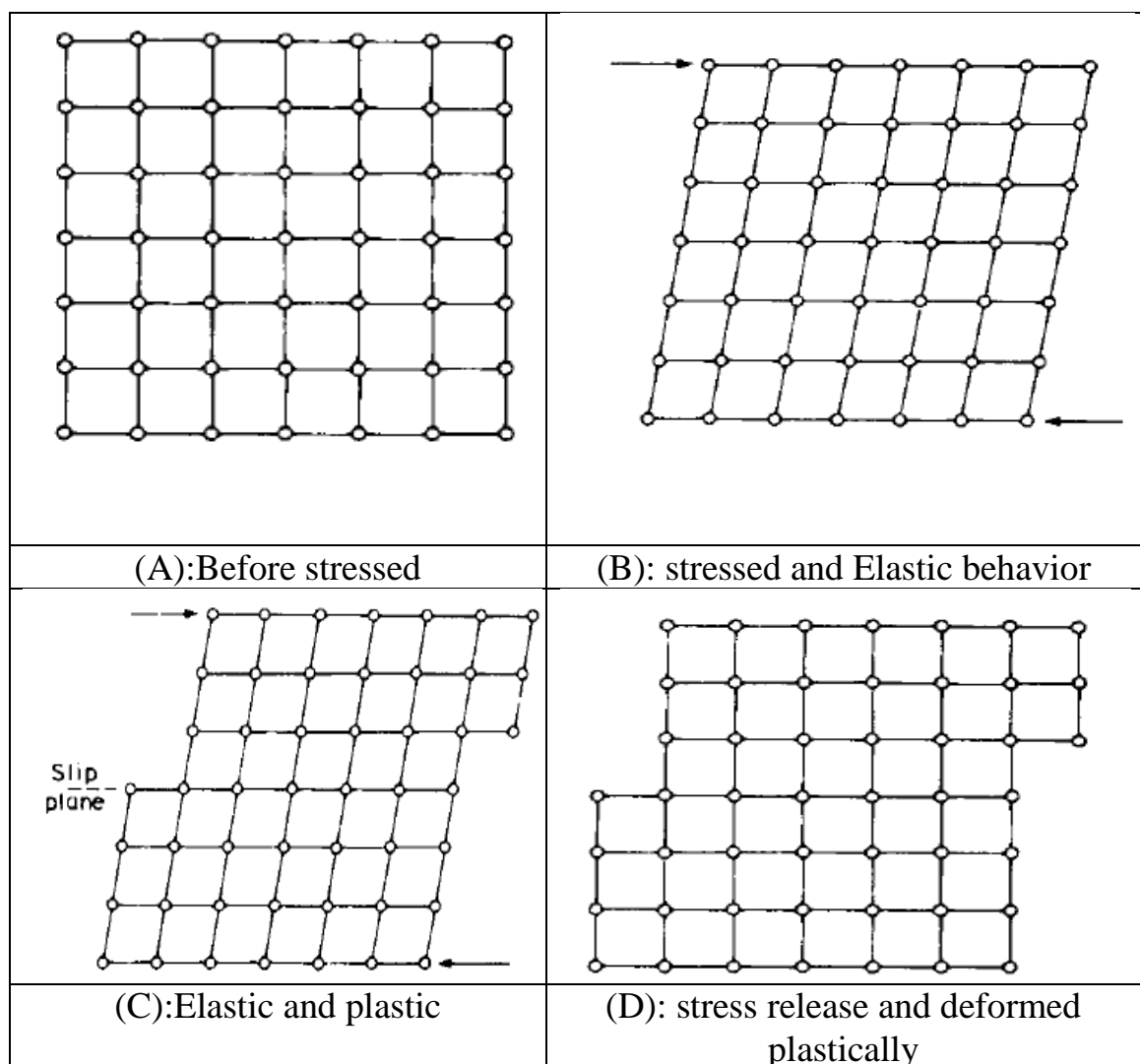
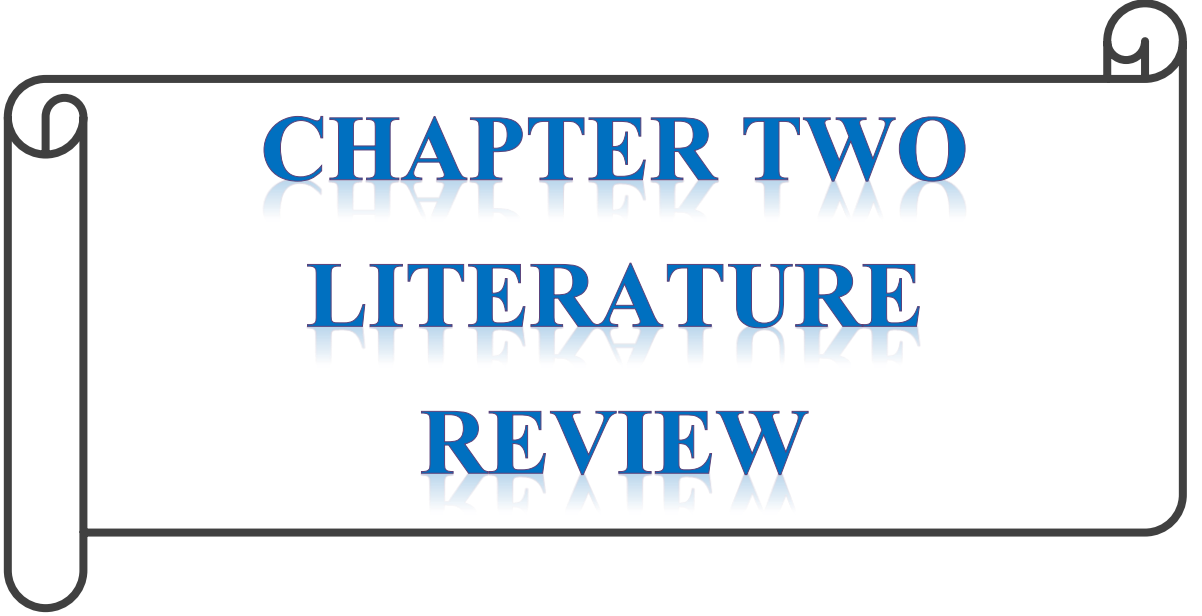


Figure (1.8): Plastic behavior of metals[5]

1.7 Thesis Objectives

The objectives to be achieved in this thesis can be summarized as follows:

- 1- Studying the effect of notch position on fatigue life with four different notch depths and two different load magnitudes and doing a comparison between the experimental and numerical (ANSYS) results.
- 2- Studying the effect of notch position on thermal behavior (heat generation due to plastic deformation) with two different notch depths and two different load magnitude.
- 3- Studying the effect of notch position on hardness of the fracture surface with four different notch depths and two different load magnitude.
- 4- Studying the effect of notch position on the area of sudden fracture region of fractured surface four different notch depths and two different load magnitude.



CHAPTER TWO
LITERATURE
REVIEW

Chapter Two

Literature Review

2.1 Introduction:

Several researches have been presented so far dealing with fatigue phenomena of metal alloys. Some of these researches are reviewed in this section.

A. Rabiei, et al, (2000), [14], studied heat generation during the fatigue of a Cellular Al-alloy. They applied Compression- compression fatigue technique on a perforated plate using infrared (IR) camera to calculate temperature change during fatigue progressing to indicate thermal behavior. From the results, it was found that the heat generated by plastic cycles is too small to cause fatigue by thermal softening, and hence, it was not responsible for fatigue failure.

N. Kadi, (2001), [15], investigated the effects of notch on fatigue behavior at high fatigue cycles by using notched shafts and applying the volumetric method to estimate the fatigue life particularly for the shafts specimens with key – seats. From the results, it was found that there were geometries such as key – seats, where their (k_t) cannot be calculated by using classical method, while volumetric method gives accepted results.

A. Fatemi, et. al., (2004), [16], studied the effects of notches on fatigue life for notched around specimens and double notched plate of micro - alloyed steel, which were treated to study the ability of strain life and stress life methods in predicting fatigue behavior. From the results obtained, the effect of notch is purely clear at high fatigue cycle and be smaller step by step at low fatigue cycle. Also, stress life method is more accurate than strain life method for notch around specimens in expecting their fatigue life.

Michele Ciaverella and Giovanni Meneghetti, (2004), [17], established a new strategy for calculating (K_f) by using some results from literature experiments for many types of alloy steel, different in notch dimensions and geometries. They studied the contrast between Neuber and Peterson and the modifying equation of Neuber and many modern formulas. From the results, they found that it is possible to expect the K_f value from classical and modern criteria compared to multi experimental fatigue limit, where they concluded that the accuracy of prediction was improved by modern criteria.

Borivoj Sustarsic, et. al., (2007), [18], examined the effects of v – notch specimens of Charpy standard samples of steel spring on fatigue behavior. They planned to get a suitable comparison with testing results of real spring. It was found that Charpy testing samples can be used to study fatigue strength of real spring steel instead of the real spring, where fatigue strength of steel can be increased to 20%. Also, it was observed that the strength of fatigue is reduced when defects or notches are present in testing specimens.

Y. Verreman and H. Guo, (2009), [19], tried to study the effects of notches on fatigue life by using different dimensions of V- notch in cylindrical specimens of medium carbon steel under torsional and axial applied load. Finite element method was applied for checking the experimental data. They found that the resistance of material to crack propagation has a great influence on fatigue behavior. Furthermore, K_f was near unity because resistance to crack propagation was very high.

Dargi Stamenkovic, et. al., (2010), [20], tried to predict numerically and analytically the duration of crack growth cycles on notched structural components. From the results, it was found that the numerical way is a good method to be utilized in examining the effect of crack on the performance of the components of notched structure, where there is an

agreement between numerical, analytical and experimental data that acquired by classical method.

XU Jian, et. al., (2011), [21] focused on the hole shape effects on the connecting bolts on fatigue behavior. Finite element method was used by MSC. Software. By looking at the outcomes of this study, the effect of hole shape on fatigue behavior is clear. Also, the fatigue life decreased step by step through expanding the short axis. The calculated data can be used as outline notes in design of bolted connection.

N.A, Alang, et. al., (2011), [22], studied the effect surface roughness on fatigue cycles using rotating cantilever notched beam specimens of carbon steel with 0.2 C (wt%), where rotating bending fatigue technique was also used. In this project, it was found that there is no great variation in fatigue life for specimens in the low fatigue cycle part. For the high fatigue cycle, on the other hand, the smoothest specimens produce much higher fatigue cycles, and numbers of crack initiation increase due to the increase in the surface roughness.

Masao Sakane, et. al., (2011), [23], discussed the effects of notches on fatigue in low cycles utilizing multi-axial load (torsion and tension) at 873 K. Experimental work was done on notched specimens of stainless steel (SUS304) load condition. An easy way was used to calculate strain at notches. The results revealed that notch has a great influence on crack initiation cycles, while it has small influence on crack propagation cycles. So, the life cycles to failure were influenced by propagation and initiation effects.

Goanta Viorel, et. al., (2011),[24], established in their paper a relation between the hardness value and plastic deformation level. The study was done in the vicinity of the fractured surface of the tested specimens by applying Vickers micro hardness technique. The material used in the experiments was normal and annealed steel (OLC45) under

static and fatigue loading. From the results, it was found that the hardness of the final area of fractured surfaces is high because the speed of crack propagation is higher; and for crack propagation area has lower value of hardness.

Nasim Daemi and Gholam Hossein Majzoubi, (2011), [25] focused on the effects of notches dimensions for different shapes on the fatigue life. In the experimental work, rotating bending machine specimens of low carbon steel alloy were used under constant load (bending fatigue life) and room temperature. Analytically, they used Manson – Coffin's way to create S/N curves for testing samples and compare between the experimentally and analytically calculated results. From the results, the analytical method (Manson Coffin) cannot able to expect the fatigue life of the notched samples.

Deepan Marudachalam, et al., (2011), [26], studied shaft design of drive system manufactured from CC55 Mn75 under various conditions of fatigue loading using Good man method, and investigated the failed by implemented the shaft in spanning machine. ANSYS software program was utilized for finite element analysis technique to check values of stresses. The shaft was subjected to shear and bending stresses. On the other hand, the forces and torques that acting on the shaft were estimated, where the stresses revolving at the fracture surface, fatigue limit, and safety factor were all calculated in addition to plotting the stress life curve. In this project, it was found that failure is likely to occur at the notch position when the fillet radius of the shaft is increased from (0.6) mm to (2) mm, and the support position changed, the factor of stress concentration is decreased also factor of safety increased from (0.71) to (1.05) and endurance limit of fatigue is increasing.

Bikash Joadder, et. al., (2011), [27], tried to predict the fatigue life of stainless steel (SS316) for notched specimens with different geometries

under different strain amplitudes. Strain-life data and Low cycle fatigue were performed for all specimens. The modeling of finite element analysis was implemented using ABAQUS software program. So, it was concluded that the maximum strain occurs at notch tip and there was a difference between the applied strain and the total strain life curve generated. Also, it was found the predicted life is less than the experimental result for all notched specimens with variation ratio up to 27.7%.

Caroline Hyll, et. al., (2012), [28], studied the heat generation during plastic deformation to fracture. In this experimental work, uniaxial tensile load was applied on a sock paper samples with using infrared camera for thermal indication. It was found that 40%-60% of thermal energy is coming from mechanical energy. At rupture time, a sharp temperature increase was acquired. Furthermore, the increase in thermal energy at rupture time was because of the elastic energy stored in the sample at that time.

G. Meneghetti and S. Masaggia, (2012), [29], evaluated experimentally and theoretically the effect of notch depth on fatigue limit by testing V-notches with 120° notch opening angle on a round samples and gears samples made of Austempered ductile iron grad (1050) . Tension to tension fatigue tests were implemented on all samples with R (0.2) at frequency ranging from (15-20) Hz and the room temperature. ANSYS program was used for finite element analyses. Theoretical results were in acceptable error with respect to experimental results, i.e $\leq 20\%$. Furthermore, it was proved that when the notch radius reached to zero, the stress concentration factor (K_t) will not be true anymore because stresses approach to an infinity value unlike when the notch radius tends to large value, where stress concentration factor is matched.

Reda I. Elghnam, (2013), [30], studied the heat transferred from horizontal rotating cylinder in constant round air. On the other hands, a new relation was applied between the Nu and Re numbers compatible with this work cases.

Qasim Bader, (2014), [31], experimented the effect of v – notch location on fatigue life by using cantilever beam specimens of (Low, Medium, and high) Carbone Steel, which were applied in cantilever rotating–bending fatigue testing machine. Their experimental data were compared with numerical results obtained from ANSYS software program. From the results found that, there is no significant effect of notch locution on fatigue life.

2.2 Summary of Literature Survey

In this section, the researches reviewed in previous section were summarized in Table (2-1).

Table (2-1): Summary of Literature Review

No.	Author and year	Paper	Type of Work	Case Study	Type of load	Results
1	A.Rabiei, et. al. (2000) [14]	Heat Generation during the Fatigue of a Cellar Al Alloy	Experimental	Cellar Al- Alloy holed plate	Compression – compression fatigue with thermal camera	* Generated heat was due to plastic deformation. * The temperature calculated was very small to be responsible for fatigue failure.
2	N. Kadi (2001) [15]	Notch effect in High Cycle Fatigue	Experimental	Notched shaft with key-seats	High Cycle Fatigue	Estimate different way for fatigue life duration of notched shaft for not applicable geometries (cannot calculate stress concentration factor by classic way) such as key-seats.
3	A. Fatemi, et. al. (2004) [16]	Fatigue Behavior and Life Predictions of Notched Specimens Made of QT and Forged Micro Alloyed Steels	Experimental	Notched bar and double notched flat plate of treated medium carbon steel AISI (1141)	R=-1 for notched bar and pulsating tension for notched flat plate	*S/N method is more accurate than strain life method for longer life. *S/N approach was more accurate for notched bar in fatigue prediction than flat plate. *The effect of notch is purely clear at high fatigue cycle and be smaller step by step at low fatigue cycle.

4	Michele Ciavarella and Giovanni Meneghetti (2004) [17]	On fatigue limit in the presence of notches: classical vs. recent unified formulations	Theoretical based on experimental results are getting from the literature for various steels and alloys	various steels and alloys		Modern criteria improve the accuracy of prediction of Kf with respect to older ones.
5	Borivoj Sustarsic, et. al. (2007) [18]	The Notch Effect on the Fatigue Strength of 51CrV4Mo Spring Steel	Experimental	Charpy V-notched specimens of steel springs (51CrV4Mo)	Pulsating fatigue	<p>*Possible to determine fatigue strength of spring steel by using Charpy V test specimens.</p> <p>* Fatigue strength of steel can be increased up to 20%.</p> <p>* Strength of fatigue was reduced when defects or notches were present in testing specimens.</p> <p>*Fatigue strength is affected by surface roughness and notch, also residual stress caused by machining and shoot-peening.</p>
6	Y. Verreman, H. Guo (2009) [19]	Short cracks at notches and fatigue life prediction under mode I and mode III loadings	Experimental and Numerical (FEM)	Circumferential V-notched plane cylindrical of medium carbon steel	Axial and torsional fatigue	<p>*Fatigue behavior was affected by material resistance to crack propagation.</p> <p>*Fatigue notch factor was close to unity because of high resistance to crack propagation.</p>

7	Dragi Stamenkovic & Katarina Maksimovic (2010) [20]	Fatigue Life Estimation of Notched Structural Components	Analytical and Numerical (FEM) (Calculating stress intensity factor)	Fatigue crack growth in 1- Air craft wing lug. 2- Riveted holes.		*FEM is efficient method for investigating the impact crack on the performance of notched structural components. *Good agreement between analytical and numerical results with respect to classical methods (photo elasticity and fatigue tests).
8	XU Jian-Xin, et. al. (2011) [21]	The effect of hole shape on fatigue life of bolted connectors	Numerical(FEM) with using MSC software	Bolted connection		*Fatigue life of bolted connectors is affected by hole's shape. *Fatigue life decreases gradually by increasing short axis. *Calculated results can give reference outline of bolted connection in air craft and vehicle structures.
9	N.A, Alang, et. al. (2011) [22]	Effect of Surface Roughness on Fatigue Life of Notched Carbon Steel	Experimental	Notched rotating cantilever beam specimen of carbon steel (0.2C wt. %) With different surface roughness	rotating bending fatigue (R= -1)	*In low cycle, there was no significant influence of surface roughness, but in high fatigue cycle, the smoothest specimens produce much higher fatigue cycle. *Increasing the number of crack initiation due to increasing the surface roughness.

10	Masao Sakane, et. al. (2011) [23]	Notch Effect on Multiaxial Low Cycle Fatigue	Experimental and Numerical (FEA)	Notched round specimens of SUS 304 stainless steel	Multi axial low cyclic fatigue (tension and torsion)	*Crack initiation is affected by notch while crack propagation is slightly affected by notch. *cycles to failure combined effects (initiation and propagation).
11	Goanta Viorel, et. al. (2011) [24]	The Variation of the Vickers Micro – Hardness in the Vicinity of the Fracture Surface at Static Loading	Experimental	normal and annealed steel (OLC45)	Static and fatigue loading	The hardness of the final area of fractured surfaces was high because the crack propagation speed is higher, and for crack propagation area has lower value of hardness.
12	Nasim Daemi & Gholam Hossein Majzoobi (2011) [25]	Experimental and Theoretical Investigation on Notched Specimens Life Under Bending Loading	Experimental and Analytical	Notched round specimens different in shapes and dimension of notches	Bending fatigue life	Manson-caffin analytical method cannot satisfactory predict the fatigue life of notched specimens
13	Deepan Marudachalam & R.Krishnaraj (2011) [26]	Optimization of shaft design under fatigue loading using Goodman method	Experimental and Numerical (FEM) with using ANSYS software	Steel shaft of C55Mn75	Torsional - bending fatigue	*Failure would occur at the notch position. *Increase in fillet radii of the shaft and change in the position of the support decreases the stress concentration factor and increases the endurance limit and fatigue factor of safety of the shaft from 0.71 to 1.05

14	Bikash Joadder, et. al. (2011) [27]	Fatigue Failure of Notched Specimen -A Strain-Life Approach	Experimental and Numerical (FEA) with using ABAQUS software	Plane and notched round specimens of stainless steel (SS316)	Strain controlled cyclic load	Predicted life was less than the experimental result for all notched specimens with variation up to 27.7%.
15	Caroline Hyll, et. al. (2012) [28]	Analysis of the Plastic and Elastic Energy during the Deformation and rupture of Paper Sample Using Thermography	Experimental	sock paper samples	Uniaxial tensile load with using infrared camera	*40%-60% of thermal energy is coming from mechanical energy. * At rupture time, a sharp temperature increase is acquired. *increasing in thermal energy at rupture, that because of stored elastic energy in the sample at that time.
16	G. Meneghetti and S. Masaggia (2012) [29]	Estimation of the fatigue limit of components made of Austempered Ductile Iron weakened by V-shaped notches	Experimental and Numerical (FEM) with using ANSYS software	V-notched specimen of Austempered Ductile Iron		*Acceptable error with respect to experimental results, i.e. $\leq 20\%$. *Proved that when the notch radius reached to zero, the stress concentration factor (K_t) will not be true anymore because of stresses growth to infinity value, unlike that when the notch

17	Reda I. Elghnam, (2013) [30]	Experimental and Numerical Investigation of Heat Transfer from Rotating Horizontal Cylinder Rotating in Still Air Round its own Horizontal Axes	Experimental and Analytical	Rotating specimen		Applied a new relation between the Nu Number and Re number can be used in these work cases.
18	Qasim Bader (2014) [31]	Effect of V Shape Notch Location on Fatigue Life in Steel Beam Made of Carbon Steel Alloys with Different Content of Carbon	Experimental and Numerical (FEM) with using ANSYS software	Notched rotating cantilever beam specimen of Low, Medium and High Carbone Steel	Bending fatigue load	There is no significant effect of notch locution on fatigue life. *S-N curve of this material can be used to predict the life of notched specimens based on the real stress developed at the notch tip

2.3 Concluding Remarks

From the previous review, several points of new researches can be concluded. In this work, the following points will be considered:

- 1-Effects of notch location on fatigue life were little considered in previous papers, especially when the fatigue test is implemented for cantilever configuration under applying load.
- 2-The heat generation due to plastic deformation during fatigue test with bending load was not studied previously. In the case of Health monitoring, the heat generation due to plastic deformation will be studied in this work as a phenomenon appears in fatigue test.



CHAPTER THREE
THEORETICAL
BACKGROUND

Chapter Three

Theoretical Background

This chapter contains three main parts: the first one is about theoretical considerations of fatigue analysis (Analytical or Empirical method), the second one is concerning the numerical investigation using the finite element method (using ANSYS Software), and the final part is dedicated for heat indication.

3.1 Theoretical Considerations

Generally, fatigue is a problem occurring in 90% of moving structural components subjected to constant or variable amplitude loading and other parameters affecting the fatigue phenomenon [12]. So types and magnitude of loading and environment effects, also type of material, microstructure, mechanical properties, surface finishing and stress concentration all of these and others can effect on fatigue life. So, it is very difficult to predict the fatigue life [32]. In this work, the main parameters affecting fatigue life were loading magnitude, S/N curve of the material and notch.

3.2 Fatigue Methodologies

There are three methods for studying fatigue behavior through predicting fatigue life as a number of cycle to fracture in specific loading level, where the fatigue life " $1 \leq N \leq 10^4$ " is classified into the low cycle fatigue region, while " $N > 10^4$ " in the high cycle fatigue region [3]. These methods are as follows:

- 1- Stress – life method.
- 2- Strain – life method.
- 3- Fracture mechanic method.

Where stress life method depends on stress level only. It is the least accurate especially for low cycle application, most traditional and simple. Also, it can be applied for a wide range of applications of high fatigue

cycle and infinite cycle with being in safe region. In Strain life method, strain and stress are considered for predicting fatigue life, hence, it needs more detailed analysis of plastic deformation and is used for low cycle fatigue. Finally, fracture mechanics method supposes a crack to be already formed and employed to predict crack growth with respect to stress intensity, and thus, it is suitable for practical application [3].

3.3 Fatigue Parameters

There are a lot of parameters should be considered in predicting fatigue life. Below are some important parameters used in fatigue life prediction [33].

Mean stress $\sigma_m = (\sigma_{max} + \sigma_{min})/2$... (3.1)

Amplitude stress $\sigma_a = (\sigma_{max} - \sigma_{min})/2$... (3.2)

Range stress $\Delta\sigma = (\sigma_{max} - \sigma_{min}) = 2\sigma_a$... (3.3)

Also stress ratio $R = (\sigma_{min}/ \sigma_{max})$... (3.4)

Where σ_{max} and σ_{min} are respectively the maximum and minimum stress level as illustrated in figure (3.1).

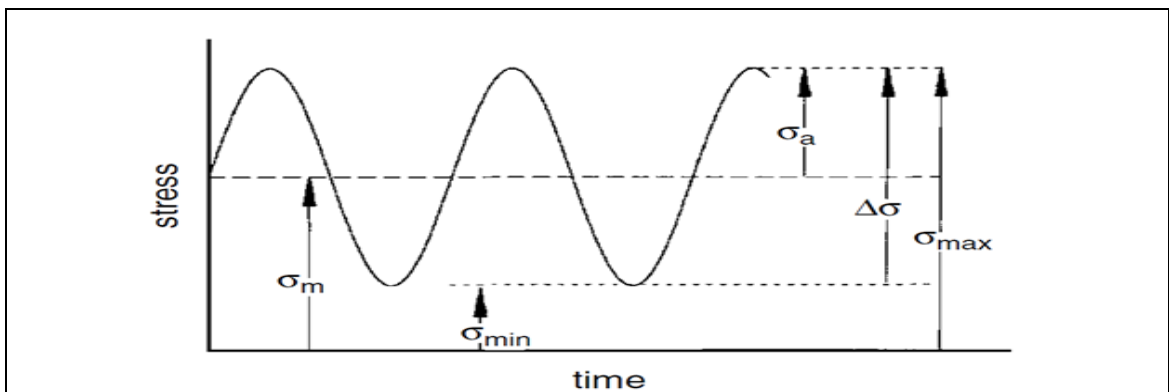


Figure (3.1): Fatigue Stress Profile[4]

These parameters are influenced by the type and nature of loading (bending, tension, torsion and combination, repeating, fluctuating or alternating), as well as frequency of loading, and other factors such as geometrical, metallurgical and mechanical properties. All of these and other can effect on fatigue behavior [33].

In this work the loading type condition is fully reversed loading ($R = -1$) with mean stress equal to zero, which was due to fatigue testing machine availability.

3.4 Notch

A lot of engineering structural designs contain stress concentration regions causing failure due to a discontinuity in section called a *notch*. The notch produces an increase in the stress, which can be calculated in terms of the stress concentration factor K_t . In fatigue process, the crack initiation and then propagation occur at this region (notched region).

3.4.1 Stress Concentration Factor K_t

Stress concentration results from ununiformed stress distribution through a cross section creating a stress increase in this region as shown figures (3.2) and (3.3).

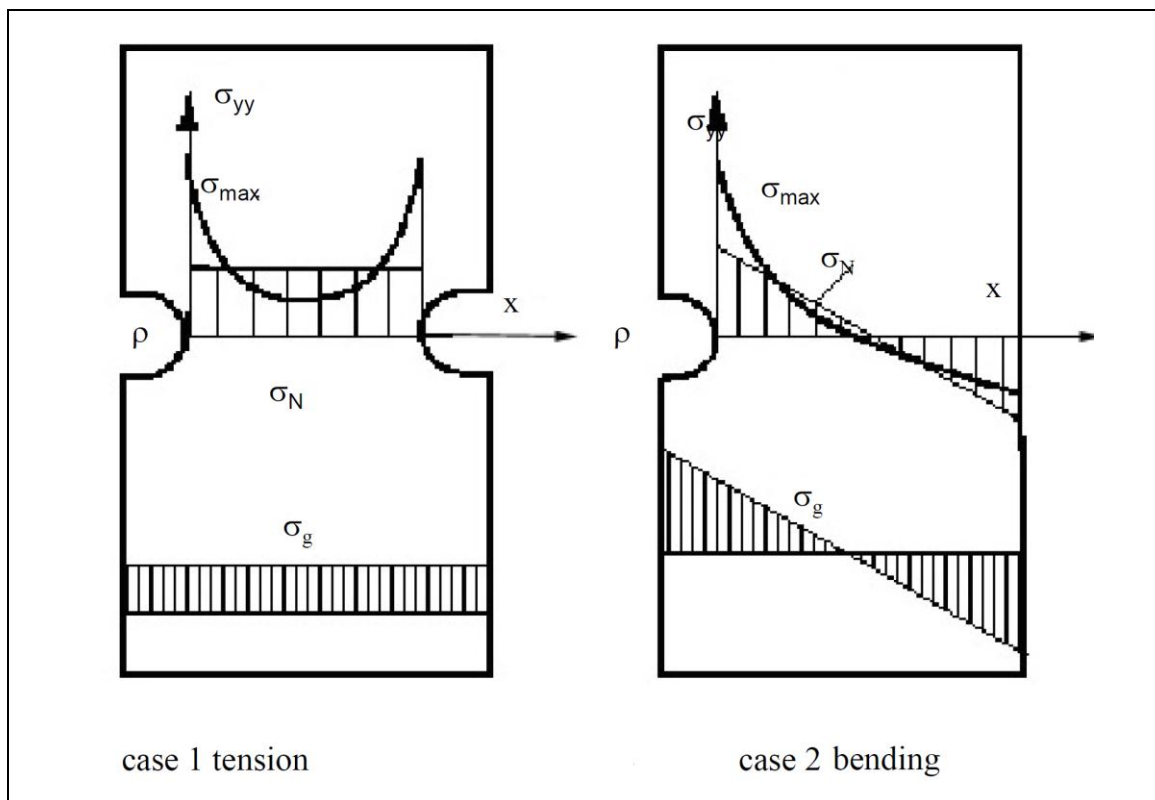


Figure (3.2): Stress concentration Due to Two Edge Notches in Tension and Bending [9]

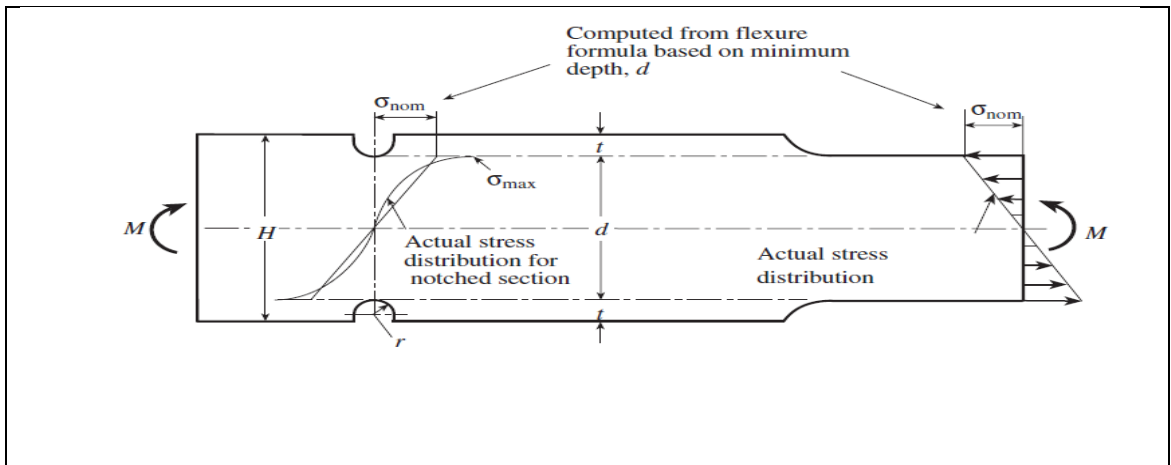


Figure (3.3): Stress concentration Due to Notches in Shouldered Beam [37]

Stress concentration factor K_t is defined as the ratio of peak stress to the nominal stress in case of no stress concentration. It depends on the geometry of notch and type of loading [6].

$$K_t = \frac{\sigma_{\text{maximum}}}{\sigma_{\text{nominal}}} \quad \dots$$

(3.6)

3.4.2 Fatigue Notch Factor K_f

It is the effective stress concentration in fatigue or may be defined as a decreased K_t values. So, it depends on the stress concentration value and material [3].

$$K_f = \frac{\text{fatigue strength of smooth specimen}}{\text{fatigue strength of notched specimen}}$$

There is another parameter joining the K_t and K_f known as the *Notch Sensitivity Factor* (q) that is defined by the relation below and it has an experimental value between zero to unity as shown in figure (3.4) [1].

$$q = \frac{K_f - 1}{K_t - 1} \quad \dots (3.7)$$

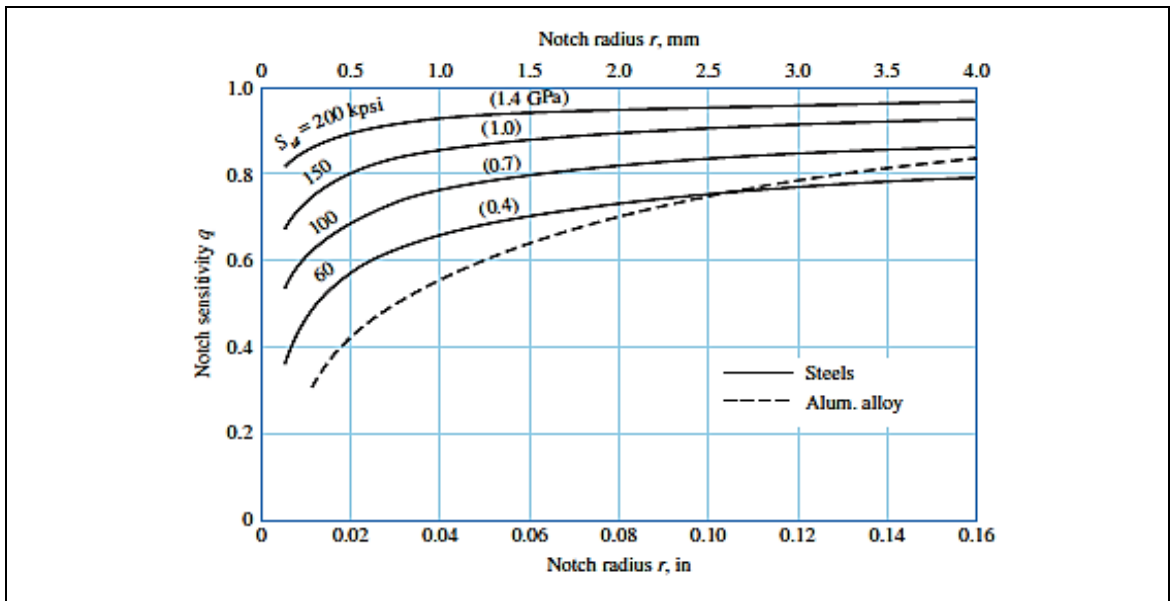


Figure (3.4): Chart of Notch sensitivity of steel and UNS A92024-T Wrought Aluminum Alloys under axial and reversed bending load[3]

This work includes two sources of stress concentration different in geometry under bending loading. The first one is a filet, which can be calculated from figure (3.5).

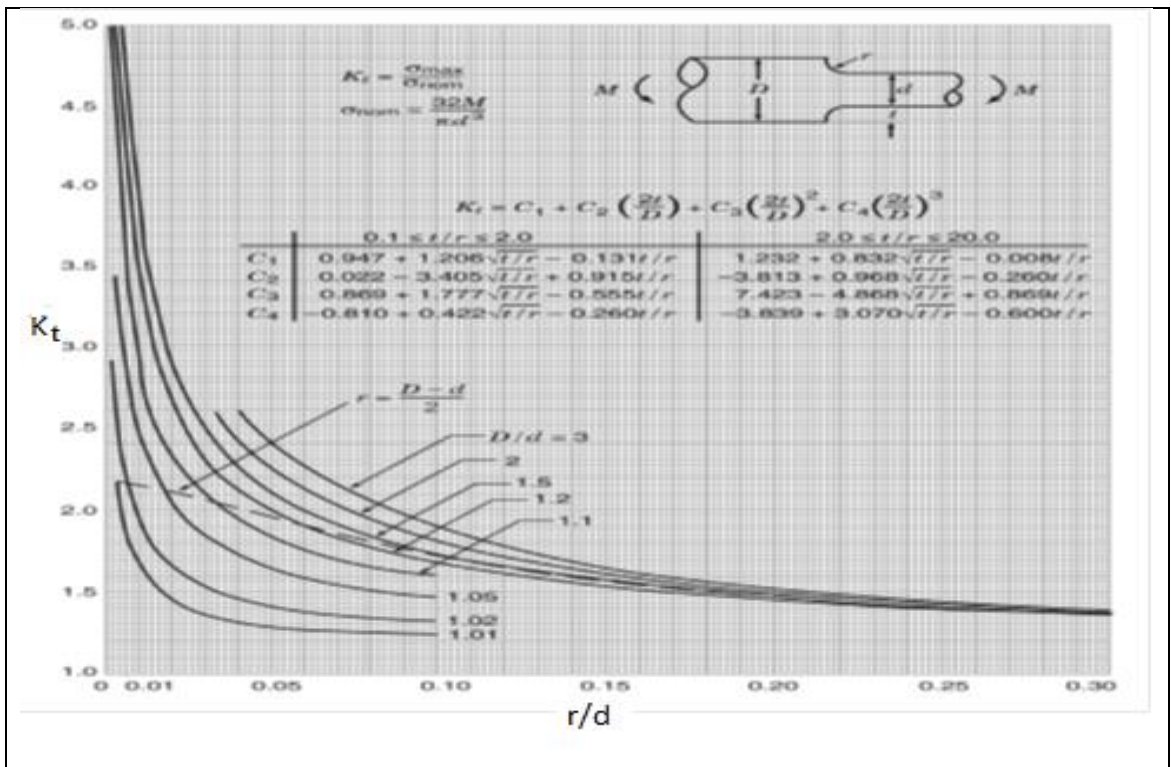


Figure (3.5): Stress Concentration Factor of Shouldered Beam Under Bending [34]

The other source of stress concentration is the v-notch on round bar. The stress concentration factor (K_t) of this type can be calculated using figure (3.6)

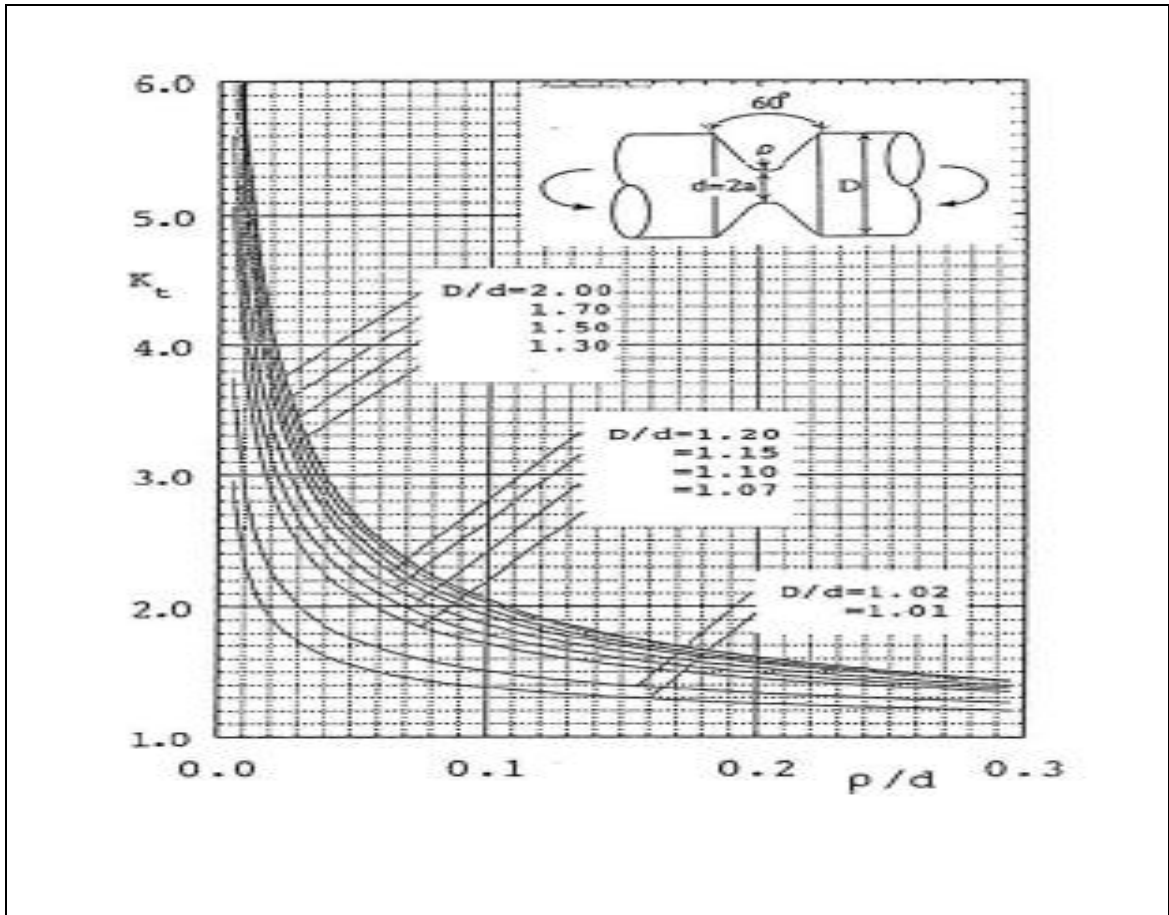


Figure (3.6): Stress Concentration Factor of V-Notched Beam Under Bending [35]

3.5 ANSYS Procedure

The most accurate numerical method used to solve engineering problems is the *Finite Element Analysis (FEA)*. Currently, there are many software programs, e.g. ANSYS, using this method for solving such problems [36]. In this work, ANSYS workbench15.0 is used.

3.6 Fatigue Analysis by ANSYS

The steps generally applied for ANSYS analysis are building the geometry, applying the boundary conditions, and finally getting the solution and results illustration [37].

From ANSYS program, the following results can be obtained [37]:

- Fatigue life.
- Safety factor.
- Stress biaxiality.
- Fatigue damage.
- Fatigue sensitivity chart.
- Rain flow and damage matrix chart (for strain-life method only).

Fatigue analysis includes three parts: material, analysis and results. Also, three methods are available for analysis; stress – life, strain – life, and fracture mechanics methods. On the other hand, there are five important inputs that fatigue results depend on [37]:

- Type of fatigue analysis.
- Mean stress type.
- Load type.
- Fatigue modification factor.
- Multiaxial stress correction.

3.7 Steps for ANSYS Analysis

1- Building the geometry; it is done by using *AutoCAD15* program to draw the geometry of all modules and then import it to the ANSYS program as *IGES* file format, as shown in figure (3.7).

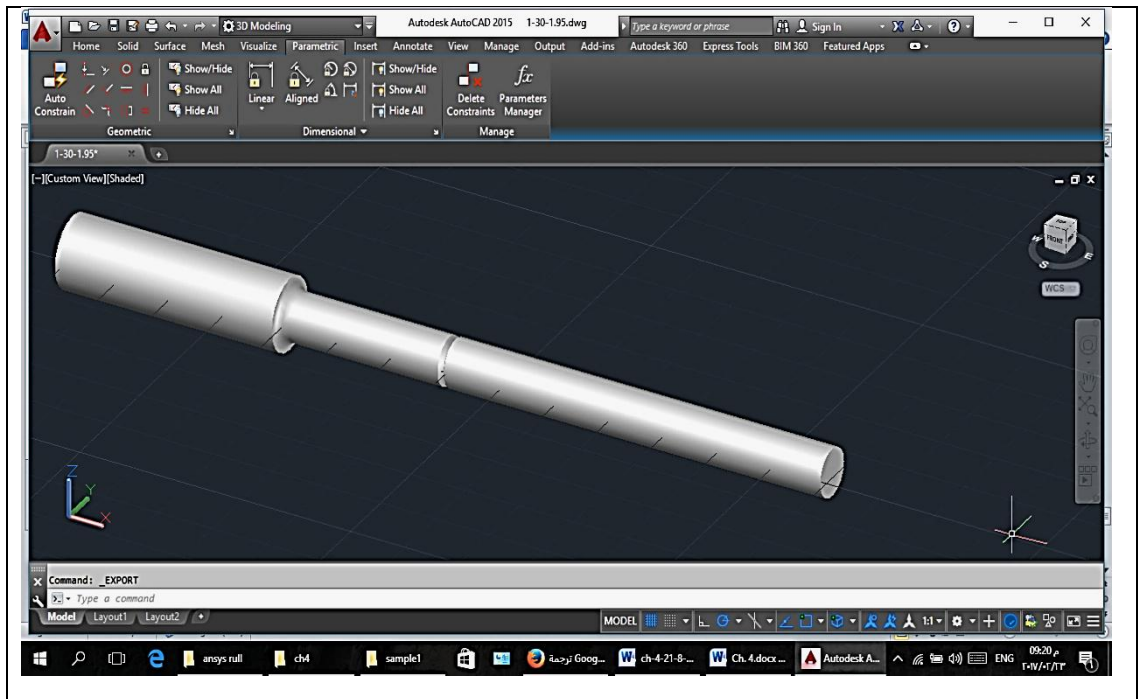


Figure (3.7): AutoCAD Program Window With a Sample

2-Opening ANSYS program window and choosing *Metric* units from menu bar icons, and the choosing *Static Structural* in order to go to the *Engineering Data*.

3-From *Engineering Data* window, the mechanical properties will be set and the experimental S/N curve of the material is specified as shown in figure (3.8).

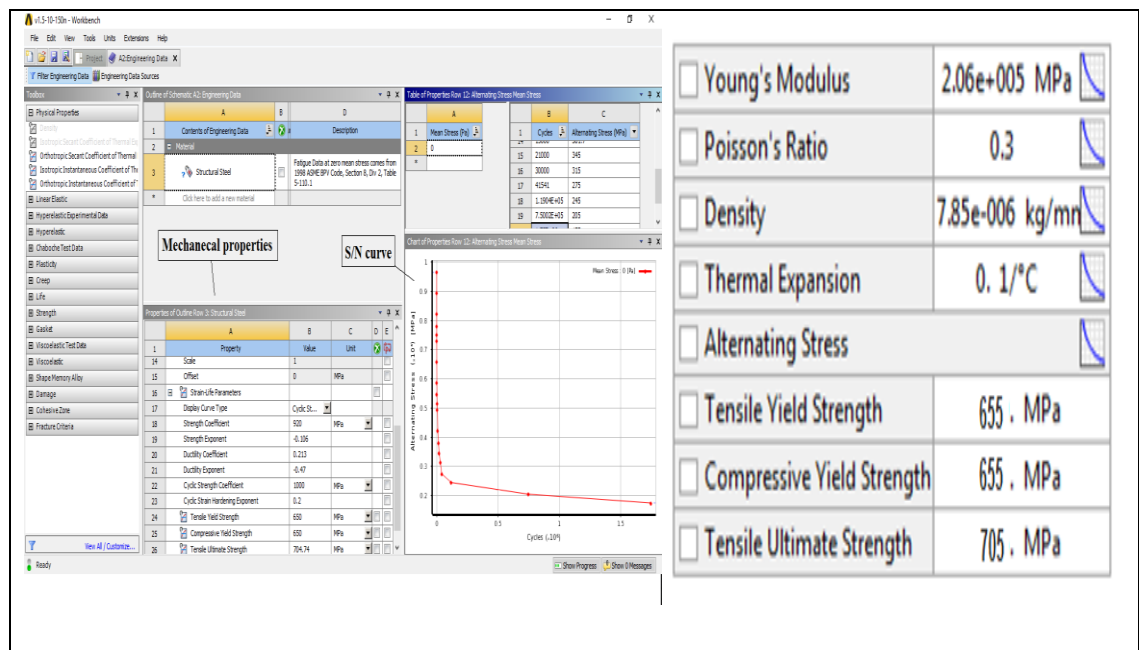


Figure (3.8): ANSYS Engineering Data window

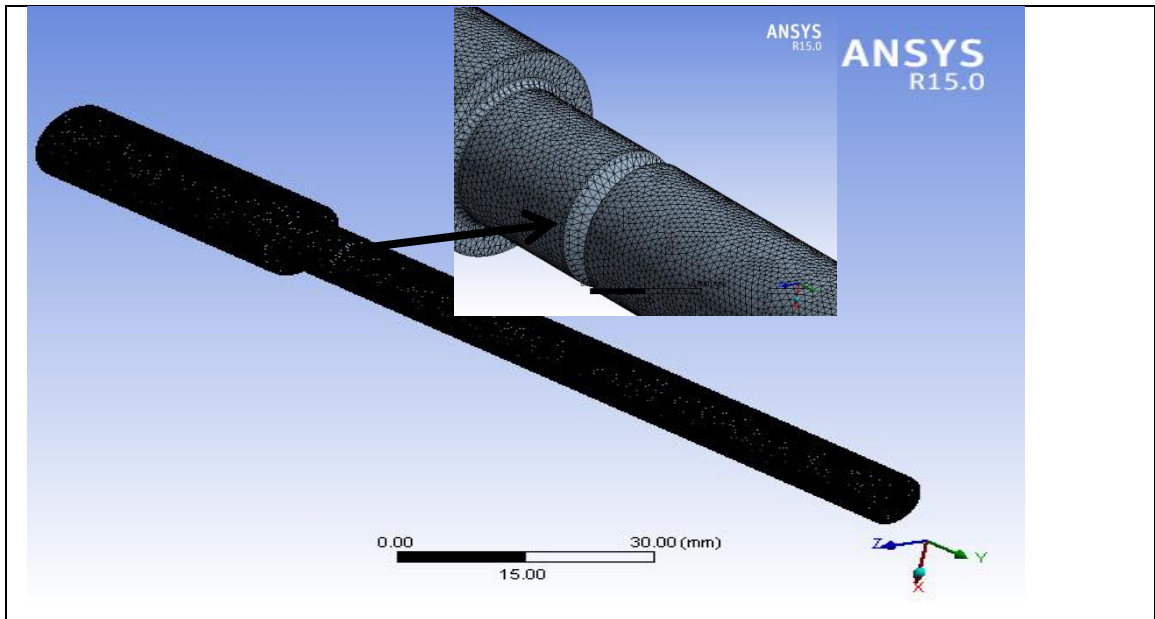


Figure (3.9): Meshed model

4- Closing the *Engineering Data* window and then opening the *Geometry* window to import the designed model that has been drawn before. After that, Model window is opened to start analysis procedure. Firstly, apply a mesh with element type *Tetrahedron* (SOLID 187), to obtain about (335000) elements and (507000) nods, as shown in figure (3.9). In this work, the suitable element size was found by calculating fatigue life for one case. For different element size and then figure (3.10) was drawn.

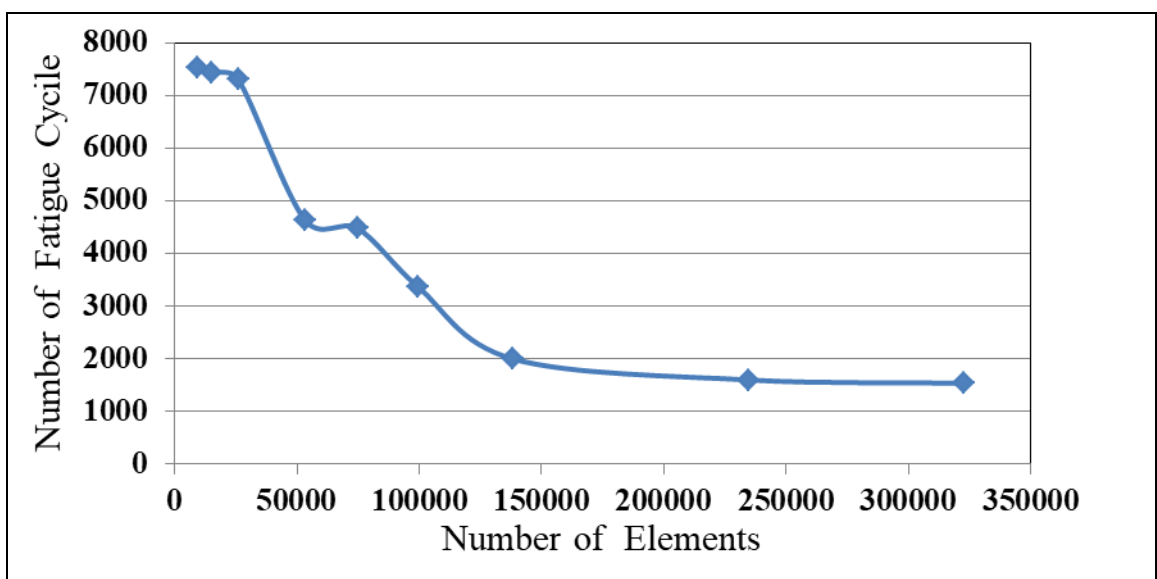


Figure (3.10): Effect of Number of Elements on Fatigue Cycle Results

5- Boundary conditions; fixed support is applied on one side while a force is applied on the other side, as shown in figure (3.11).

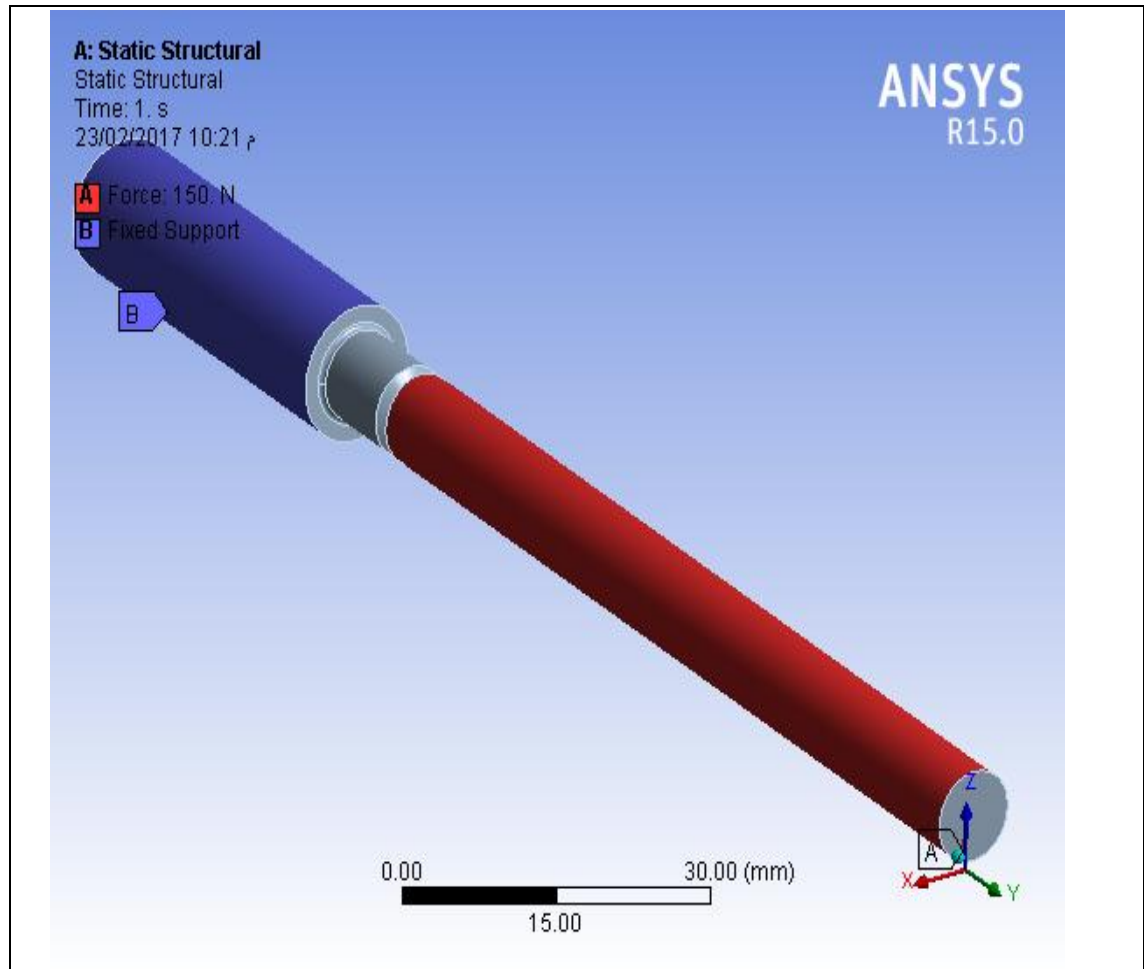


Figure (3.11): Model with Applied Load and Fixed Support

6-Frame choosing *Wizard* (1, 2) choosing *Fatigue analysis: Finding Fatigue Life and Safety Factor* (3), and then inserting *Fatigue Tools* (4), finally *Solving* (5) to get the results, as shown in figure (3.12).

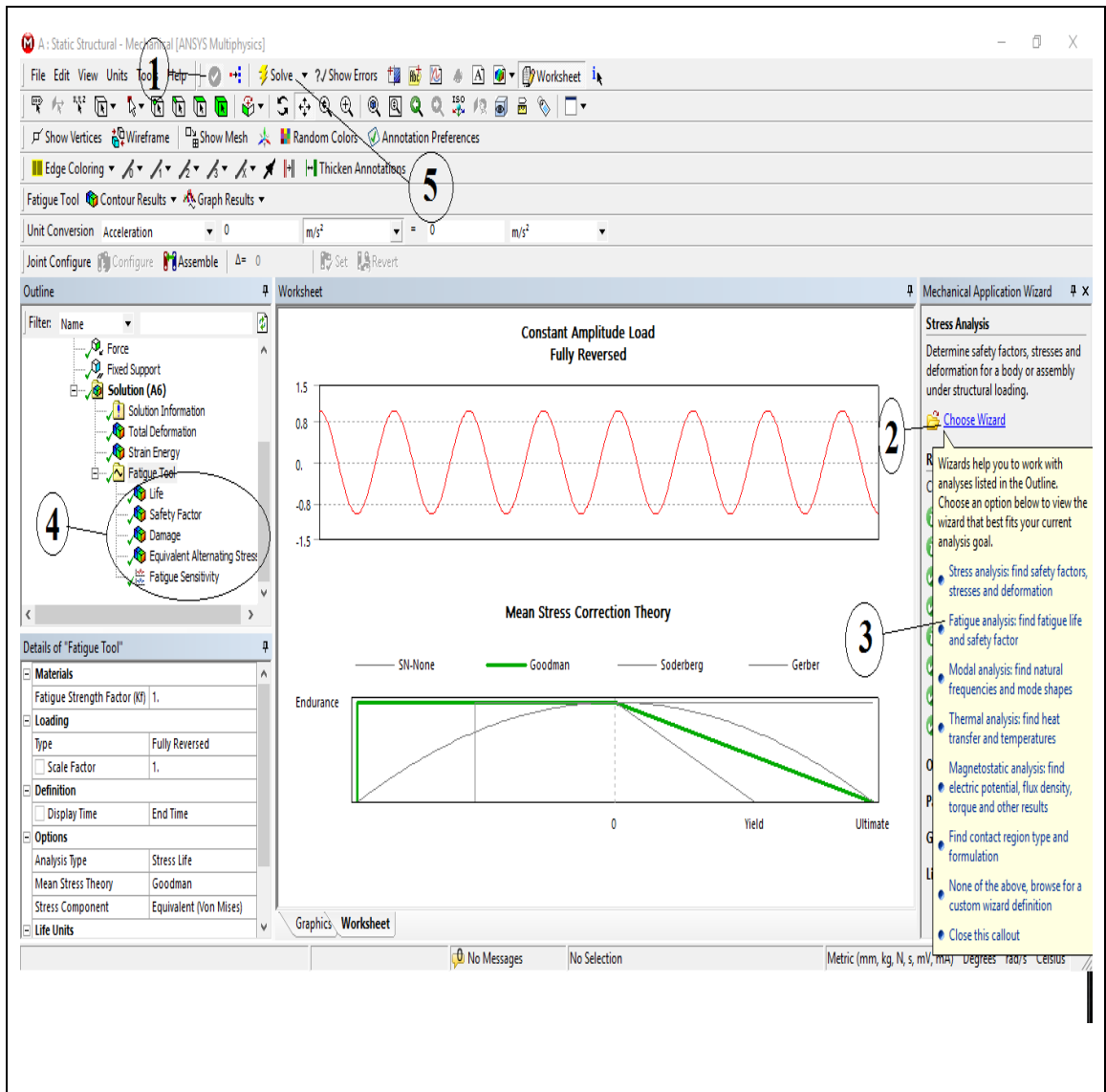
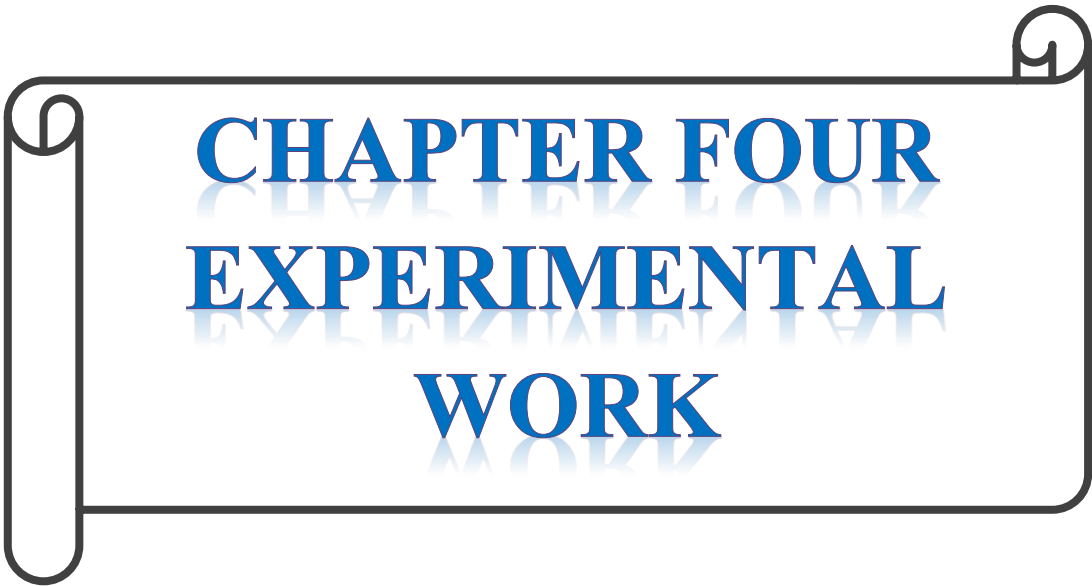


Figure (3.12): Solving Procedure



CHAPTER FOUR
EXPERIMENTAL
WORK

Chapter Four

Experimental Work

4.1 General

In this work, (28^r) standard material specimens of Low Carbon Steel (ST37-2) were provided by The State Company for Mechanical Industries. These specimens were machined to appropriate shapes in the workshop of the Mechanical Engineering Department in Faculty of Engineering/ University of Kufa. In order to study the effects of depth and location along the 60° v-notched specimens (0.5mm, 1mm, 1.5mm and 2mm) depth on fatigue life, two magnitudes of load (100N and 150N) were applied as fully reversed cyclic load. The experimental work contains six main parts. The first one was chemical composition test. The second one was tensile test. Third was fatigue test, which was divided into two parts: S/N curve plot, and the effect of notch depth and location on fatigue life. During the fatigue life test, an infrared camera was used to monitor the temperature change during the process, which was fourth part. The fifth part of experimental work was a macroscopic test for fracture surface, while the final part was a hardness test for the fracture surfaces. Figure (4.1) shows the experimental procedure followed in this work.

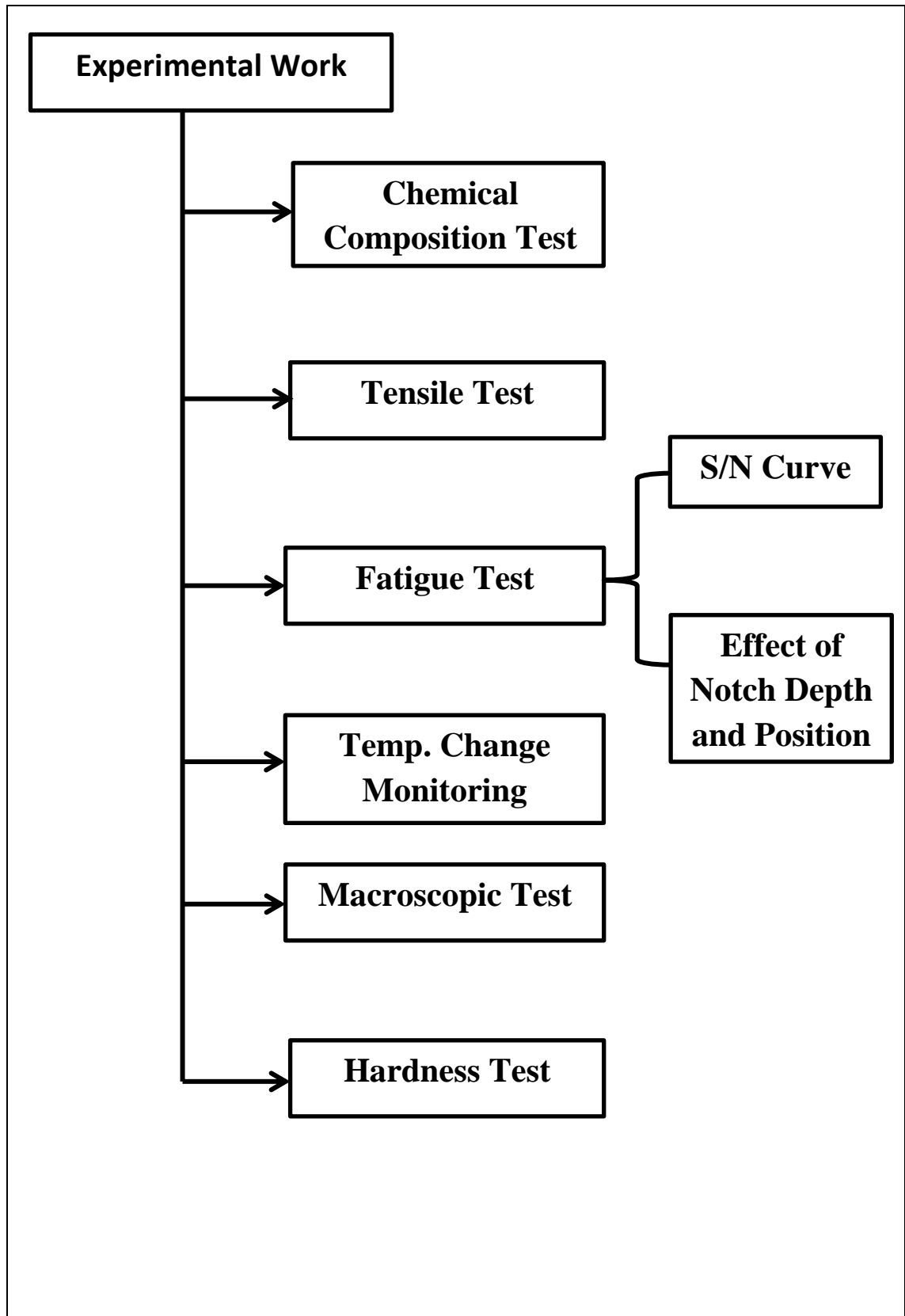


Figure (4.1): Experimental Work Strategy

4.2 Chemical Composition Test

In this work, chemical composition test of Low Carbon Steel (ST37-2) was done in State Company for Inspection and Engineering Rehabilitation (SIER) by using spectrometer device (SPECTRO MAXx) type (ARC. MET 8000) at room temperature (20.3°C) and relative humidity (35%).

Table (4.1) shows the results that were got from the testing device and certificated on appendix (A).

Table (4.1) Chemical Composition

Elem.	C%	Fe%	P%	S%	Si%	Al%	Cr%	Mn%	Ni%	Cu%	Mo%
Exp.	0.187	Bal.	0.0041	0.021	0.281	0.02	0.122	0.636	0.091	0.136	0.011
Standard	0.17	Bal.	0.05	0.05	-	-	-	-	0.009	-	-

4.3 Tensile Test

In this test, used four samples of (DIN 50125) standard, as shown in figure (4.2), were tested using device type (GUNT WP 300). The testing process was done in in the laboratory of Mechanical Engineering Department/ University of Kufa. This test was done to get the mechanical properties of the material tested, where the results are shown in table (4.2).

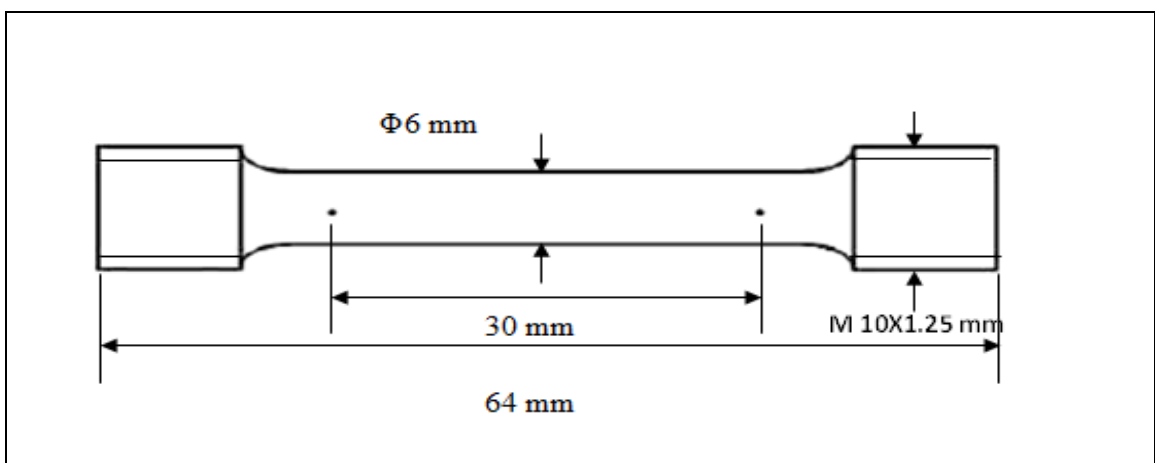


Figure (4.2): Tensile Specimens of (DIN 50125)

Table (4.2) Mechanical Properties of steel (ST37-2)

Hardness (HRB)	Yield strength (Mpa)	Tensile strength (Mpa)	Elongation %	Modulus of elasticity (Gpa)
65	655	704.74	14.17	200

4.4 Fatigue Test

4.4.1 Fatigue Testing Specimen

This test is divided into two parts. The first one was done to draw the S/N curve using 38 samples. The second part was done to investigate the effect of notch depth and location on fatigue life, as illustrated in figure (4.3), using 240 samples with about three tests for each case. The fatigue samples were machined in appropriate dimensions ($D = 12\text{mm}$ and $L = 40\text{ mm}$) and ($d = 8\text{ mm}$ and $L = 106\text{ mm}$).

- First group included smooth samples without notch in order to draw the S/N curve as shown in figure (4.4).
- Second group included notched specimens to study the effects of notch location and notch depth through doing a v-notch with angle 60° and four different depths (0.5mm, 1mm, 1.5mm and 2mm). Every notch depth was localized in different locations on different samples. The v-notches were located at distance (10, 20, 30... 100) mm from the edge as shown in figure (3.5) and this figure explained the named strategy that be used then in cases.

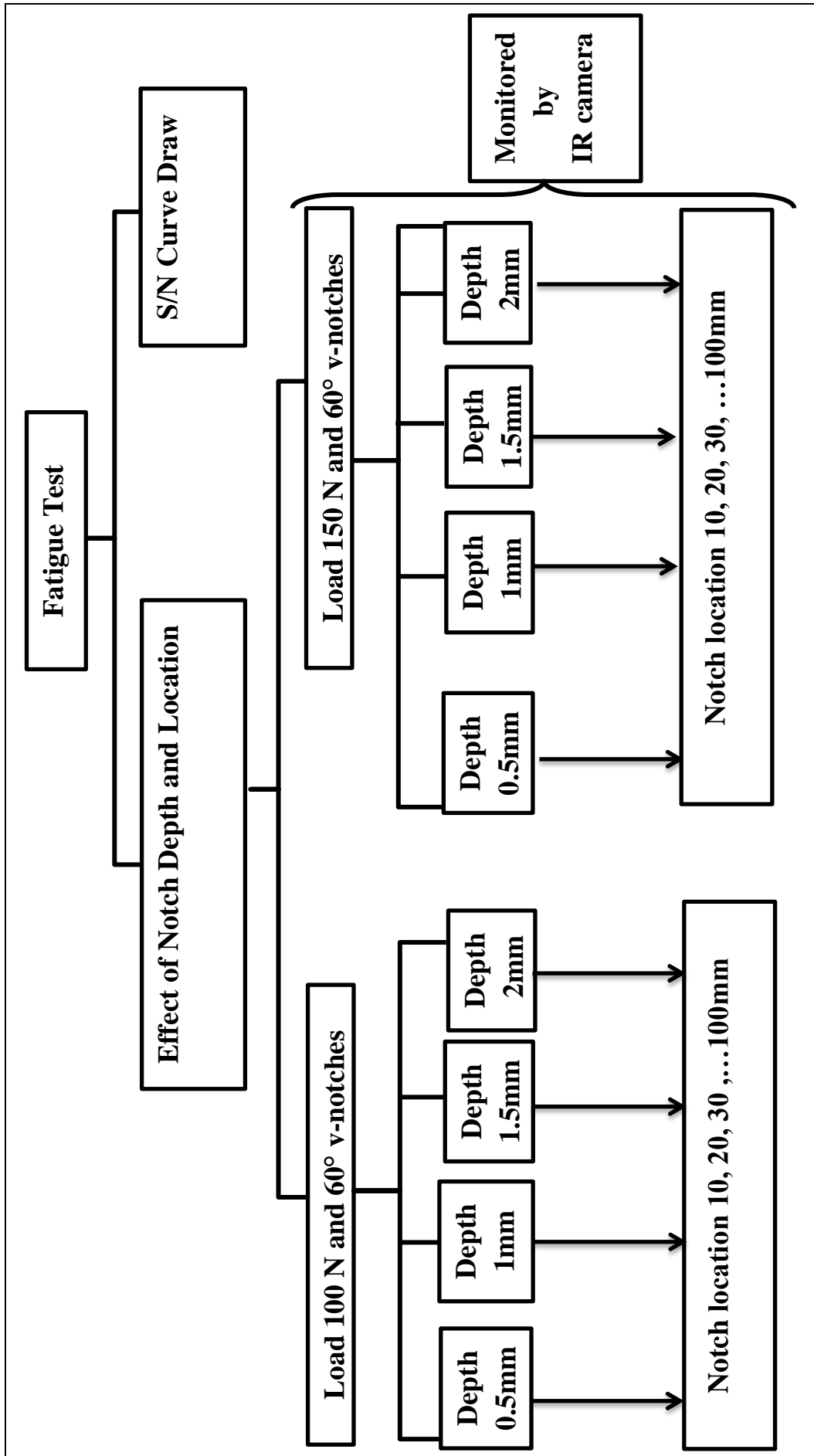


Figure (4.3): Schematic of Fatigue Test Strategy

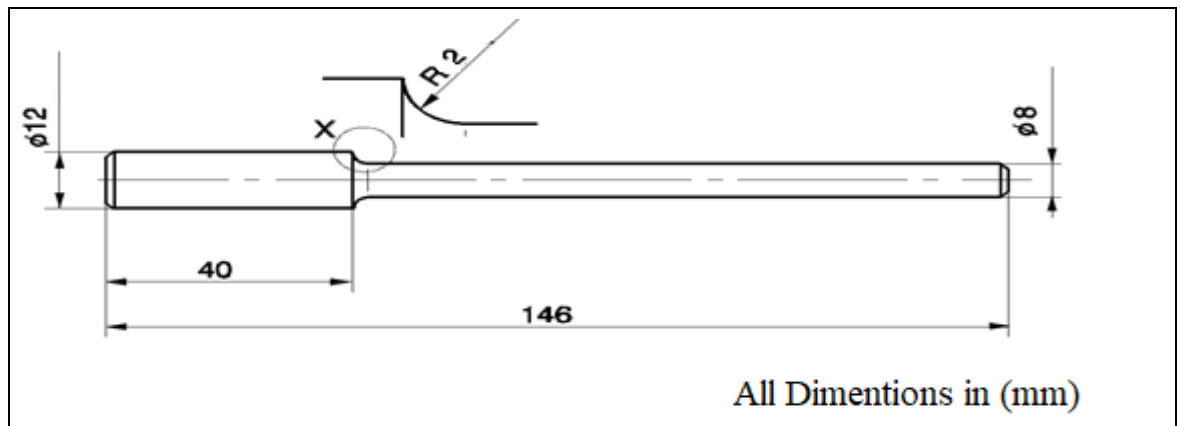


Figure (4.4): Fatigue Test Sample

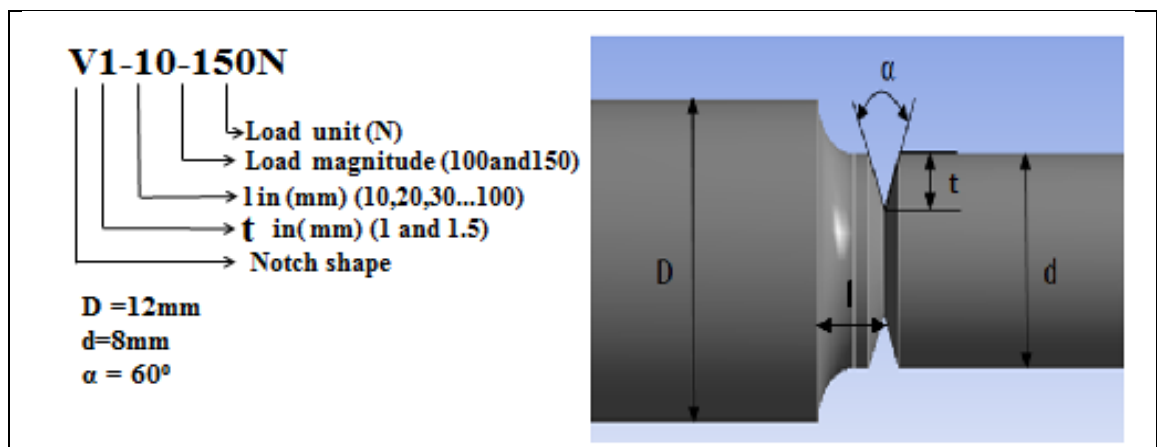


Figure (4.5): Notched Specimen Showed the Notch Position

4.4.2 Fatigue Testing Machine

It has been conducted in the laboratories of Mechanical Engineering Department/ University of Kufa. The tests were implemented using fatigue testing machine (Gunt WP140), which uses a single cantilever rotating bending beam specimen with a fully reversed bending load and constant amplitude. This testing machine can record the fatigue strength of the tested material by drawing the stress – number of fatigue life curve. Also, it is possible to investigate the effects of notch or surface finishing on fatigue

life. The amplitude stress can be adjusted according to the study requirements. This device has two digital screens displaying the number of cycle and load magnitude in (N). The tested sample was clamped from one side, while the other side was connected to the concentrated adjustable force with range (0-300 N) to produce bending load. The device has a constant frequency of (50Hz). Through the experiments, the load applied was sinusoidal cyclic with stress rate $R = (-1)$. The tests were done at room temperature (27-34) °C and environment humidity of (40-57) %. When the specimen was fractured, the testing machine stopped automatically by the shutdown sensor. There is a digital screen illustrating the number of rotation and stop accounting at failure.

The bending moment and stress amplitude that was applied as figure (4.6) calculating from the equations as below:

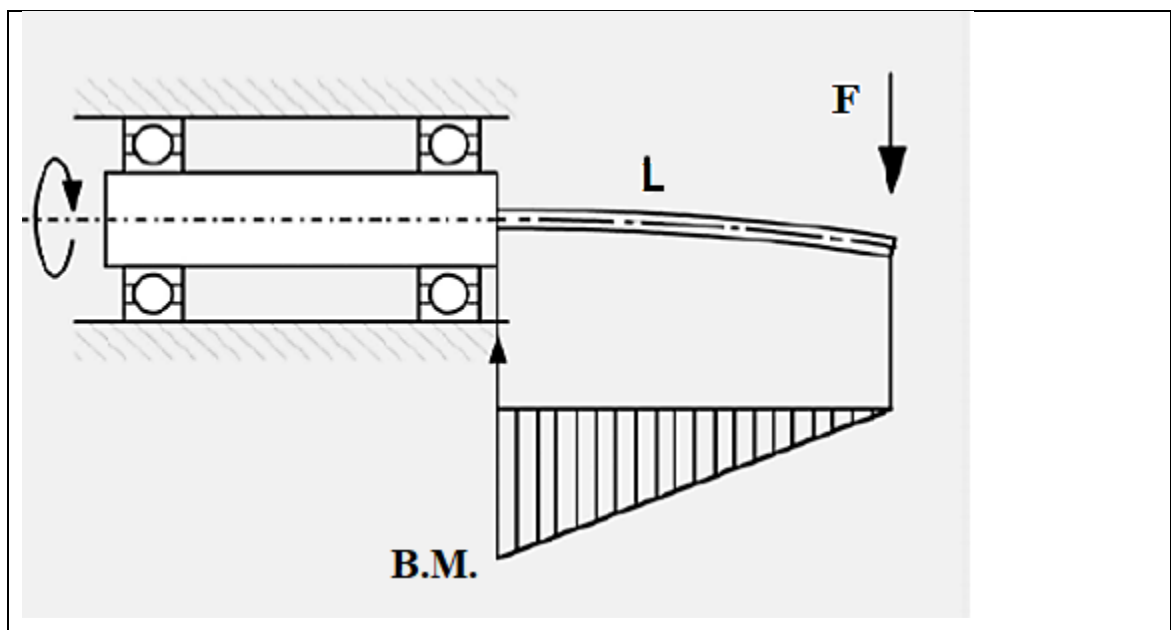


Figure (4.6): Schematic of Applied Load on The Testing Specimen

$$M_b = F \cdot L \quad \dots (4.1)$$

By using the section modulus of the specimen, the alternating stress amplitude can be calculated as shown below.

$$W_b = \frac{\pi d^3}{32} \quad \dots (4.2)$$

$$\sigma_a = \frac{M_b}{W_b} = \frac{32 \times F \times L}{\pi d^3} \quad (\text{Mpa}) \quad \dots (4.3)$$

Where;

F = Applied force (N).

L= Bending Moment arm = 106 mm ± 0.1mm.

d = Specimen Diameter = 8 mm ± 0.1mm.

M_b = Bending moment (N.mm).

W_b = Section modulus of the specimen.

4.5 Temperature Change Monitoring

This type of test was conducted in the laboratories of Mechanical Engineering Department / University of Kufa, using an infrared camera type (FILIR E50), which has a color LCD large touched monitoring screen (3.5 in), and its specification as detailed in table (4.3).

Table (4.3) Specification of IR Camera

1	Temperature Range	-20 ⁰ to 650 ⁰ C
2	Thermal Sensitivity	< 0.05 ⁰ to 30 ⁰ C
3	Accuracy Range	±2 ⁰ C or ± 2% of reading
4	IR Resolution	240X180 pixels
5	Frame Rate	60Hz
6	Digital Zoom	4X continuous
7	Dimensions	246X97X184mm
8	Weight	0.825Kg

Furthermore, this camera has the ability to monitor temperature change for three different moveable spot points and auto hot / cold spot point during the thermal viewing screen and recording. Can Record either in the form of pictures or continuous video. Also, manual focus, auto calibration, and auto orientation for screen view are all available to utilize.

4.6 Macroscopic Test

It was done on fractured surface of the fatigue test specimens by using digital camera type Canon IXY 12.1MEGA PIXELS with external amplifier lens X4. This test was implemented in the laboratories of Mechanical Engineering Department / University of Kufa. This type of test was to analyze fracture surface of fatigue test specimens, as shown in figure (4.7).

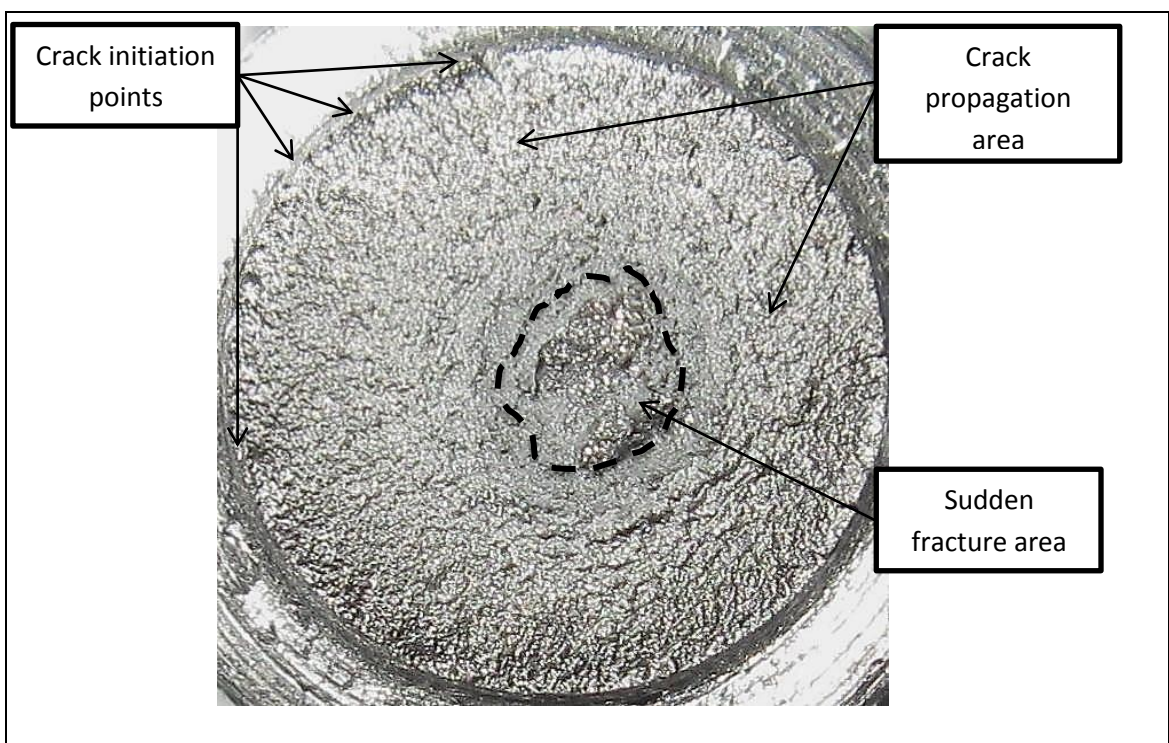
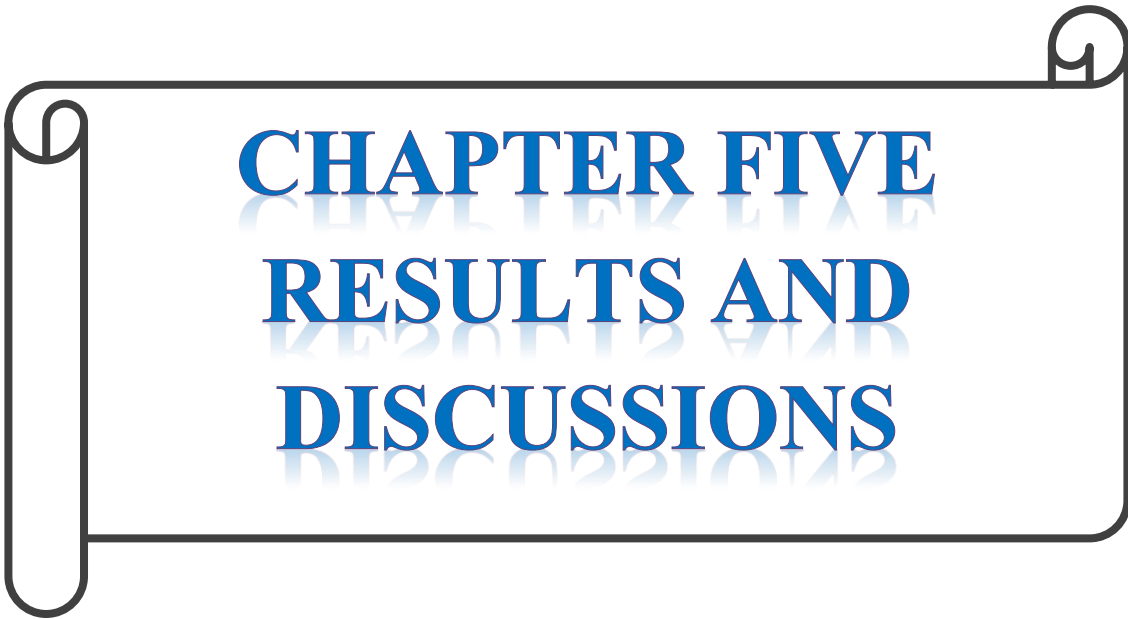


Figure (4.7): Fracture Surface of The Rotating Bending Fatigue Testing Specimen

4.7 Hardness Test

It was done on the fractured surface of the fatigue test specimens by using Brinell Hardness Test model (HB-30008). This test was conducted in the laboratories of Mechanical Engineering Department / University of Kufa. This type of test was meant to analyze the hardness of fracture surfaces of fatigue test specimens at sudden fracture and crack propagation areas, as shown in figure (4.7).



CHAPTER FIVE
RESULTS AND
DISCUSSIONS

Chapter Five

Results and Discussion

5.1 Introduction

In this chapter, the results obtained in this work will be displayed in three different sections. The first one is related to the experimental and numerical (by ANSYS work bench 15.0) results of fatigue life tests and then comparing them with the values of load, notch depth and notch position. The second section deals with changing the sudden fracture area in the fatigue testing specimens with respect to notch position. The third section discusses the hardness test results for the fracture area of the fatigue testing specimens with respect to notch position

5.2 Fatigue Test

This section is divided into two parts; the first part shows the experimental S/N curve, and the second part deals with experimentally and numerically measured effect of notch position on fatigue life. Furthermore tables (5.1) to (5.4) show the cases that were studied and the positions of fracture. Figure (5-1) shows the first part of the experimental results which was for S/N curve for the material used in this research, where the test was done to get (12) points, and found that the fatigue strength of the testing material was about (175 Mpa). The experimental results of S/N curve will be used in the theoretical part (ANSYS program) to obtain the number of fatigue life by building a mathematical model that simulates the process of failure in the fatigue. The Basquin's Formula was applied for describing the relationship between stress and number of fatigue life (see 1.4.1).

$$\sigma = (2464.1) (N_f)^{-0.189} \quad \dots (5-1)$$

The second part of the experimental aspect of the test was the testing of samples containing notch. The criteria studied in this part of study were:

- 1- Depth of the notch: where the study of four depths of the notches (0.5, 1, 1.5 and 2) mm.
- 2- Notch position: Ten positions were studied with respect to the edge of the large part of the sample (see Figure (4.5)).
- 3- The applied load magnitude: have been used two forces in this research, (100 and 150) N.

The results will be compared with the theoretical results obtained from the ANSYS program.

Figures (5 - 2) to (5 - 5) show the comparison between the experimental and ANSYS results of the samples with notch depths of (0.5, 1, 1.5 and 2) mm, respectively and load magnitude (100) N. While Figures (5-6) to (5-9) show the comparison between the experimental and ANSYS results for the samples with notch depths of (0.5, 1, 1.5 and 2) mm respectively and load magnitude (150) N. Also the figures (5-10) and (5-11) illustrated the effect of changing the depth of notch on the value of experimental fatigue life when the applied load is (100 and 150) N respectively. While (5 - 12) and (5 - 13) explained the effect of changing the depth of notch on the value of fatigue life calculated by ANSYS at load magnitude (100 and 150) N. From these figures, the following points can observe:

- 1- The presence of the notch will change the location of the fracture in the smooth sample (un – notched sample) where the fracture position in the smooth sample is always on the wide edge (supported edge) and this is observed during the experimental work. This is due to two points; the first one: the greatest value of stress at the wide edge (the largest arm and the least diameter observed in equation 4-3)). The second one: there is a source of stress concentration at this edge (see figure (3-5)). In the case of notched sample, the fracture will change its position. Once the

fracture located in the notch and then the fracture located at the edge (see Tables (5-1) – (5-4)). The changing of fracture location necessarily means changing the location of the greatest stress affecting on the sample. Therefore, the factors affecting on the smooth sample, arm length and source of stress concentration, are no longer influential alone, but other factors influence the fracture.

- 2- When the notch is creating in the sample at appropriate position that will increase the fatigue life of this sample by a ratio depending on the depth of the notch and its position and the magnitude of applied load. So with the increasing the depth of notch, the amount of increasing in the fatigue life will decrease with proven applied load. Also with the increasing in applied load, the increasing in fatigue life will decrease at proven notch depth. For the location of the notch, when the notch go away from the edge, the increasing in the value of the fatigue life until reach the highest value and then the fatigue life begin to decrease, and all of this occurs when proven the depth of notch and the applied load. This shown clearly when the depth of notch (1 and 1, 5) mm. The highest value for the fatigue life can be getting when the fracture position is moved from the notch to the edge. In other words, if the notch is located between the wide edge and the position of highest fatigue life, the fracture location is in the notch position. And when the notch located between the position of highest fatigue life and free end, the fracture position will be at the edge.
- 3- The location of the highest value of the fatigue life calculated experimentally is different from those calculated using the ANSYS program by not more than 20 mm. The depth of the notch is the factor that greatly effects on the location of the highest value of the fatigue life.
- 4- Maximum increasing in fatigue life was experimentally by the ratio more than (75) % and numerically by the ratio more than (73) % with respect to the smooth sample.

To explain this phenomenon it is necessary to draw the stress causing the fracture experimentally using Basquin's Formula obtained from the S/N curve (see equation (5-1)). Figures (5 - 14) to (5 - 17) show the comparison between the fracture stress value calculated from the experimental and ANSYS results when the notch depth is (0.5, 1, 1.5 and 2) mm respectively, and at a load of 100 N. When the applied load is 150N, the figures from (5-18) to (5-21) illustrate the comparison between the value of fracture stress calculated from the experimental and ANSYS results when the notch depth is (0.5, 1, 1.5 and 2) mm, respectively. Figures (5-22) and (5-23) show the comparison between fracture stress calculated from the experimental results when the notch depth is (0.5, 1, 1.5 and 2) mm at the load is (100 and 150) N respectively. Finally, the figures (5-24) and (5-25) show the comparison between fractional stress calculated from the ANSYS results when the depth of the notch is (0.5, 1, 1.5 and 2) mm at the load is (100 and 150) N respectively. From these curves, the following points can be observed:

- 1- The fracture stress (maximum stress) decreased gradually with the progress of the notch position toward the free end until it reached a certain point after which the stress begins to increase again. This point is the point of the coup in which the fracture position is transformed from the notch to the edge. This condition is clearly shown when the depth is (1 and 1.5 mm) and the load is (100 and 150) N and also shown when the depth of notch is (0.5) mm and the load (150) N.
- 2- When the depth of the notch is (2) mm, the point of the coup does not appear experimentally because of the position of the fracture is always in the notch position (because of maximum stress was always at notch) when the applied load was (100 and 150) N. In ANSYS, the fracture position will move from the notch position to the edge when the notch position is (90) mm and the load was (100 and 150) N.

3- When the depth of the notch was (0.5) mm and the applied load was (100) N, the point of the coup point does not appear experimentally or theoretically (using ANSYS). In this case, the stress is equal to the minimum stress in the S/N curve (Endurance Limit), so there is no fracture.

When notch depth (0.5 and 2) mm the phenomenon is not clearly appeared to be explained, so the case of notch depth (1.5) mm will be discussed the phenomenon of decreasing and increasing stress fracture depending on the following points:

- 1- The smooth sample contains two diameters; the first diameter is 12 mm and is the large diameter. The first diameter length is (10) mm. The second diameter is (8) mm and second diameter length is (106) mm. Due to the difference in length and diameter, and due to the notch (location and depth), the value of the equivalent second moment of area will change (see equation (4-3)). Figure (5-28-A) explained how the equivalent second moment of area increased by moving the position of the notch towards the free end for the notched sample when the depth of notch is (1.5) mm (see [38], [39]). As a result of this increasing in the value of equivalent second moment of area, the value of stress at the notch and at the edge will decrease as shown in Figures (5 - 28 – B) and (5-28- C). From the figures, the decreasing in stress at the notch was higher than the decreasing of stress at the edge, this is the reason of moving the fracture position from the notch to the edge.
- 2- Edge and notch were two sources of stress concentration, but the effect of notch was greater than that of the edge (see figures (3-^o) and (3-^٦)). The effect of one of them on the other will vary depending on the proximity between them and the value of stress on each of them (see paragraph 1.^o).
- 3- The effect of plastic deformation on the mechanical properties (Strain Hardening).

From above points, the changing of fracture position explain clearly, and the figures (5-26), (5 - 27), and (5 - 29) indicate the change in the equivalent second moment of area and the stresses at the edge and the notch at load 100 N and 150 N when the notch depth is 0.5, 1 and 2 mm respectively.

5.3 Fracture Surface Test

Figure (5 - 30) shows the fracture of the samples containing a notch with depth (1 and 1.5) mm and the applied load is (150) and at different positions of notches, because When notch depth (0.5 and 2) mm the phenomenon is not clearly appeared to be explained. From the figure can see there were a coarse areas and a little bit smooth areas. The coarse areas indicate sudden rapid fracture, while smooth areas indicate slow fracture (crack propagation area). On this basis, the rough fracture area was calculated for all samples. The figures were obtained from figures (5 – 31) to (5 - 34), which shown the area of the sudden fracture of samples containing a particular depth and in a specific location and when applying loads of (100 and 150) N. From these figures the following points can be observed:

- 1- The area of the sudden fracture decreased as the notch moved away from the wide edge, which is the same behavior that we observed in the fracture stress at the fracture position (note the figures from (5-14) to (5-21)). Where increasing stress on the fracture position, cause an increasing on the area of sudden fracture and vice versa. Decreasing stress on the fracture position, leads to the decreasing on the area of the sudden fracture.
- 2- The area of sudden fracture increases with the applied load on the sample. Where noticed that the area of sudden fracture when the application of (150) N load is greater than the equivalent when the applied load of (100) N (the same reason in point (1)).

- 3- The area of sudden fracture increases by increasing the depth of the notch in the sample and when applying the same load. Where noticed that the area of sudden fracture at notch depth (2) mm was greater than the others when the notch depth was less than (2) mm (the same reason in point (1)).
- 4- The results of the area of sudden fracture gives a clear indication of the increase in the fatigue life of the samples containing notches, where can see the increase in the fatigue life will necessarily decrease the area of sudden fracture because of decreasing of stress at the fracture position.

5.4 Hardness Test

Figure (5-35) shows the surface fracture of the fatigue testing specimens. This test was applied on two regions on the fracture surface. The first one is the sudden fracture area (A1), while the second is the propagation area (A2) for each tested specimens. From the results obtained, shown in figures (5.36) to (5.43), the following points are noticed;

- 1- The hardness of sudden fracture area (A1) is higher than it is in the propagation area (A2). This is due to increasing the crack propagation speed on sudden fracture area (see [24]).
- 2- Decreasing the hardness of sudden fracture area at notch region is due to moving the notch away from the edge region, which in turn leads to decreasing the maximum stress in notch region due to this shifting (note the figures from (5-14) to (5-21)), and hence, results in a decrease in plastic deformation (see [24]).
- 3- Hardness of sudden fracture surface is directly proportional to the applied load because of the increase in the stress at fracture region.
- 4- Hardness of sudden fracture surface is directly proportional to the depth of notch because of the increase in the stress calculated at this region.

Table (5.1) Cases of Experimental and ANSYS Fatigue Test of 0.5 mm Depth

No.	Notch Position (mm)	Load (N)	Crack (Fracture) Position in Experimental Work (mm)	Crack (Fracture) Position in ANSYS (mm)
1	10	100	10	10
2	20	100	20	To endurance Limit
3	30	100	30	To endurance Limit
4	40	100	To endurance Limit	Edge
5	50	100	To endurance Limit	Edge
6	60	100	Edge	Edge
7	70	100	Edge	Edge
8	80	100	Edge	Edge
9	90	100	Edge	Edge
10	100	100	Edge	Edge
11	10	150	10	10
12	20	150	20	20
13	30	150	30	Edge
14	40	150	Edge	Edge
15	50	150	Edge	Edge
16	60	150	Edge	Edge
17	70	150	Edge	Edge
18	80	150	Edge	Edge
19	90	150	Edge	Edge
20	100	150	Edge	Edge

Table (5.2) Cases of Experimental and ANSYS Fatigue Test of 1 mm Depth

No.	Notch Position (mm)	Load (N)	Crack (Fracture) Position in Experimental Work (mm)	Crack (Fracture) Position in ANSYS (mm)
1	10	100	10	10
2	20	100	20	20
3	30	100	30	30
4	40	100	40	40
5	50	100	50	Edge
6	60	100	60	Edge
7	70	100	Edge	Edge
8	80	100	Edge	Edge
9	90	100	Edge	Edge
10	100	100	Edge	Edge
11	10	150	10	10
12	20	150	20	20
13	30	150	30	30
14	40	150	40	40
15	50	150	50	Edge
16	60	150	60	Edge
17	70	150	Edge	Edge
18	80	150	Edge	Edge
19	90	150	Edge	Edge
20	100	150	Edge	Edge

Table (5.3) Cases of Experimental and ANSYS Fatigue Test of 1.5 mm Depth

No.	Notch Position (mm)	Load (N)	Crack (Fracture) Position in Experimental Work (mm)	Crack (Fracture) Position in ANSYS (mm)
1	10	100	10	10
2	20	100	20	20
3	30	100	30	30
4	40	100	40	40
5	50	100	50	50
6	60	100	60	Edge
7	70	100	70	Edge
8	80	100	Edge	Edge
9	90	100	Edge	Edge
10	100	100	Edge	Edge
11	10	150	10	10
12	20	150	20	20
13	30	150	30	30
14	40	150	40	40
15	50	150	50	50
16	60	150	60	Edge
17	70	150	70	Edge
18	80	150	Edge	Edge
19	90	150	Edge	Edge
20	100	150	Edge	Edge

Table (5.4) Cases of Experimental and ANSYS Fatigue Test of 2 mm Depth

No.	Notch Position (mm)	Load (N)	Crack (Fracture) Position in Experimental Work (mm)	Crack (Fracture) Position in ANSYS (mm)
1	10	100	10	10
2	20	100	20	20
3	30	100	30	30
4	40	100	40	40
5	50	100	50	50
6	60	100	60	60
7	70	100	70	70
8	80	100	80	80
9	90	100	90	Edge
10	100	100	100	Edge
11	10	150	10	10
12	20	150	20	20
13	30	150	30	30
14	40	150	40	40
15	50	150	50	50
16	60	150	60	60
17	70	150	70	70
18	80	150	80	80
19	90	150	90	Edge
20	100	150	100	Edge

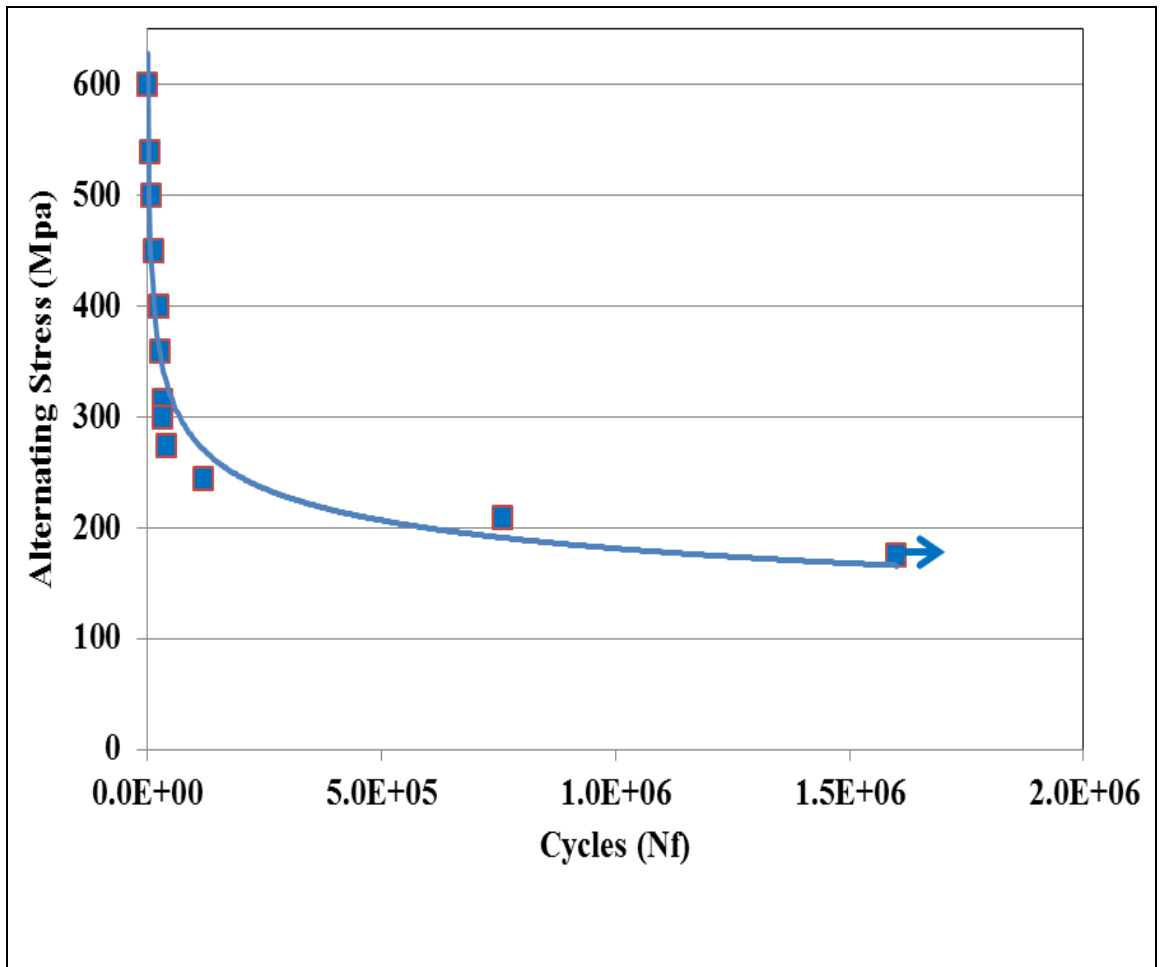


Figure (5.1): Experimental S/N Curve

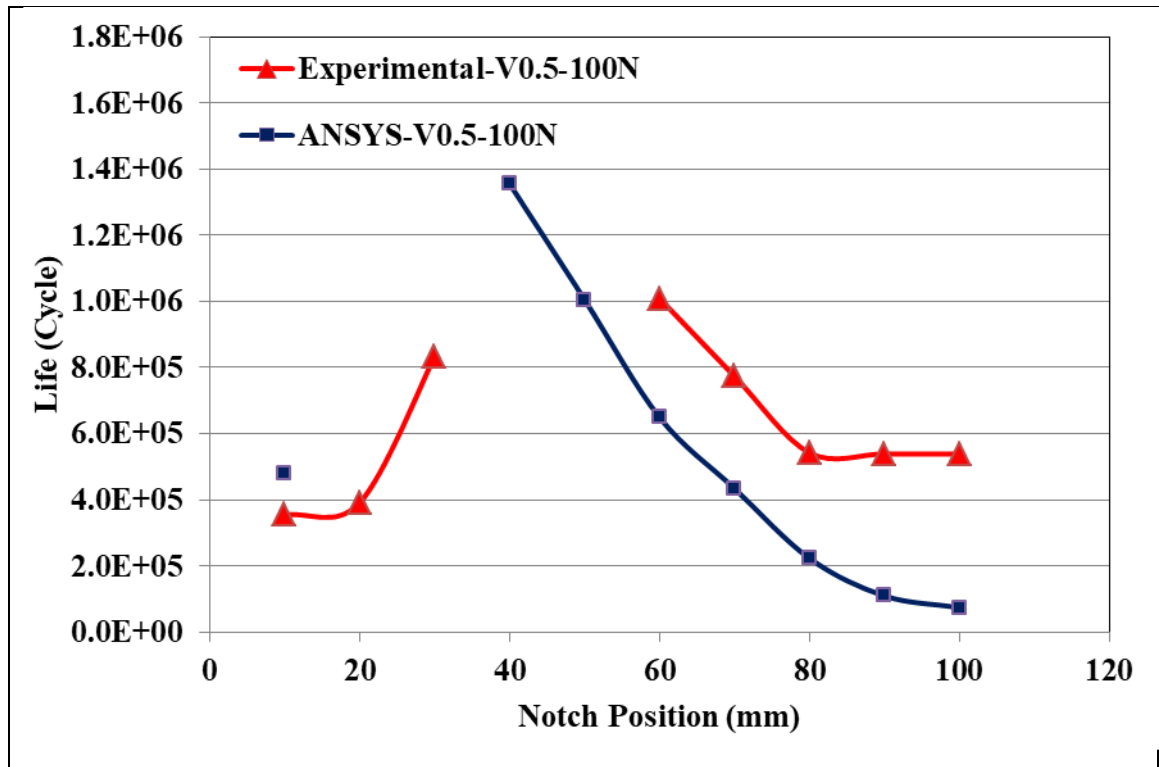


Figure (5.2): Experimental and ANSYS Fatigue Life Change Along the Notch Position When the Notch Depth is (0.5) mm and the Applied Load is 100N

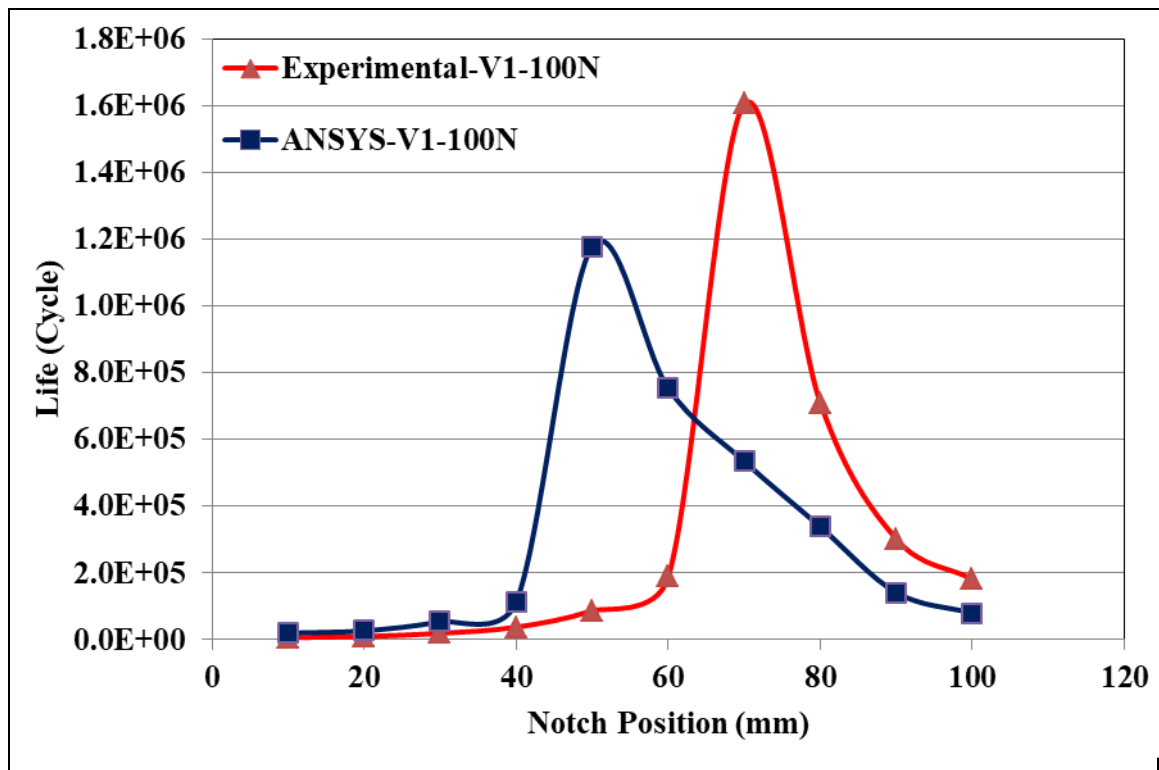


Figure (5.3): Experimental and ANSYS Fatigue Life Change Along the Notch Position When the Notch Depth is (1) mm and the Applied Load is 100N

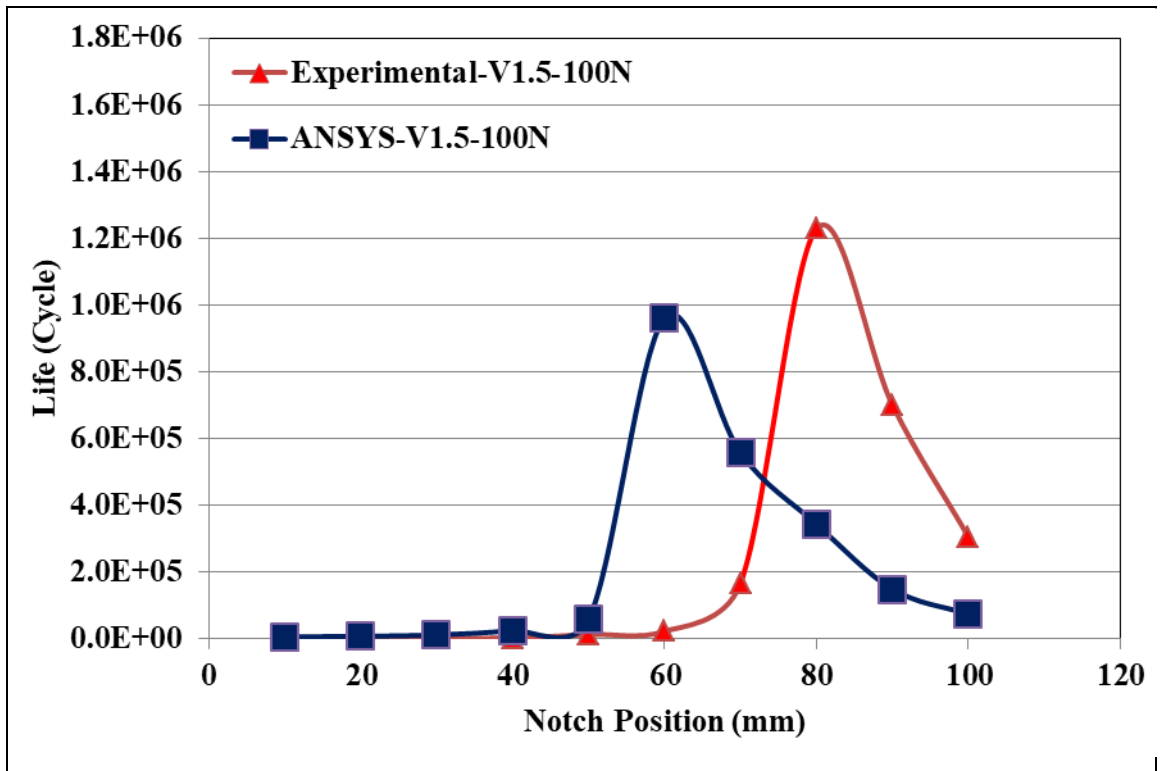


Figure (5.4): Experimental and ANSYS Fatigue Life Change Along the Notch Position When the Notch Depth is (1.5) mm and the Applied Load is 100N

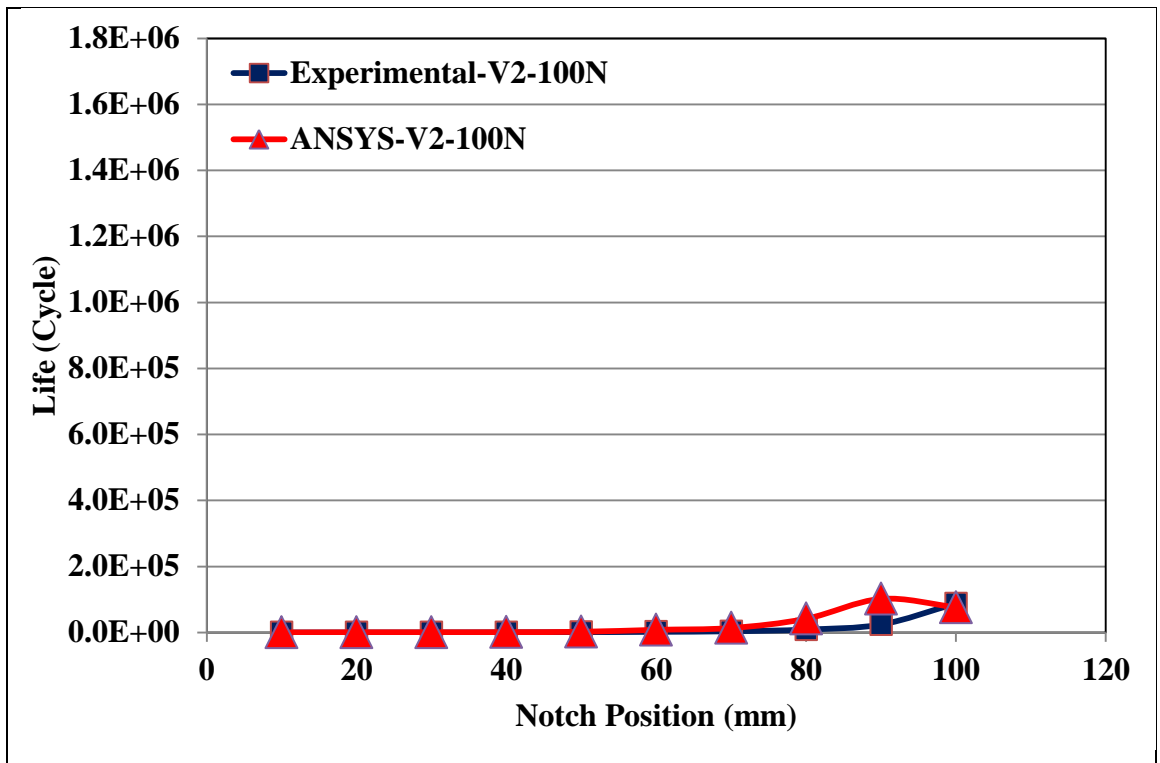


Figure (5.5): Experimental and ANSYS Fatigue Life Change Along the Notch Position When the Notch Depth is (2) mm and the Applied Load is 100N

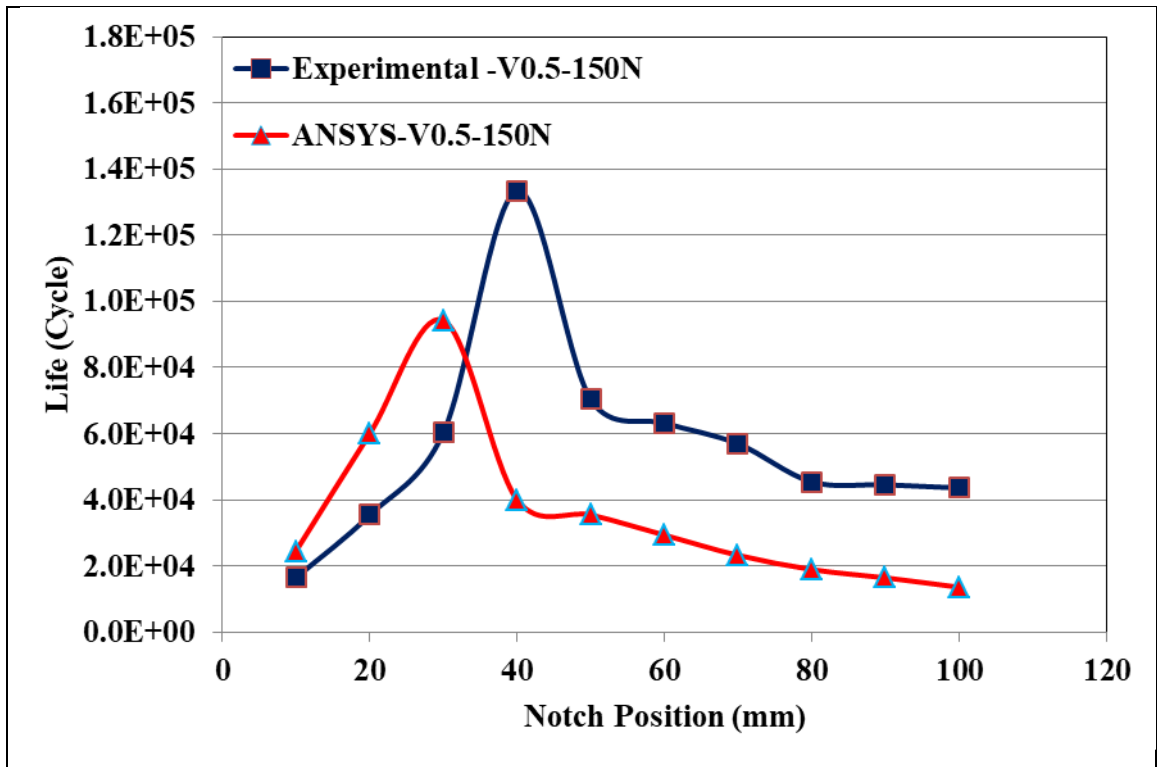


Figure (5.6): Experimental and ANSYS Fatigue Life Change Along the Notch Position When the Notch Depth is (0.5) mm and the Applied Load is 150N

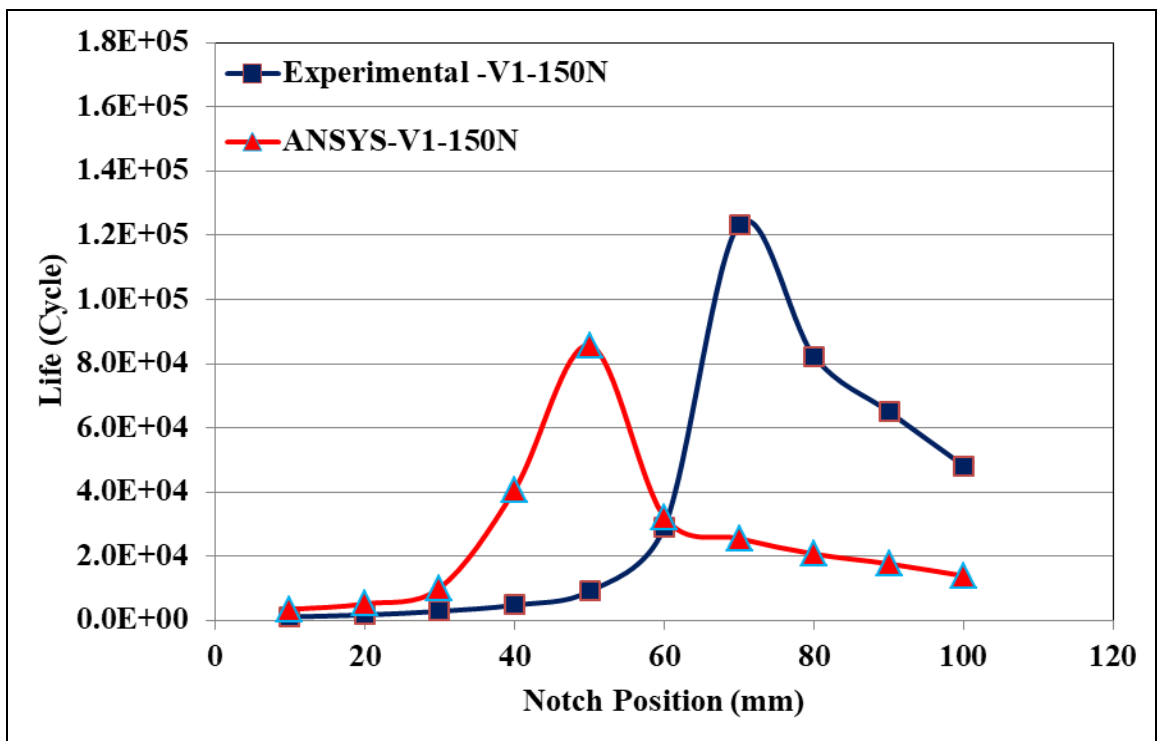


Figure (5.7): Experimental and ANSYS Fatigue Life Change Along the Notch Position When the Notch Depth is (1) mm and the Applied Load is 150N

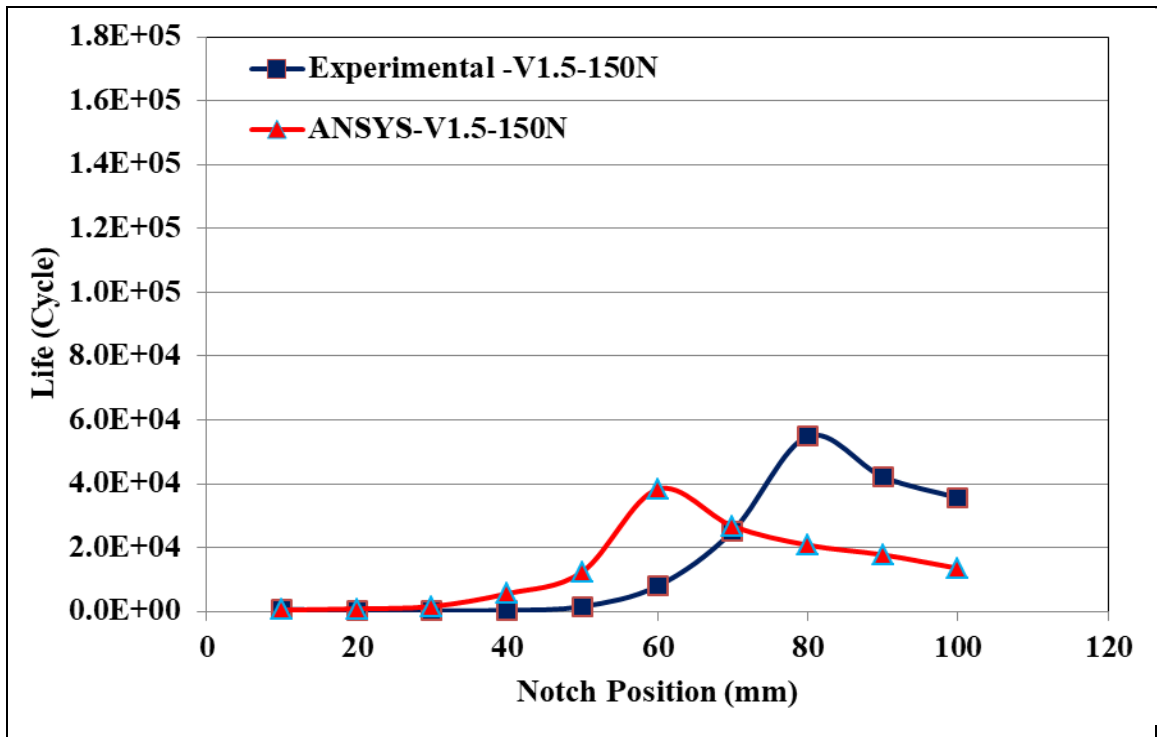


Figure (5.8): Experimental and ANSYS Fatigue Life Change Along the Notch Position When the Notch Depth is (1.5) mm and the Applied Load is 150N

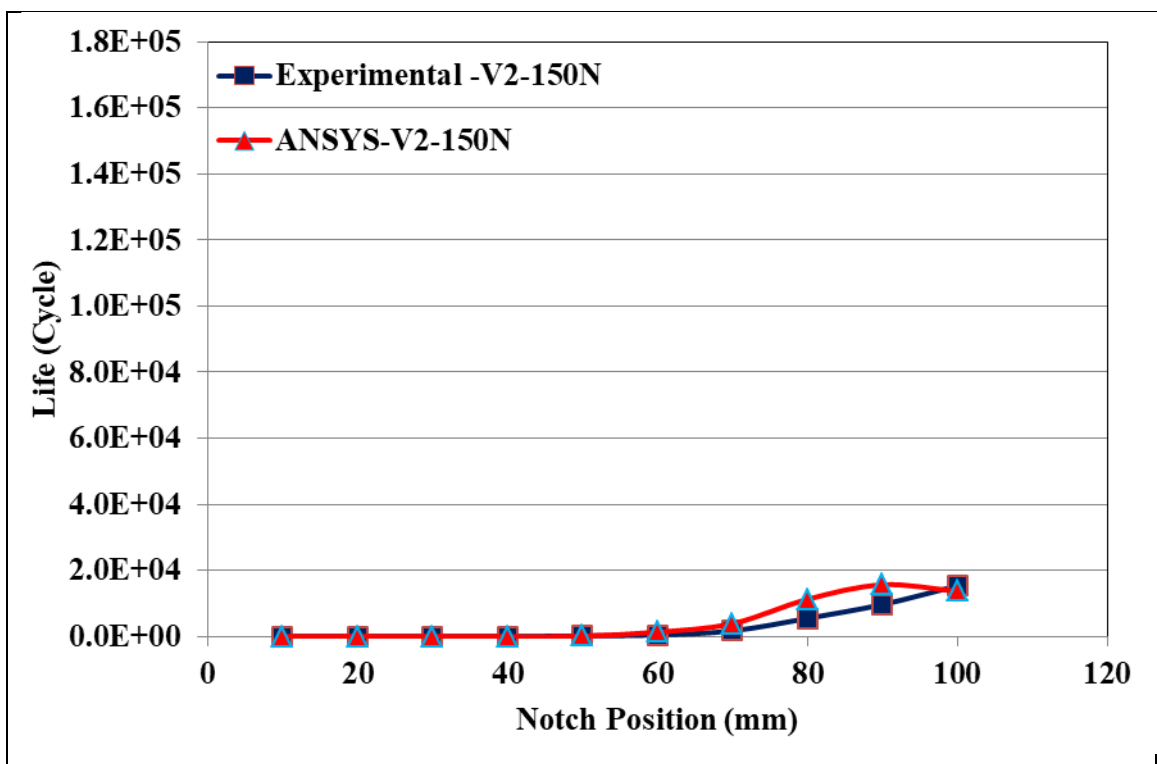


Figure (5.9): Experimental and ANSYS Fatigue Life Change Along the Notch Position When the Notch Depth is (2) mm and the Applied Load is 150N

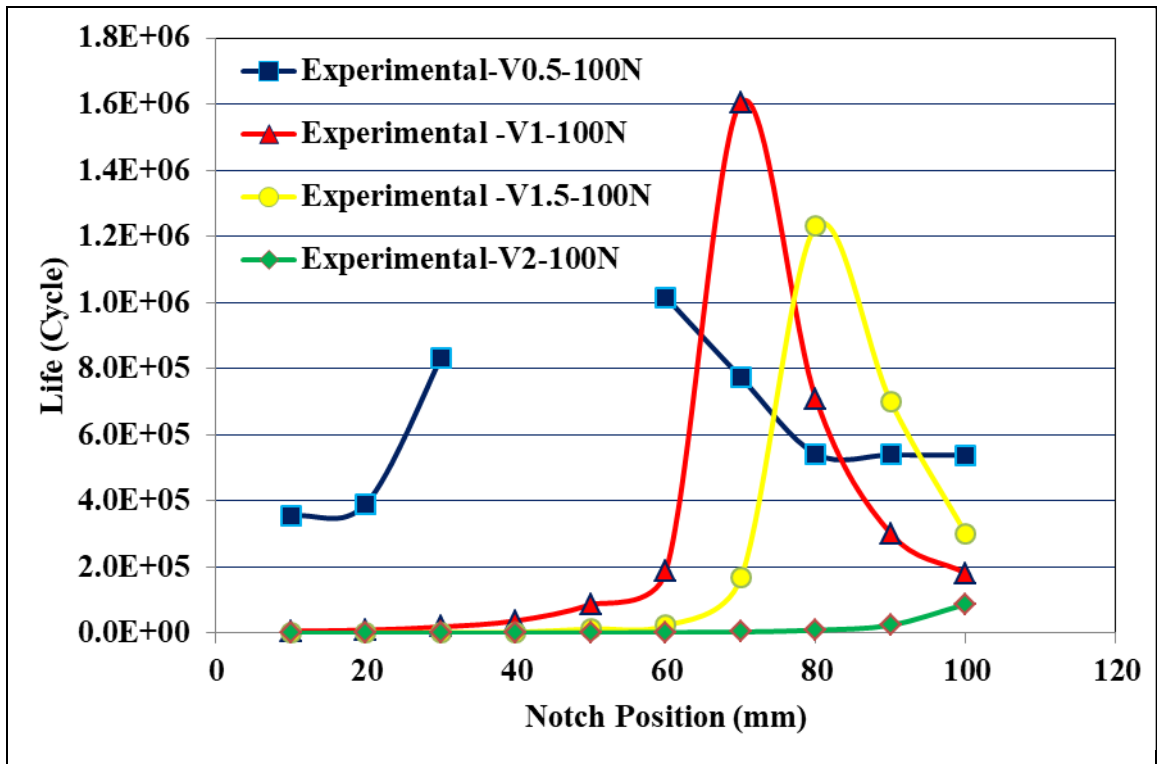


Figure (5.10): Comparison Among Experimental Fatigue Life for Different Notch Positions When the Applied Load is 100N

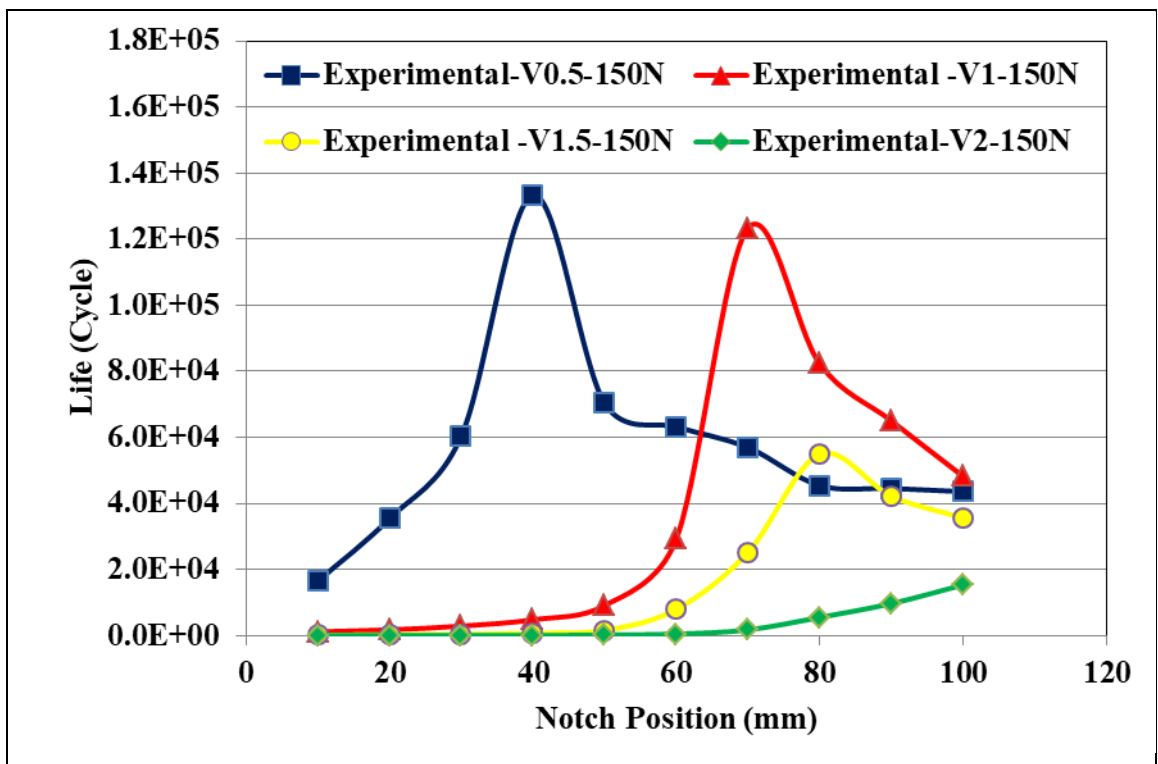


Figure (5.11): Comparison Among Experimental Fatigue Life for Different Notch Positions When the Applied Load is 150N

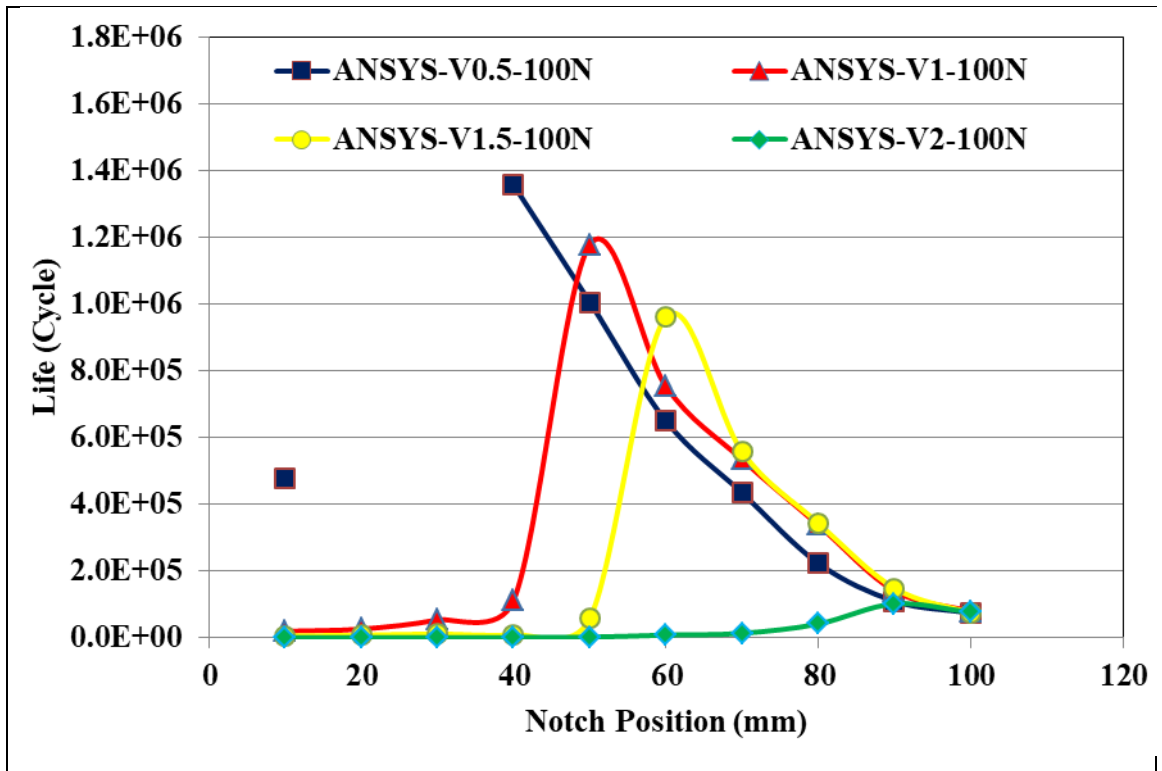


Figure (5.12): Comparison Among ANSYS Fatigue Life for Different Notch Positions When the Applied Load is 100N

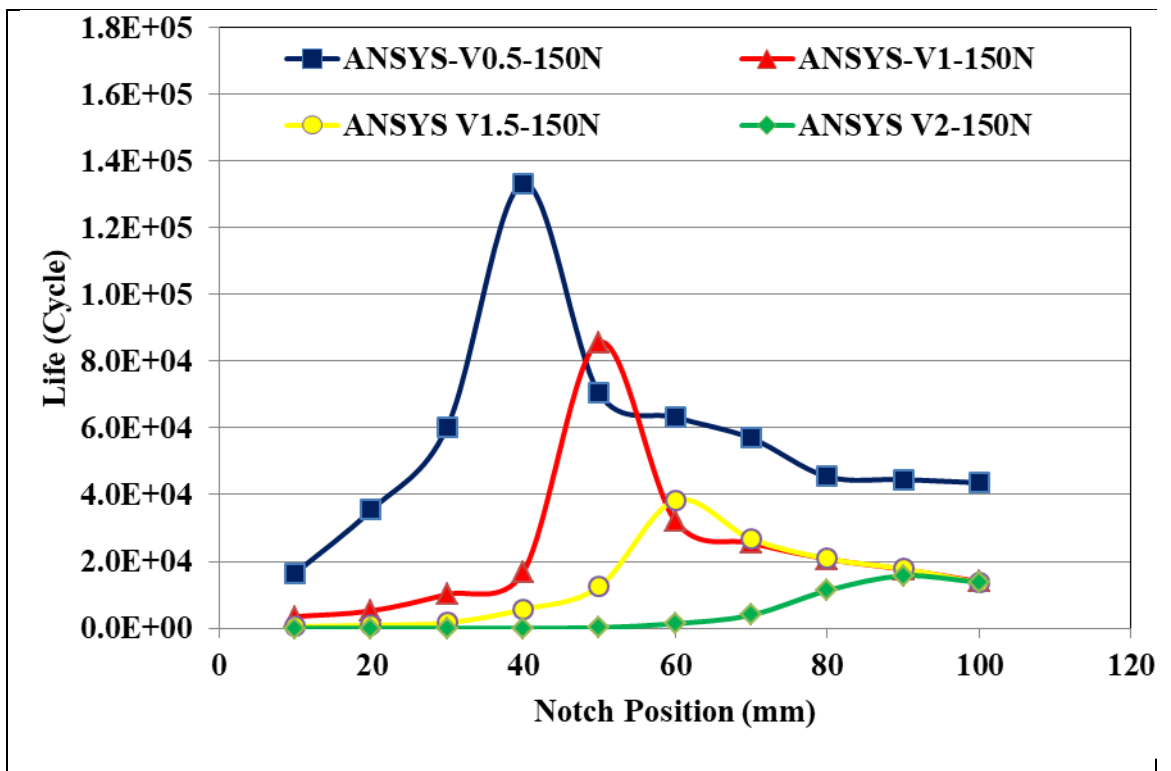


Figure (5.13): Comparison Among ANSYS Fatigue Life for Different Notch Positions When the Applied Load is 150N

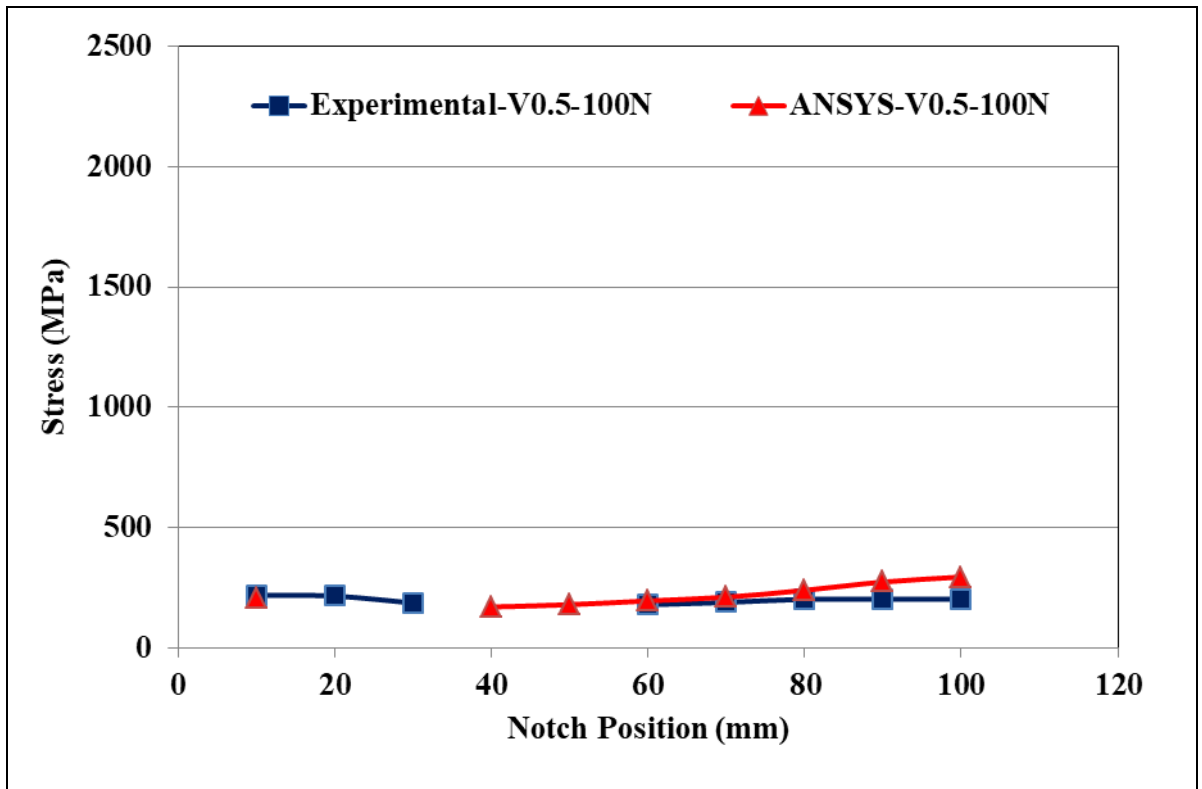


Figure (5.14): Comparison Between Experimental and ANSYS Stresses When the Notch Depth is (0.5) mm and the Applied Load is 100N

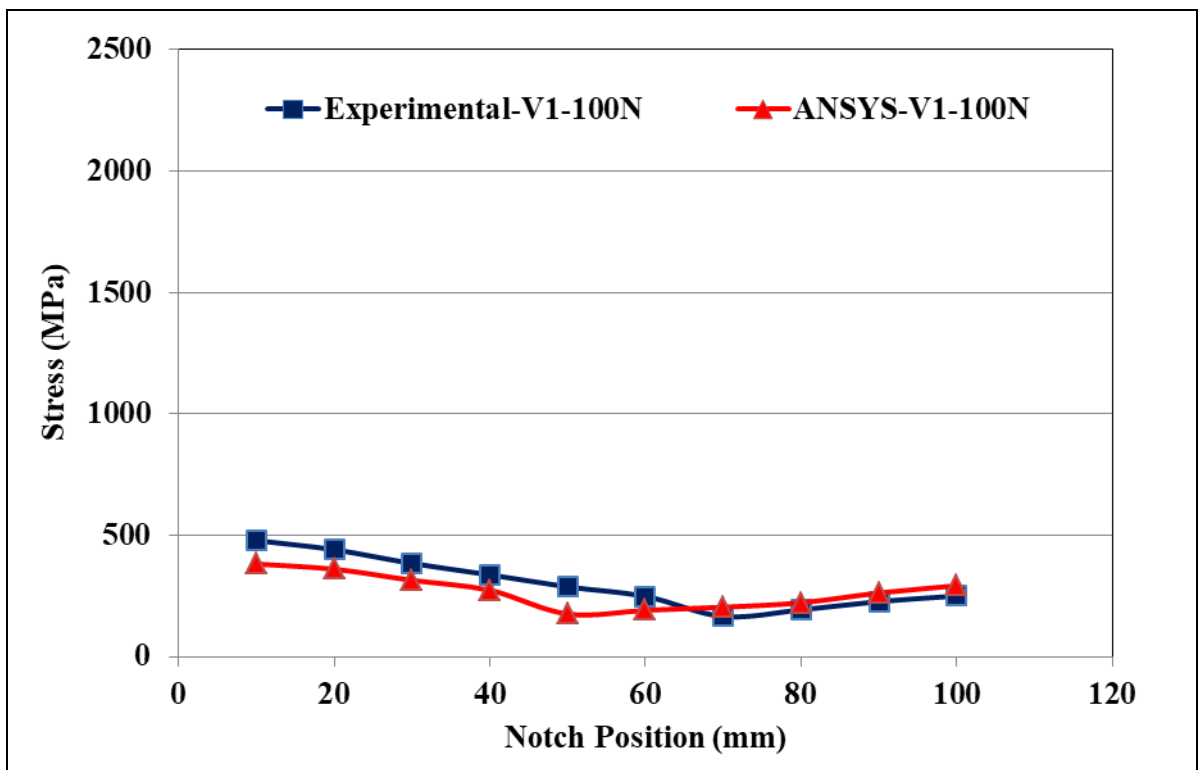


Figure (5.15): Comparison Between Experimental and ANSYS Stresses When the Notch Depth is (1) mm and the Applied Load is 100N

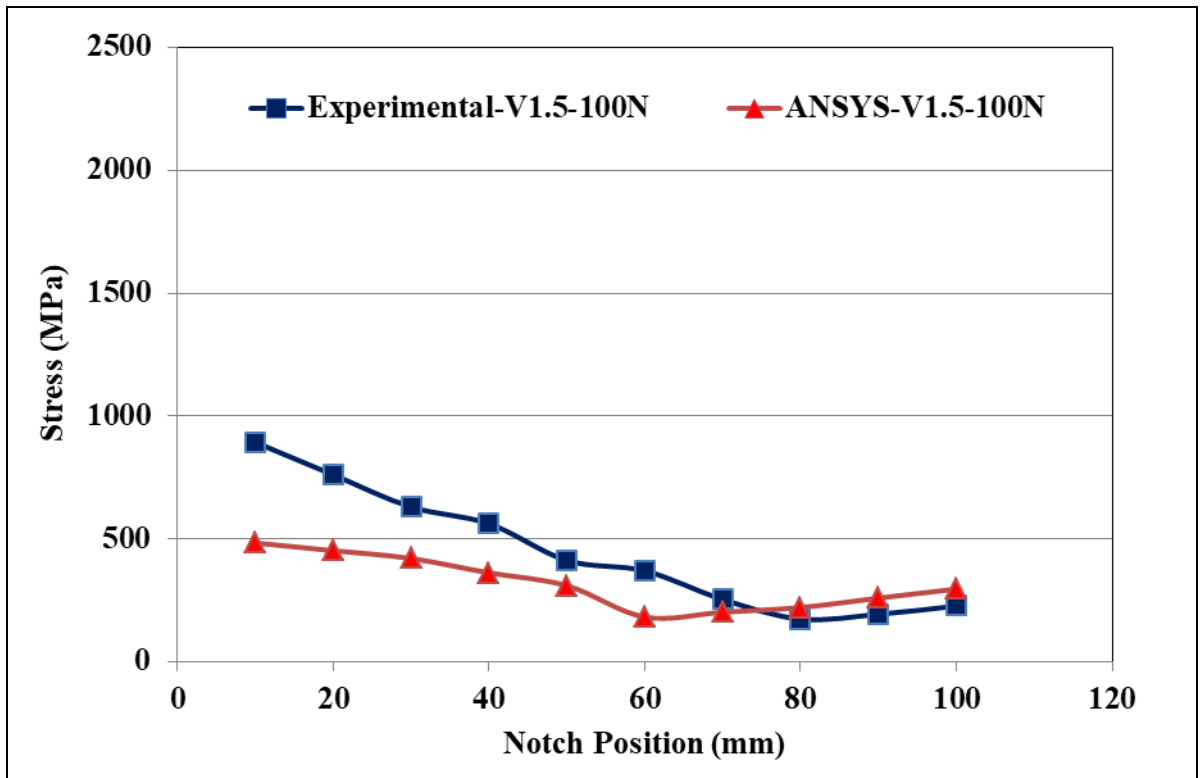


Figure (5.16): Comparison Between Experimental and ANSYS Stresses When the Notch Depth is (1.5) mm and the Applied Load is 100N

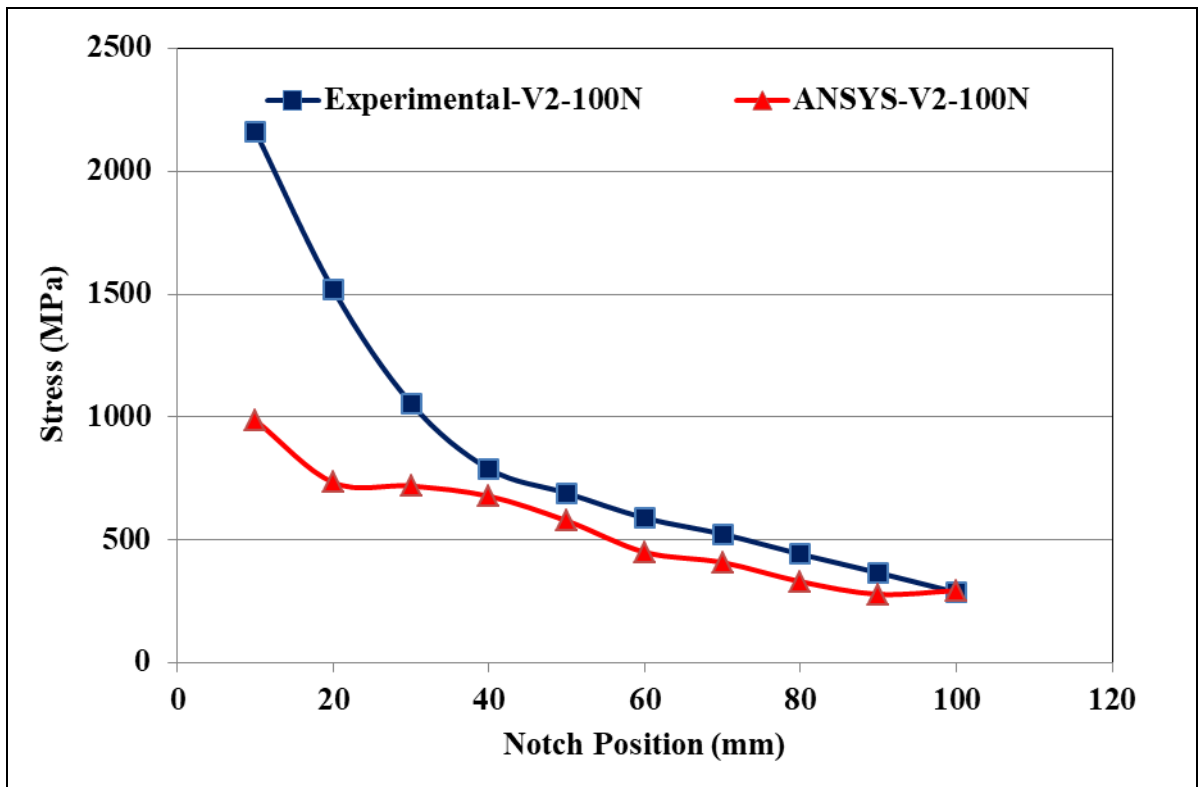


Figure (5.17): Comparison Between Experimental and ANSYS Stresses When the Notch Depth is (2) mm and the Applied Load is 100N

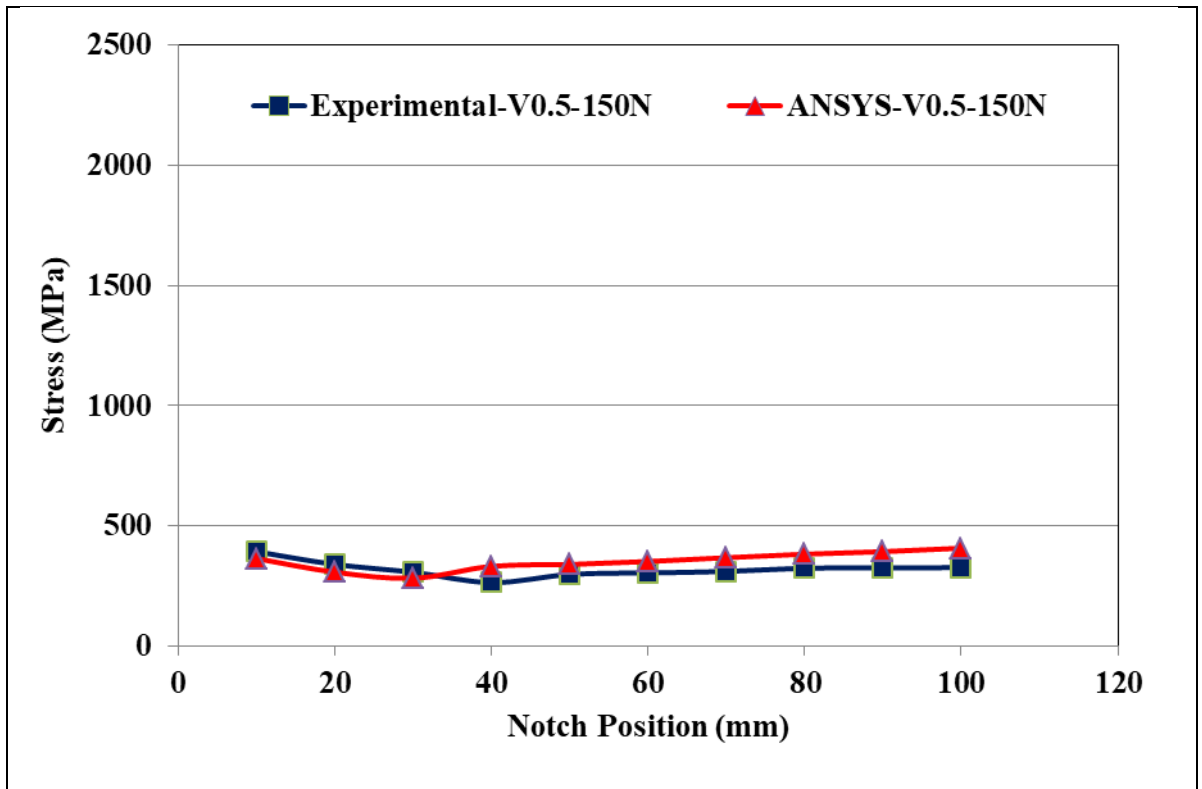


Figure (5.18): Comparison Between Experimental and ANSYS Stresses When the Notch Depth is (0.5) mm and the Applied Load is 150N

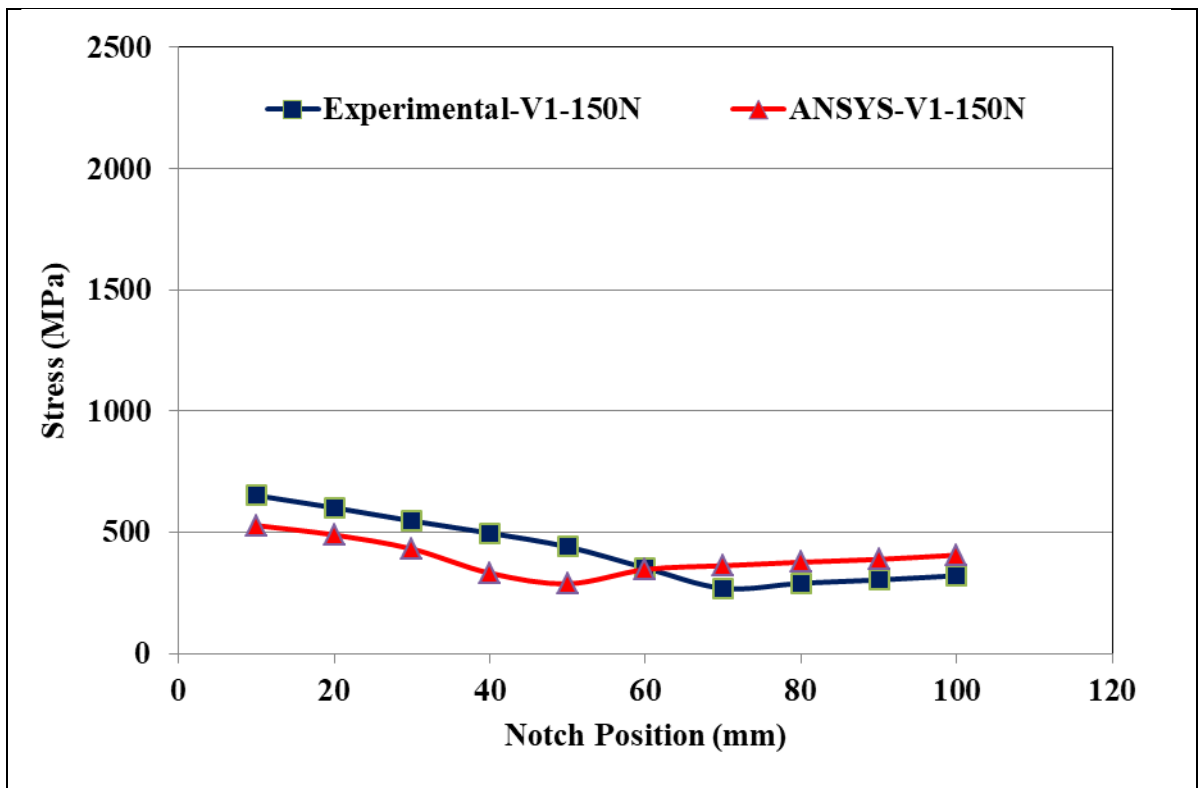


Figure (5.19): Comparison Between Experimental and ANSYS Stresses When the Notch Depth is (1) mm and the Applied Load is 150N

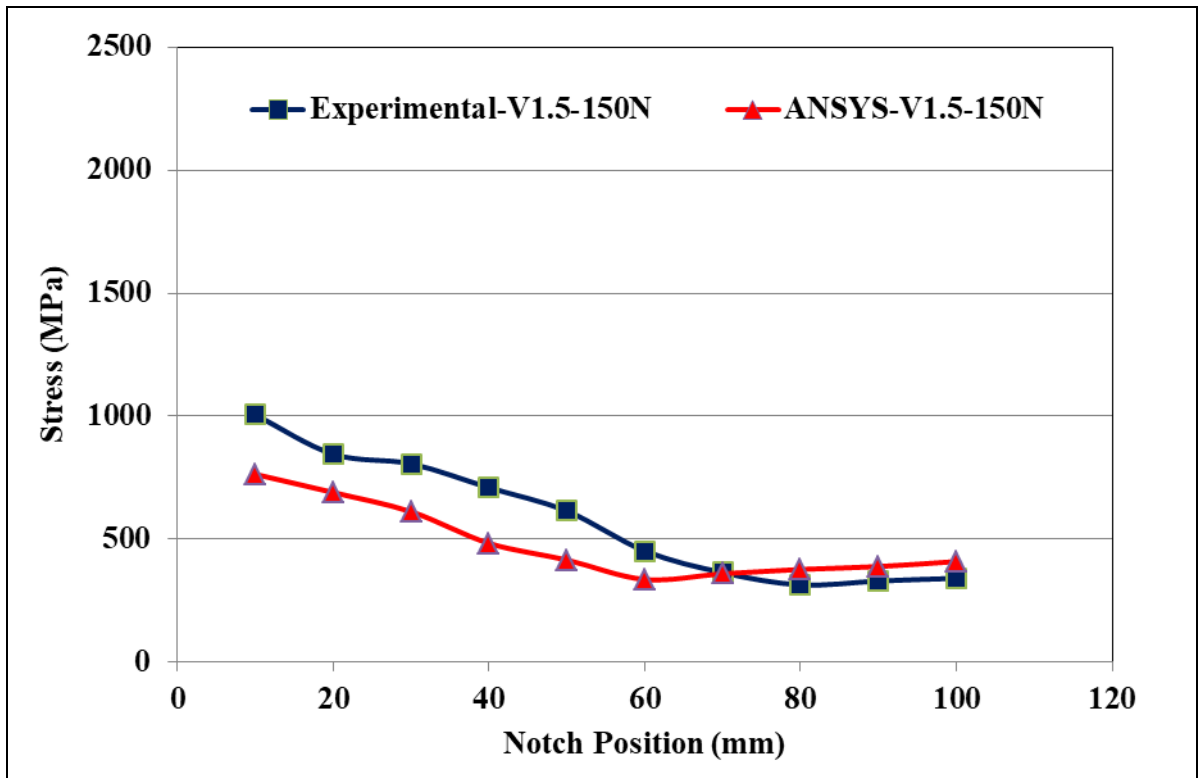


Figure (5.20): Comparison Between Experimental and ANSYS Stresses When the Notch Depth is (1.5) mm and the Applied Load is 150N

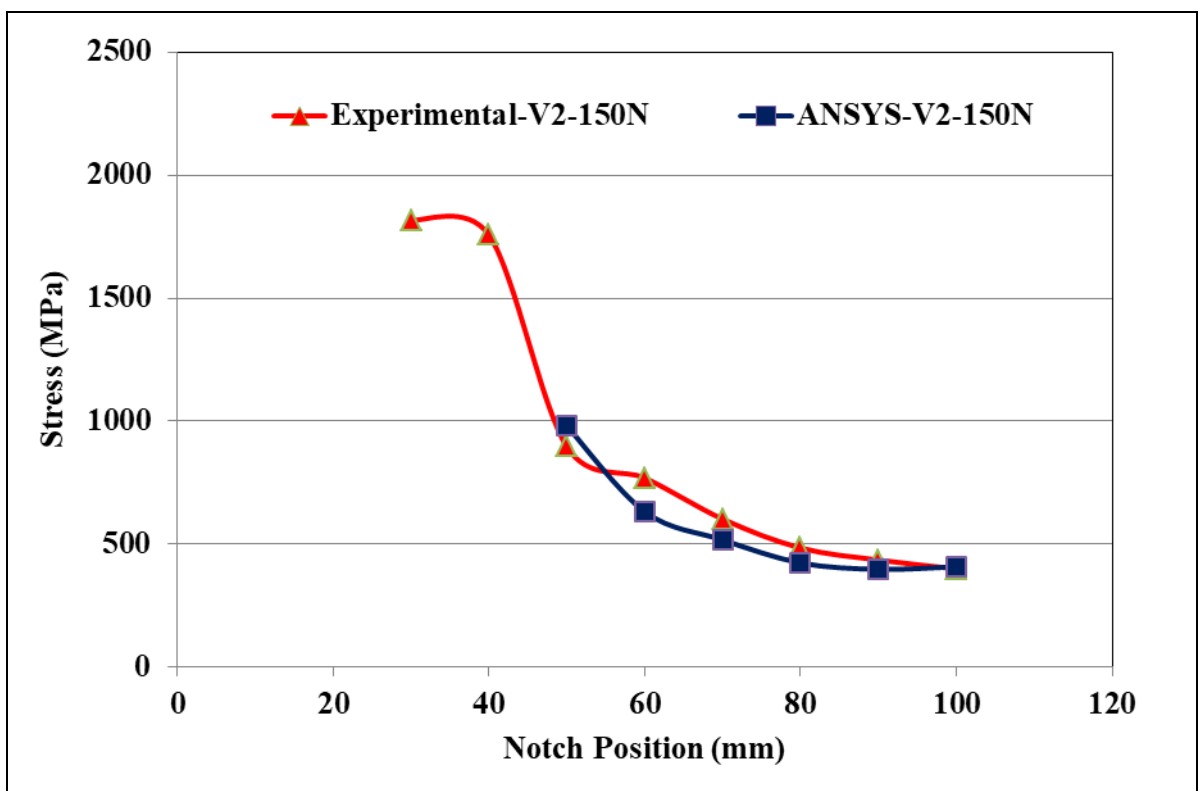


Figure (5.21): Comparison Between Experimental and ANSYS Stresses When the Notch Depth is (2) mm and the Applied Load is 150N

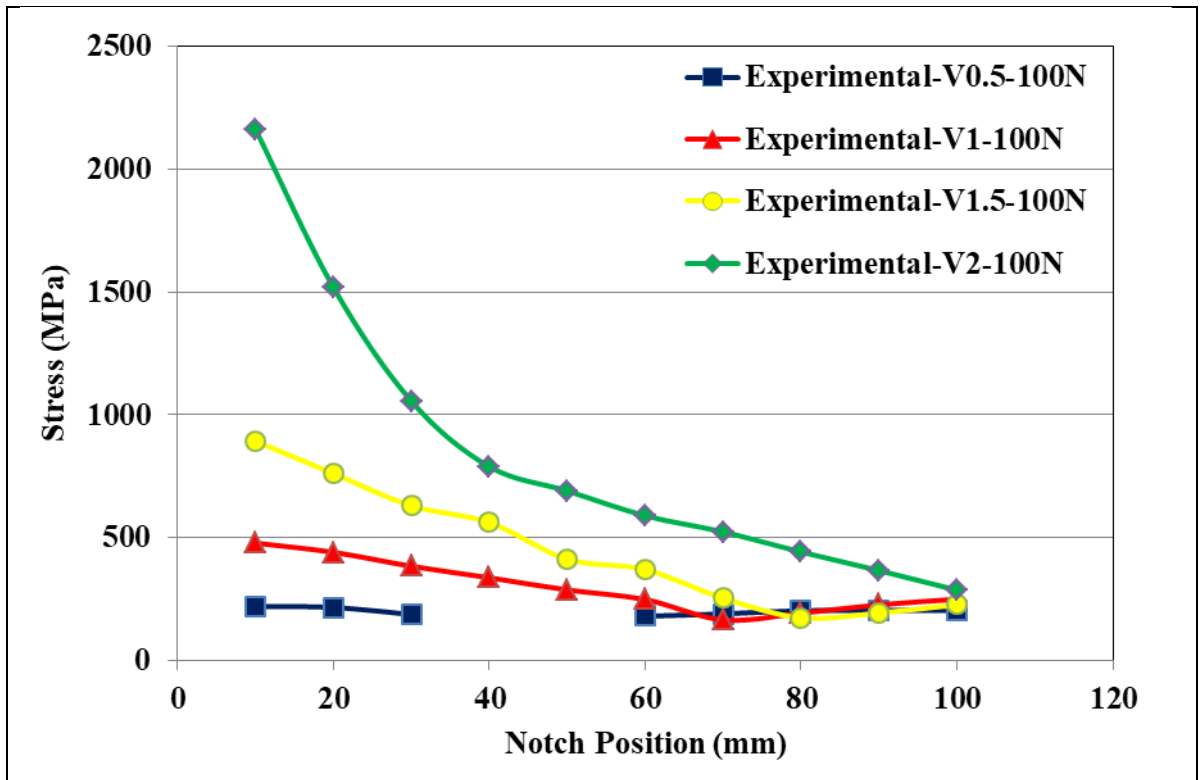


Figure (5.22): Comparison Among Experimental Stresses for Different Notch Depth When the Applied Load is 100N

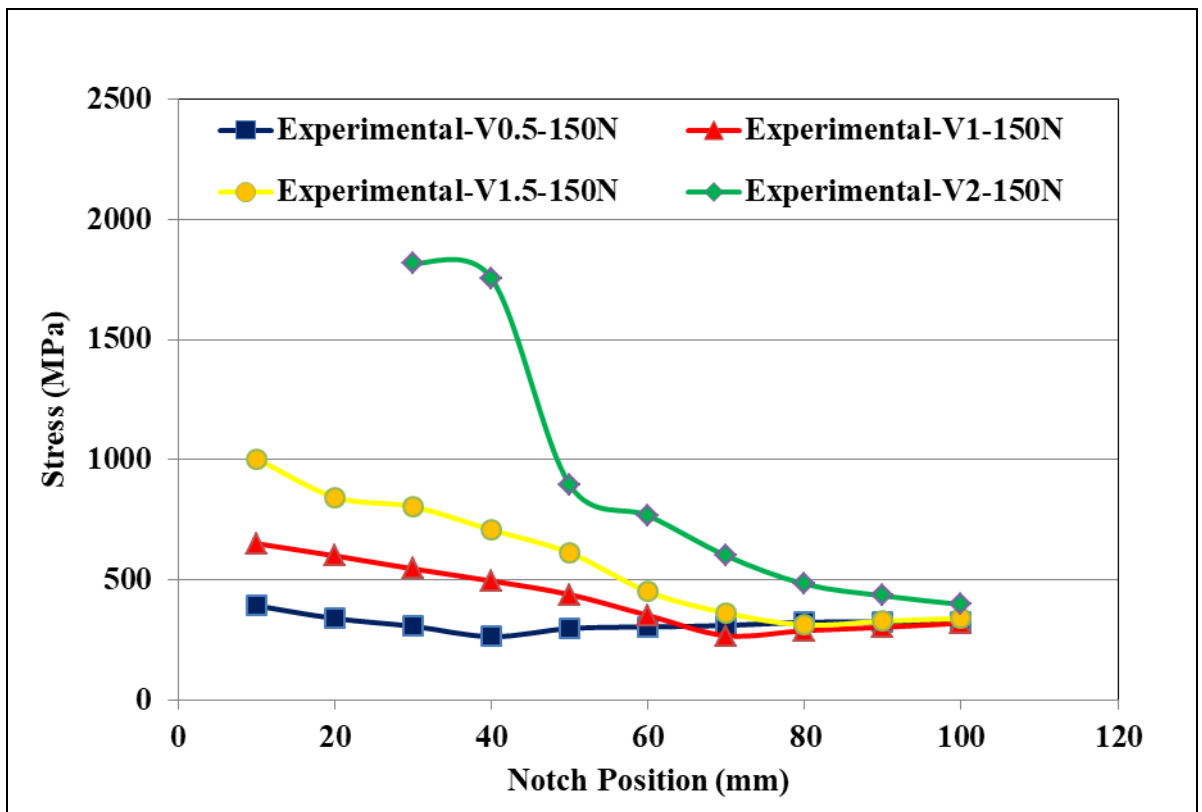


Figure (5.23): Comparison Among Experimental Stresses for Different Notch Depth When the Applied Load is 150N

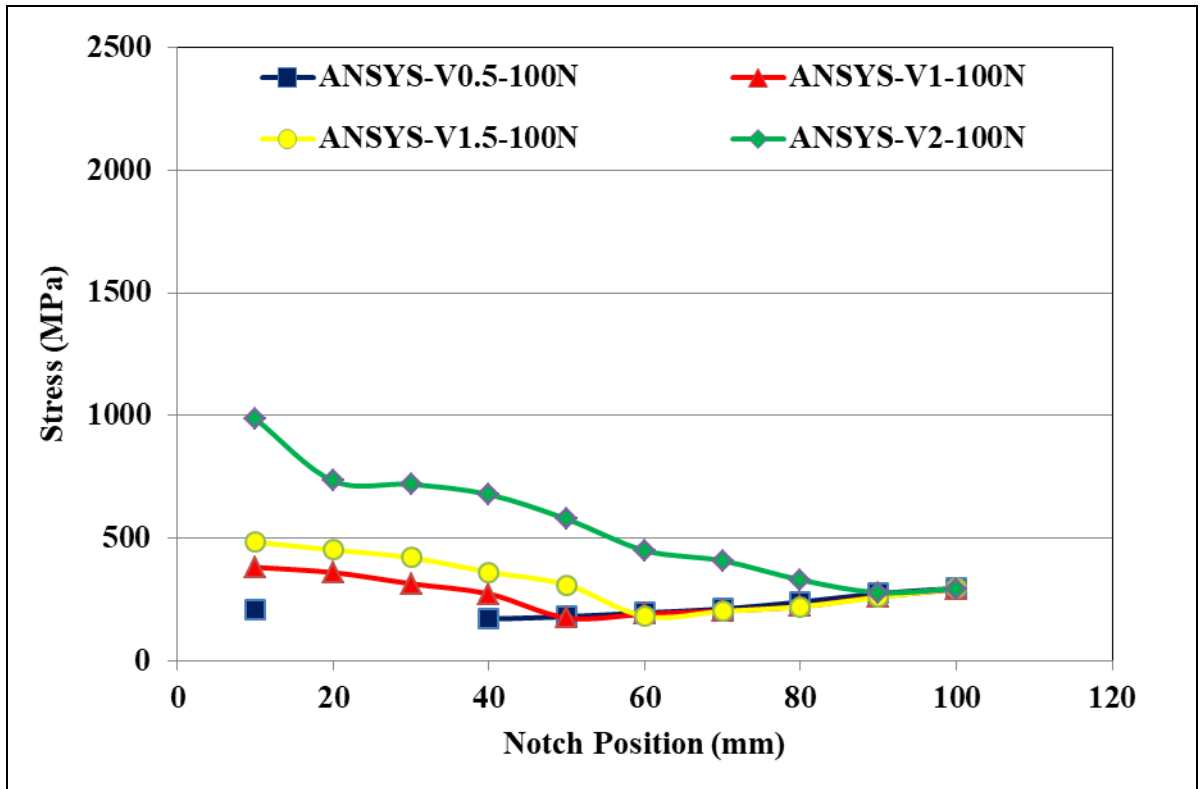


Figure (5.24): Comparison Among ANSYS Stresses for Different Notch Depth When the Applied Load is 100N

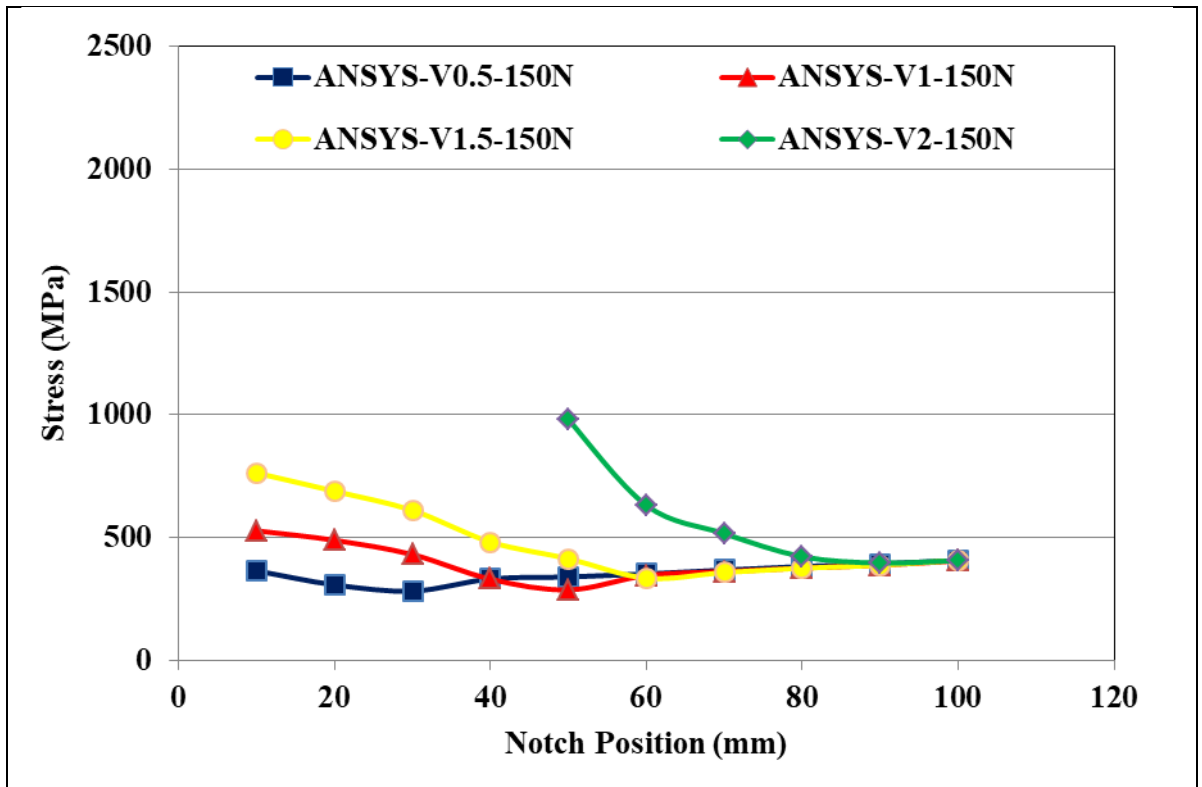
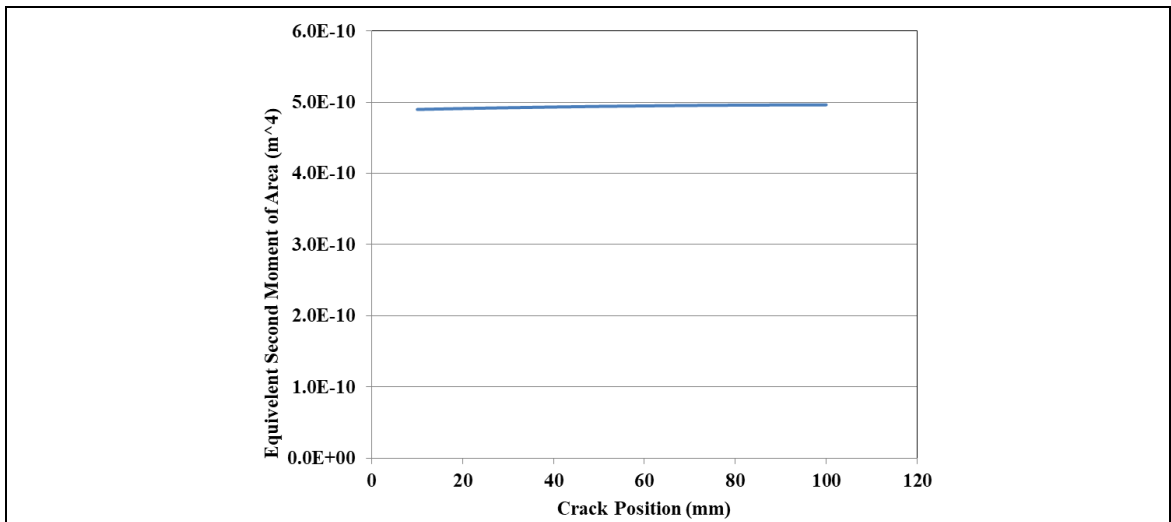
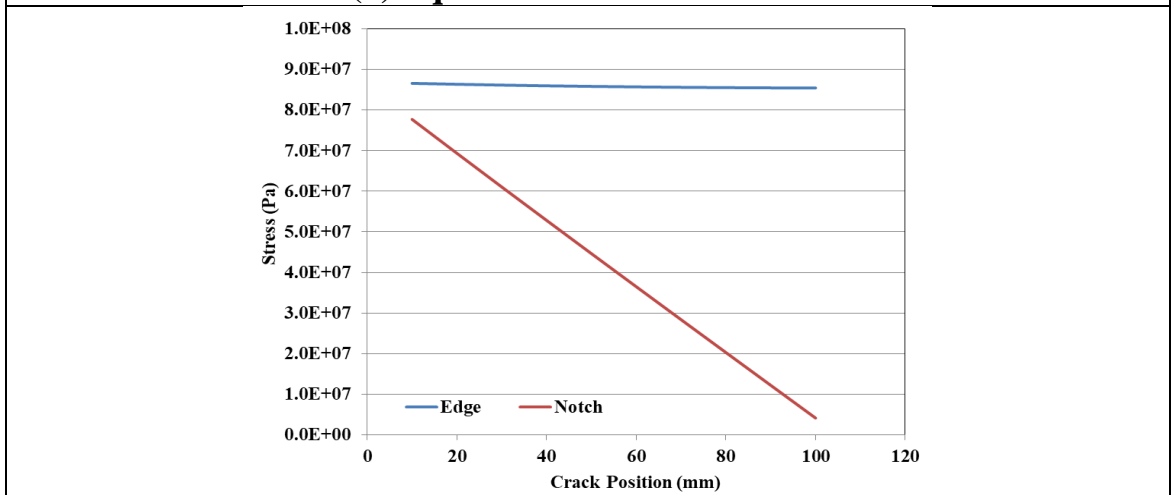


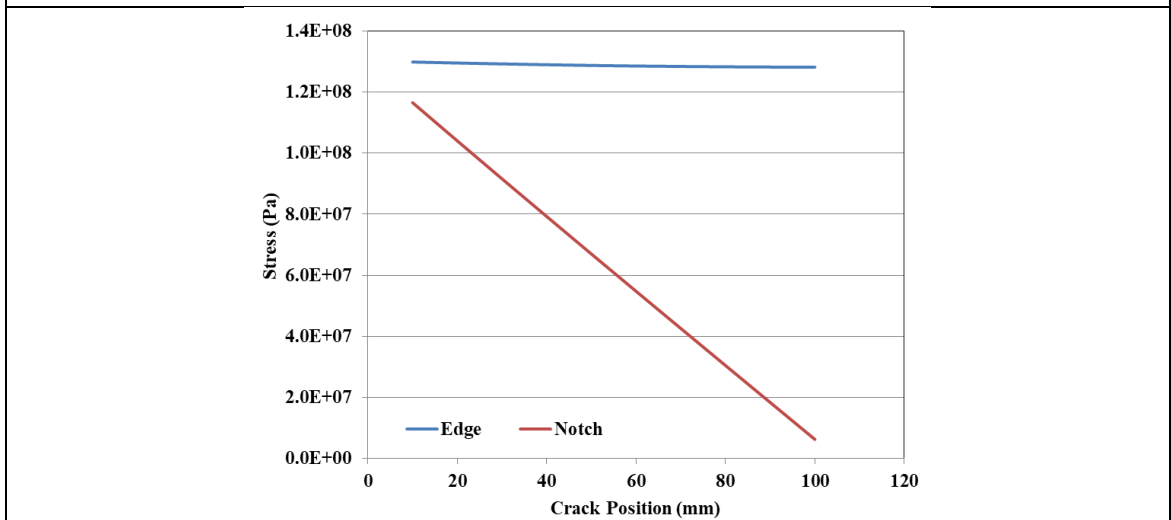
Figure (5.25): Comparison Among ANSYS Stresses for Different Notch Depth When the Applied Load is 150N



(a) Equivalent Second Moment of Area



(b) Stress Due to Equivalent Second Moment of Area When the Load is 100 N



(c) Stress Due to Equivalent Second Moment of Area When the Load is 150 N

Figure (5.26): Equivalent Second Moment of Area and Stress Due to Equivalent Second Moment of Area When the Depth of Notch is (0.5) mm

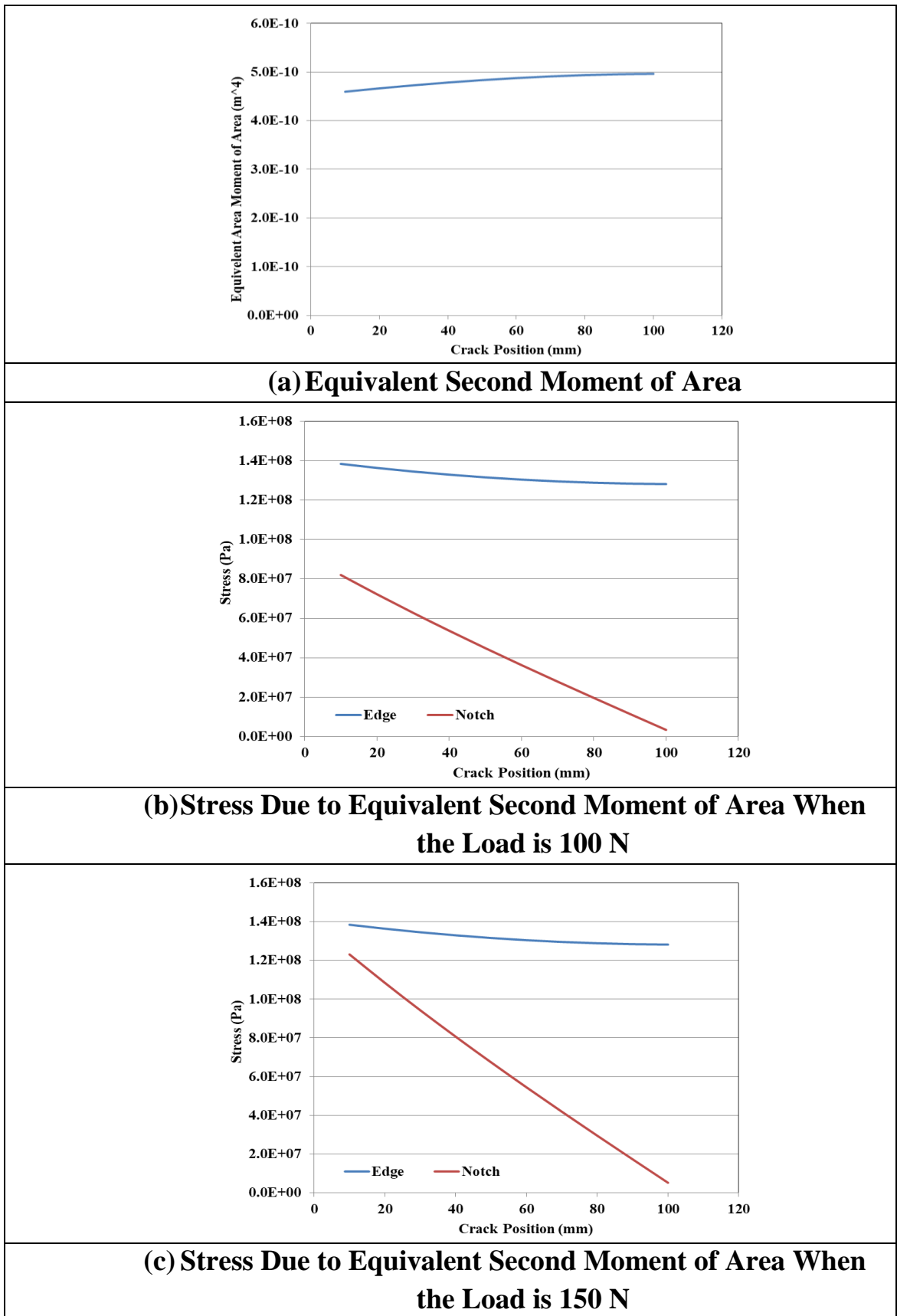
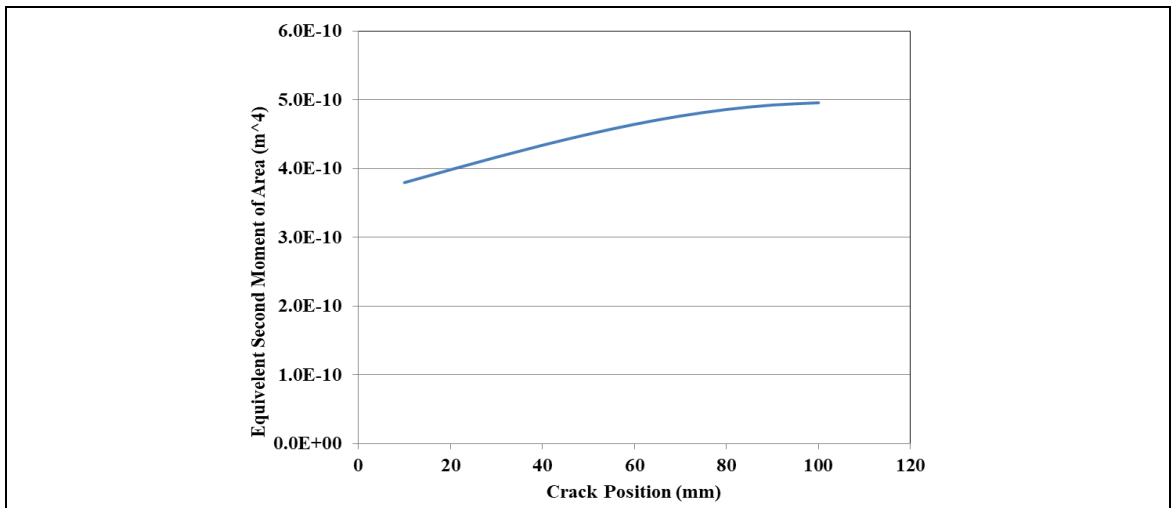
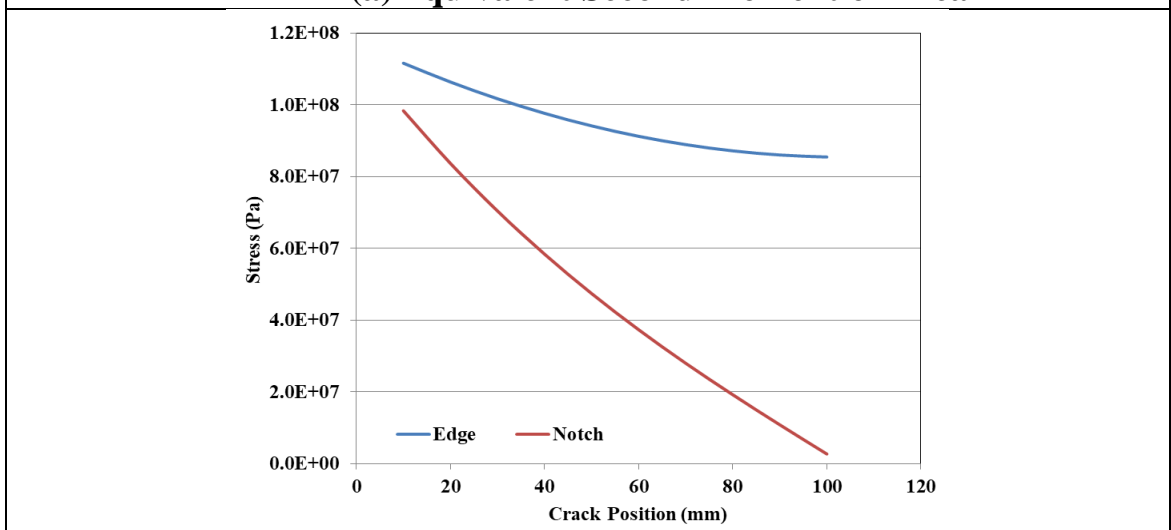


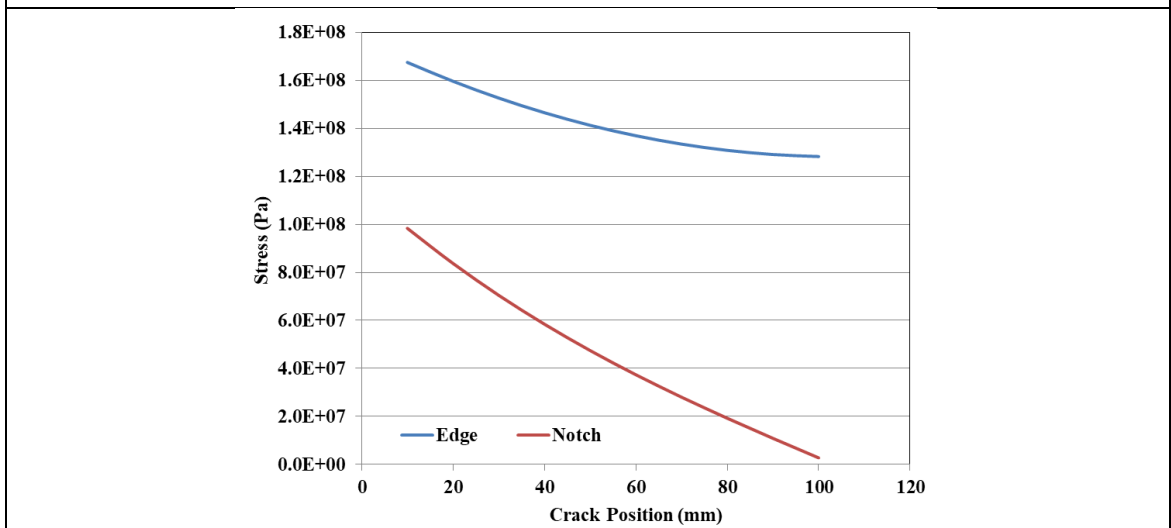
Figure (5.27): Equivalent Second Moment of Area and Stress Due to Equivalent Second Moment of Area When the Depth of Notch is (1) mm



(a) Equivalent Second Moment of Area

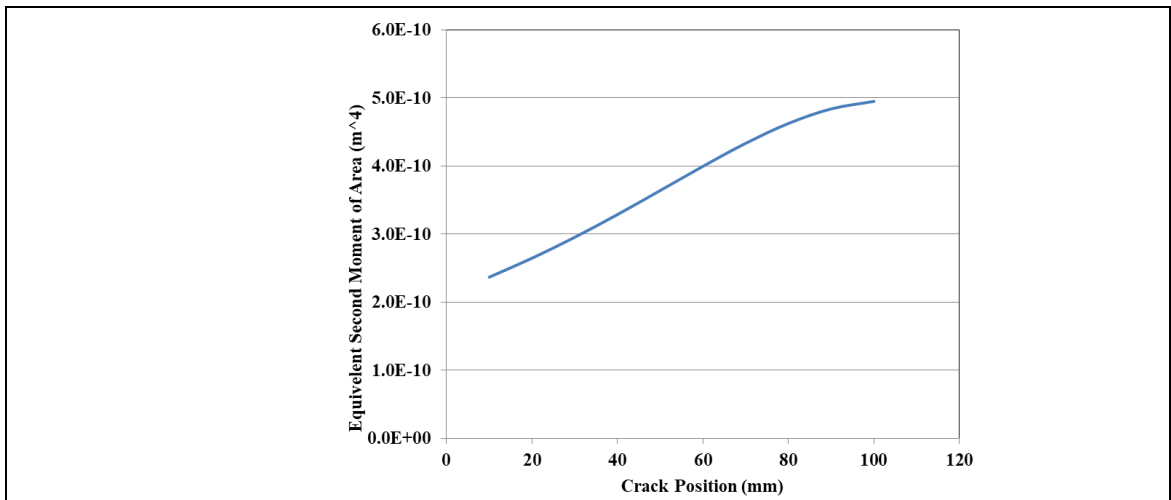


(b) Stress Due to Equivalent Second Moment of Area When the Load is 100 N

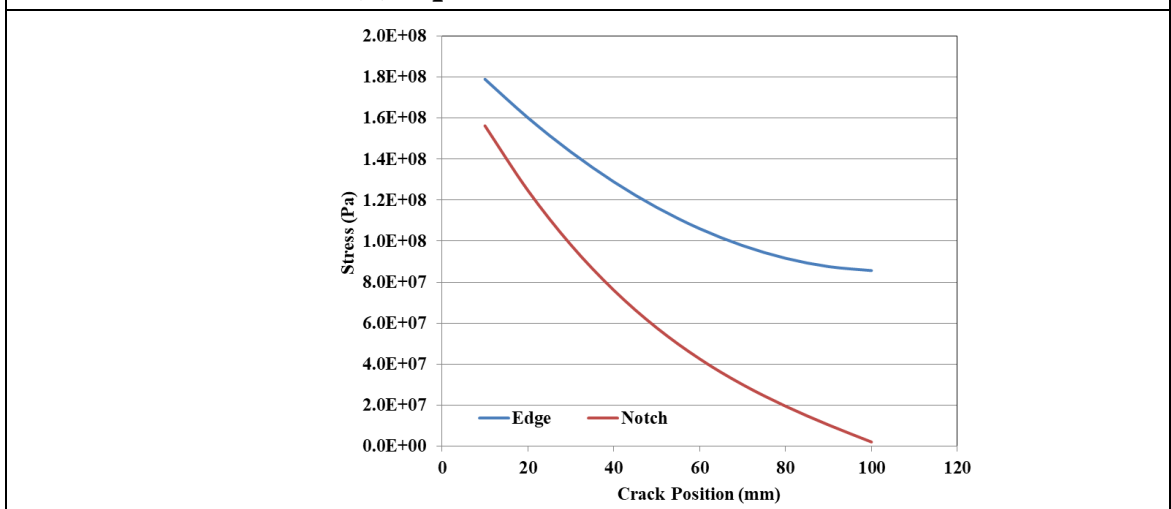


(c) Stress Due to Equivalent Moment of Inertia When the Load is 150 N

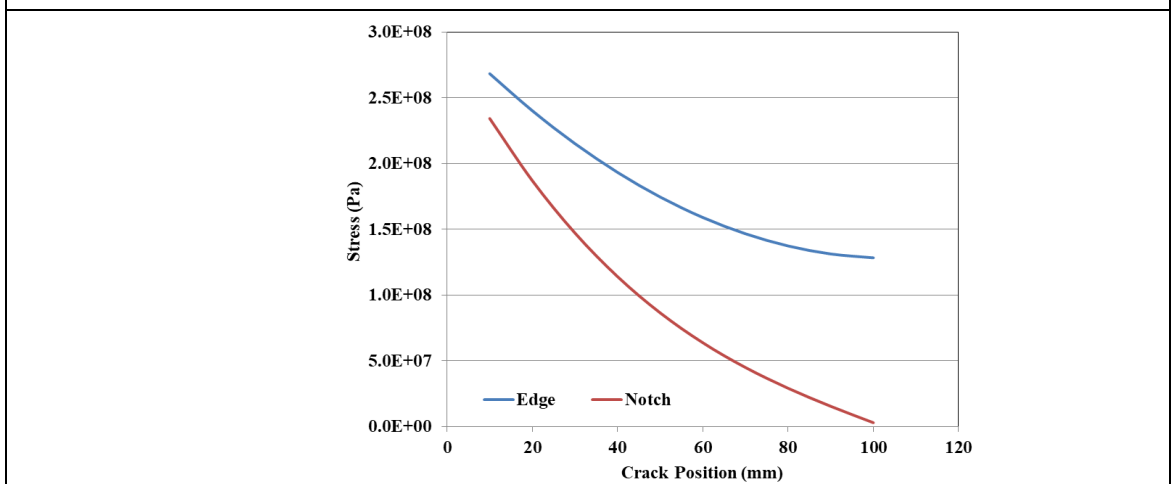
Figure (5.28): Equivalent Second Moment of Area and Stress Due to Equivalent Second Moment of Area When the Depth of Notch is 1.5 mm



(a) Equivalent Second Moment of Area



(b) Stress Due to Equivalent Second Moment of Area When the Load is 100 N



(c) Stress Due to Equivalent Second Moment of Area When the Load is 150 N

Figure (5.29): Equivalent Second Moment of Area and Stress Due to Equivalent Second Moment of Area When the Depth of Notch is (2) mm

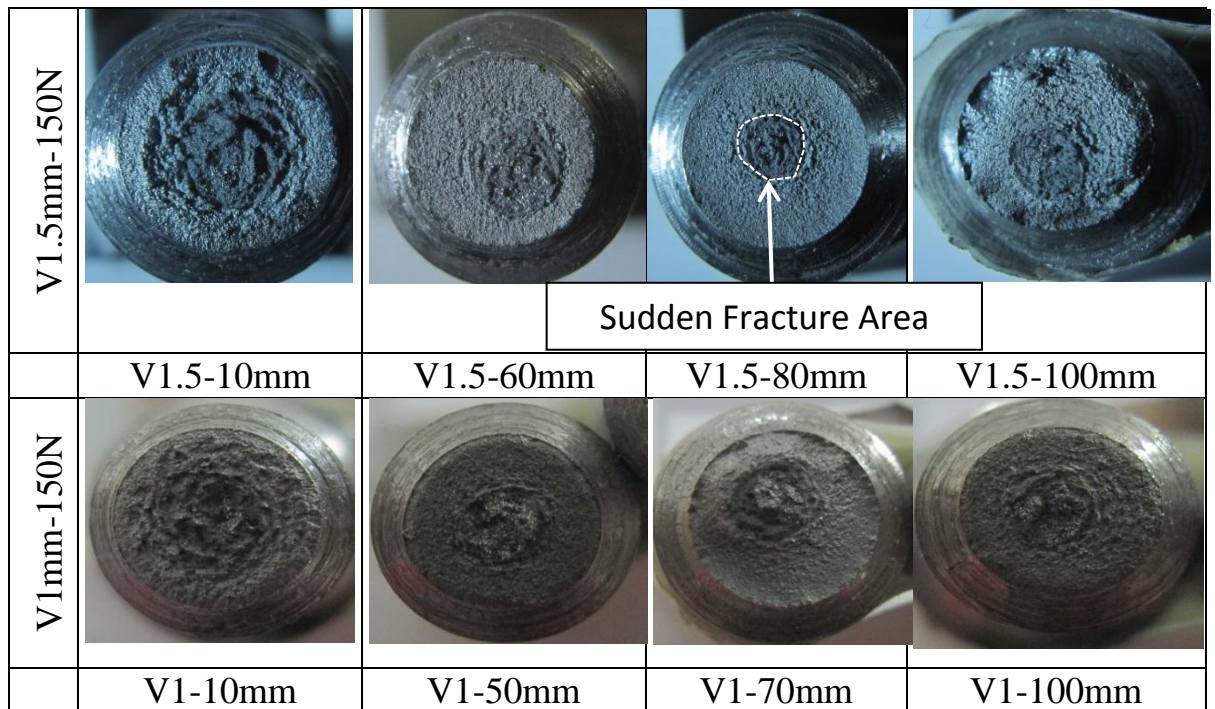


Figure (5.30): Fracture Surface Test

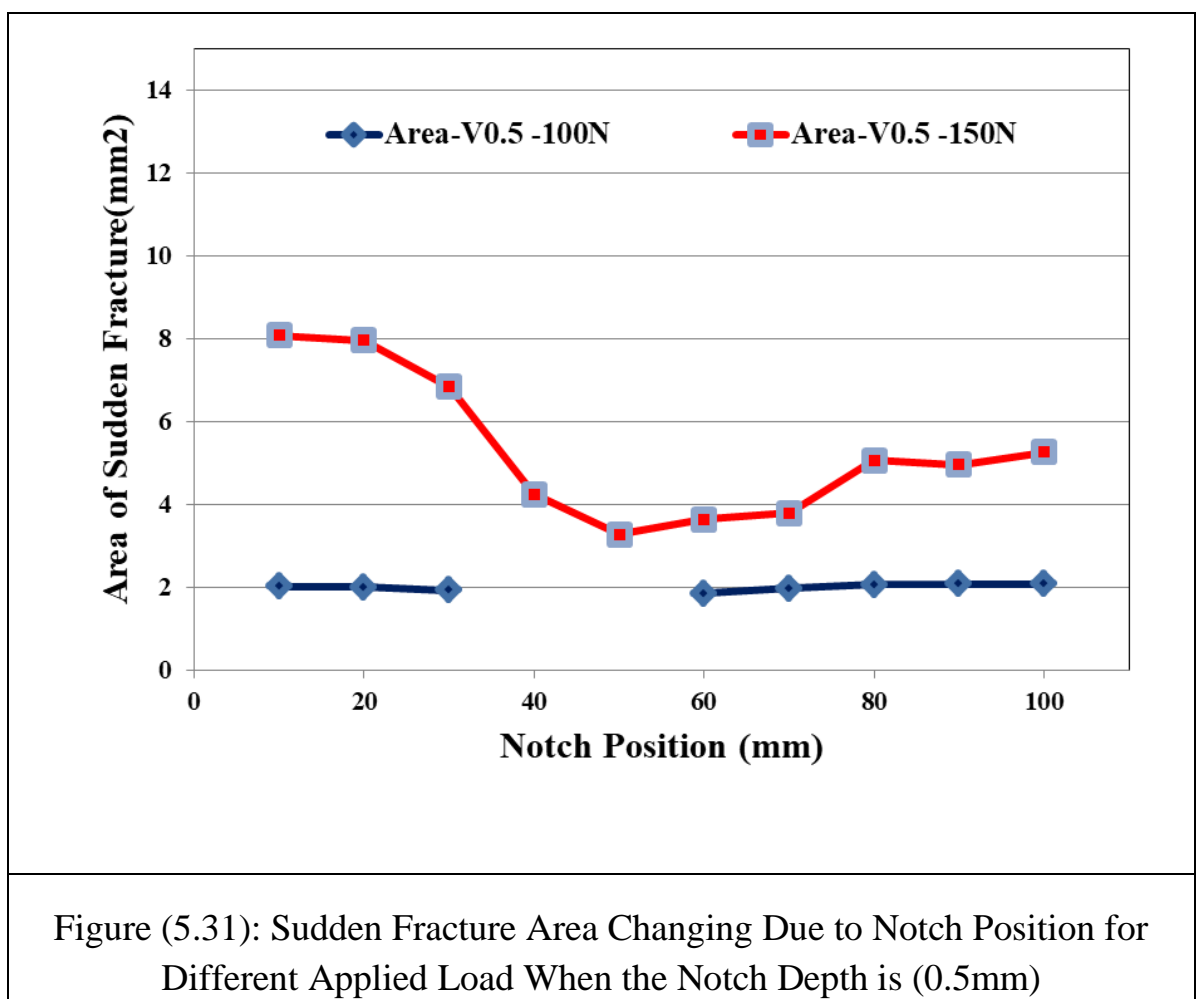


Figure (5.31): Sudden Fracture Area Changing Due to Notch Position for Different Applied Load When the Notch Depth is (0.5mm)

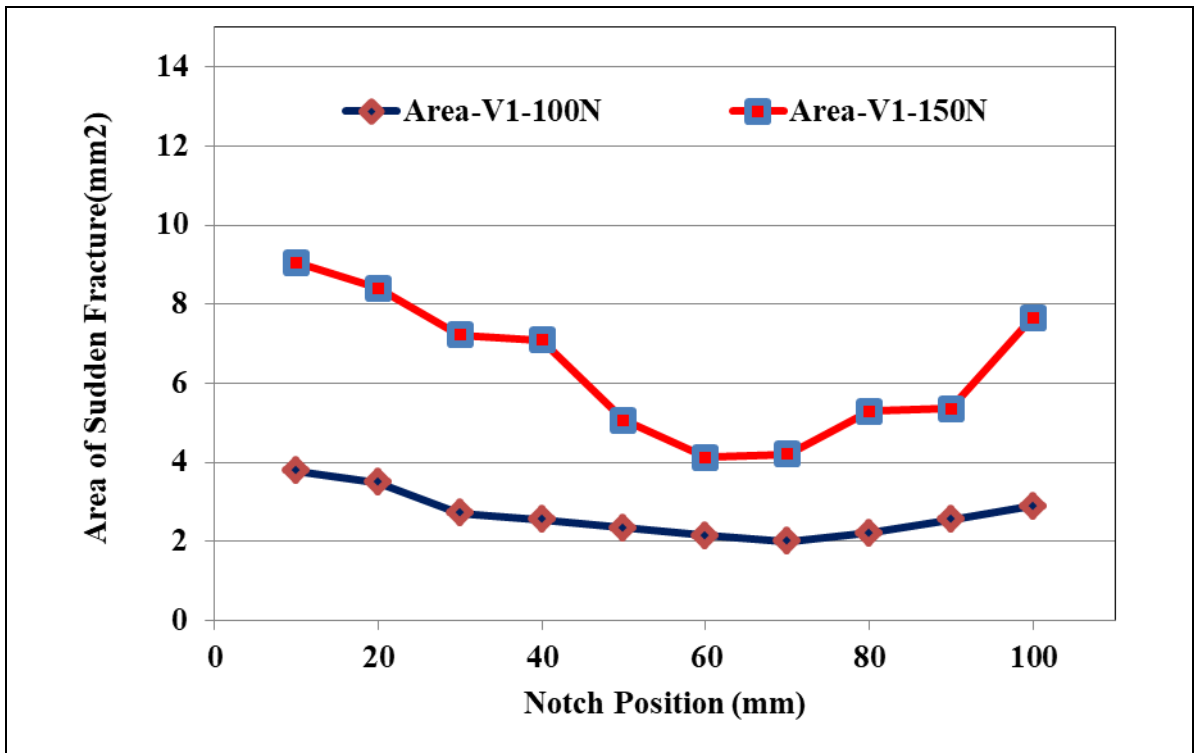


Figure (5.32): Sudden Fracture Area Changing Due to Notch Position for Different Applied Load When the Notch Depth is (1mm)

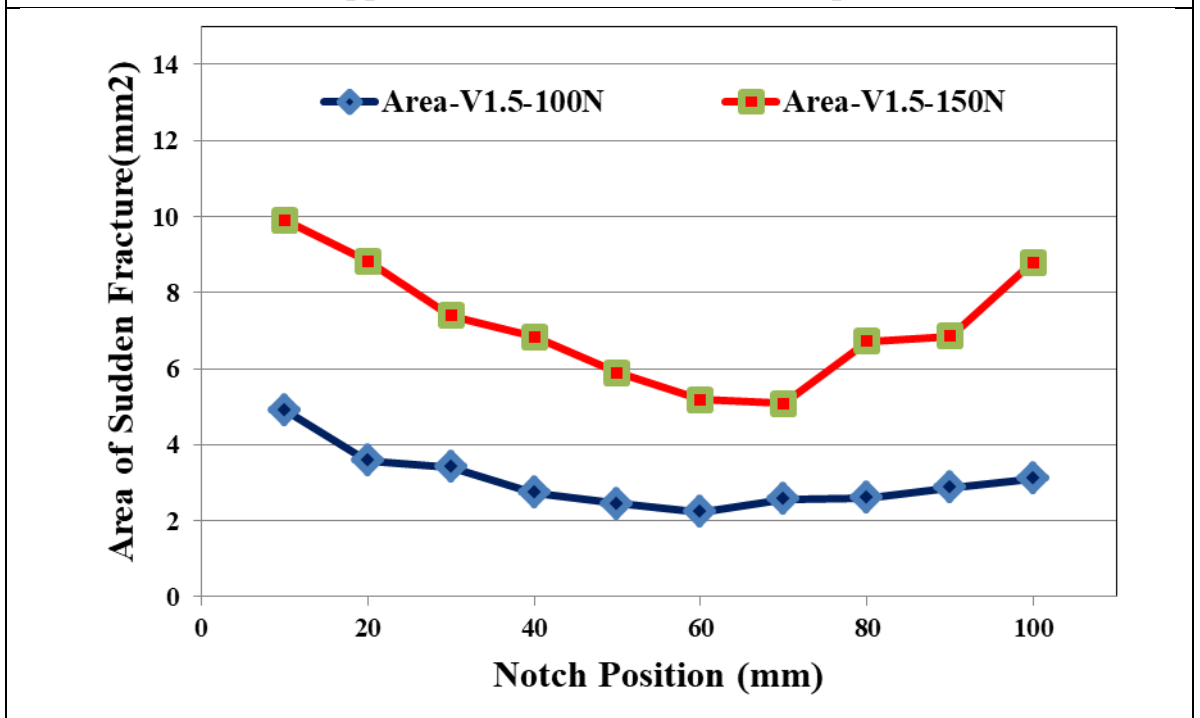


Figure (5.33): Sudden Fracture Area Changing Due to Notch Position for Different Applied Load When the Notch Depth is (1.5mm)

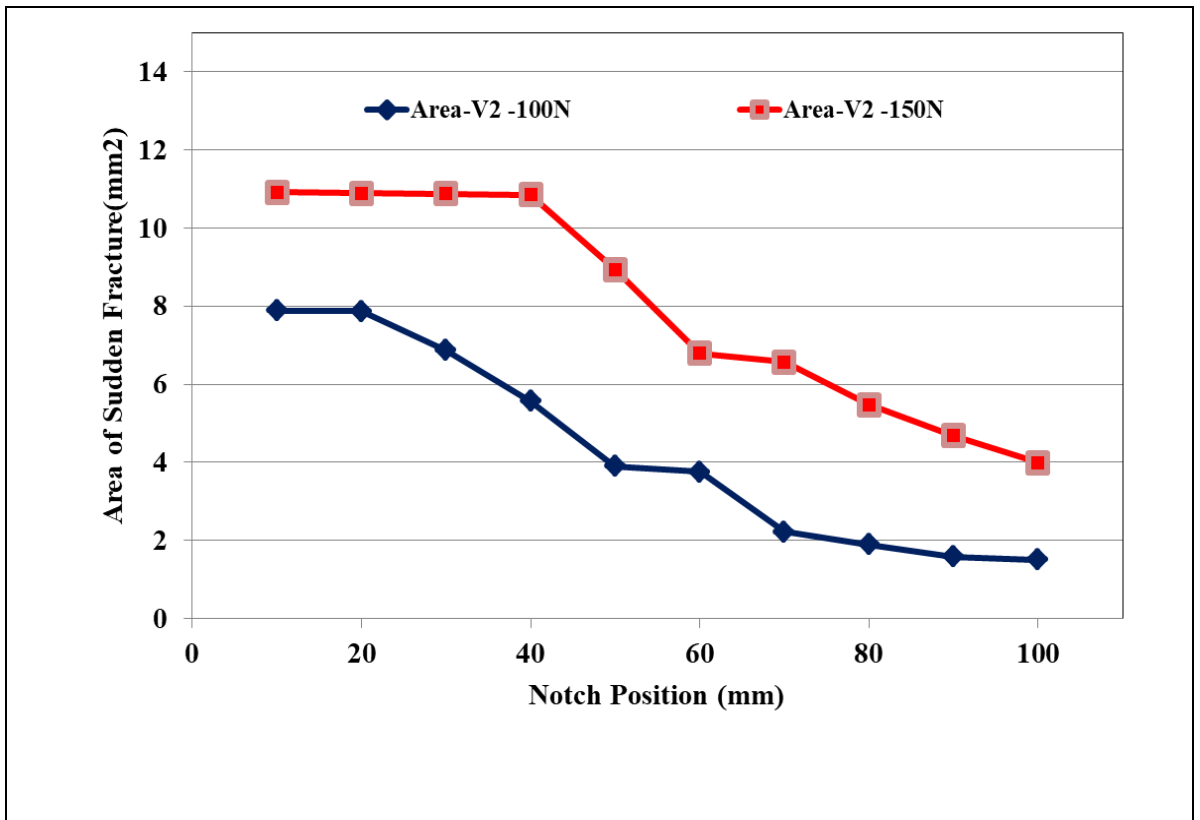


Figure (5.34): Sudden Fracture Area Changing Due to Notch Position for Different Applied Load When the Notch Depth is (2mm)

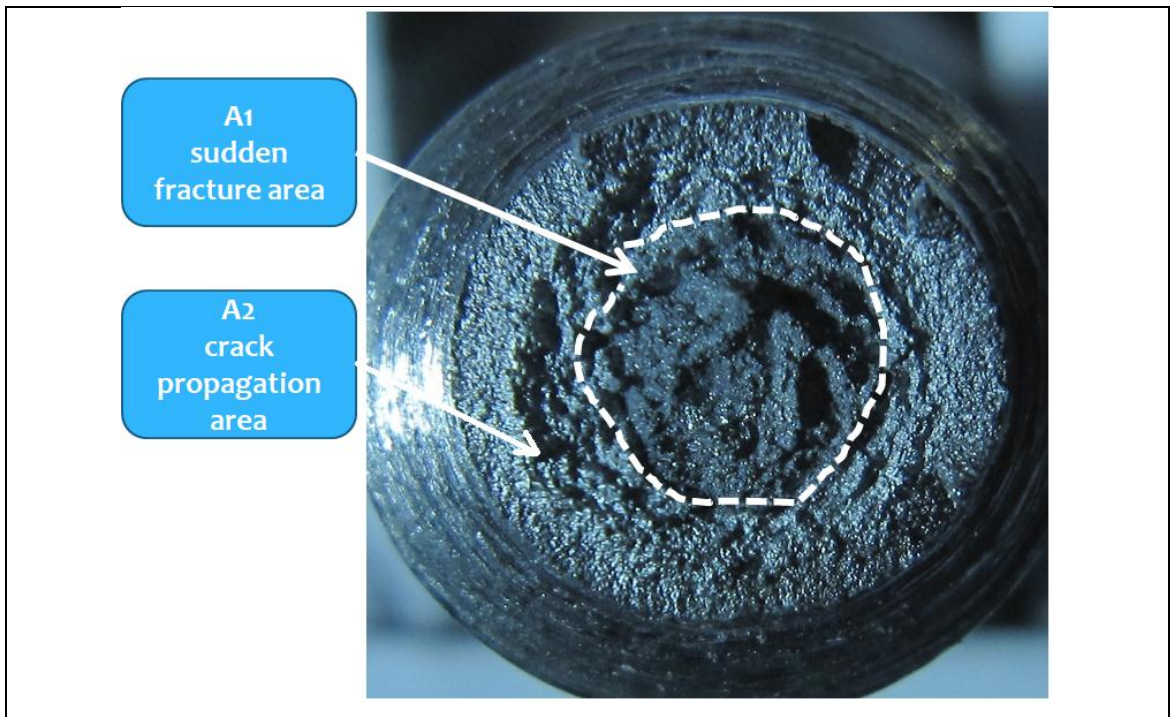


Figure (5.35): Hardness Test of Fracture Surface

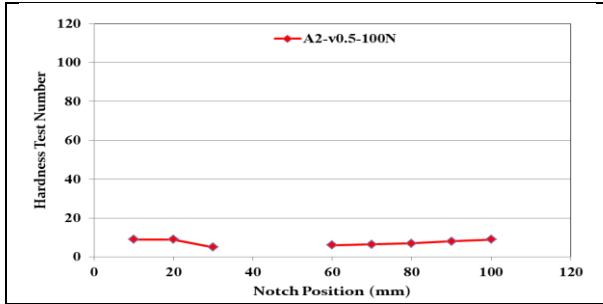


Figure (5.36):Hardness of Fracture Areas Due to Notch Position When the Notch Depth is (0.5) mm and the Applied Load is 100 N

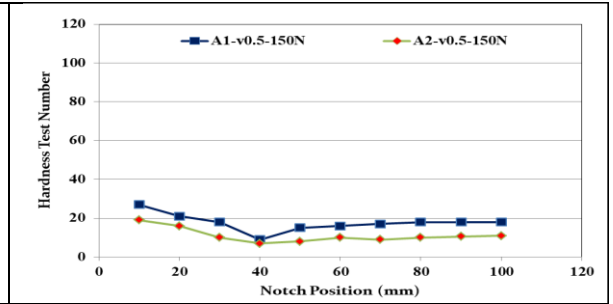


Figure (5.37):Hardness of Fracture Areas Due to Notch Position When the Notch Depth is (0.5) mm and the Applied Load is 150 N

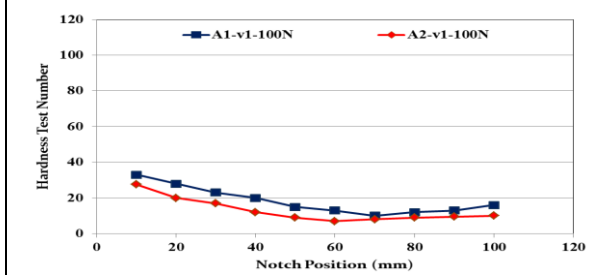


Figure (5.38):Hardness of Fracture Areas Due to Notch Position When the Notch Depth is (1) mm and the Applied Load is 100 N

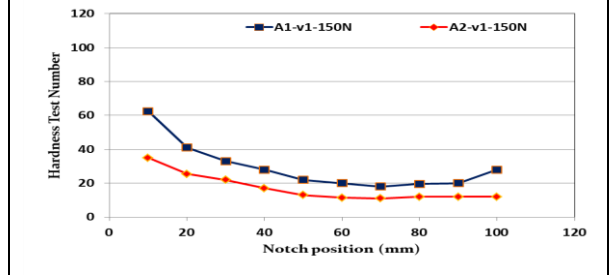


Figure (5.39):Hardness of Fracture Areas Due to Notch Position When the Notch Depth is (1) mm and the Applied Load is 150 N

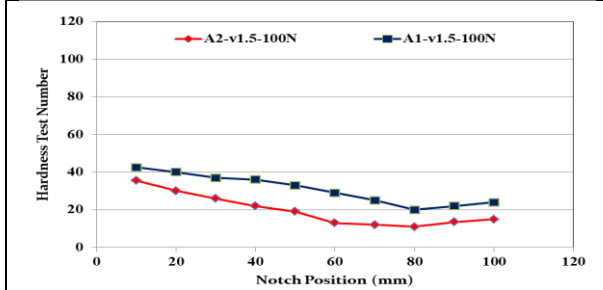


Figure (5.40):Hardness of Fracture Areas Due to Notch Position When the Notch Depth is (1.5) mm and the Applied Load is 100 N

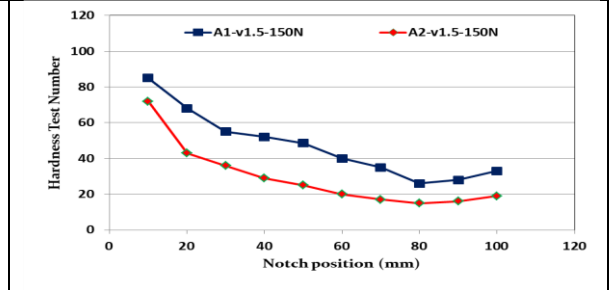


Figure (5.41):Hardness of Fracture Areas Due to Notch Position When the Notch Depth is (1.5) mm and the Applied Load is 150 N

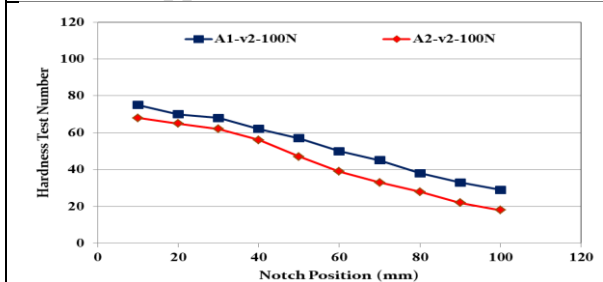


Figure (5.42):Hardness of Fracture Areas Due to Notch Position When the Notch Depth is (2) mm and the Applied Load is 100 N

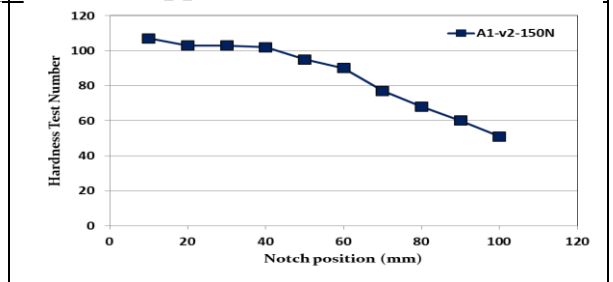
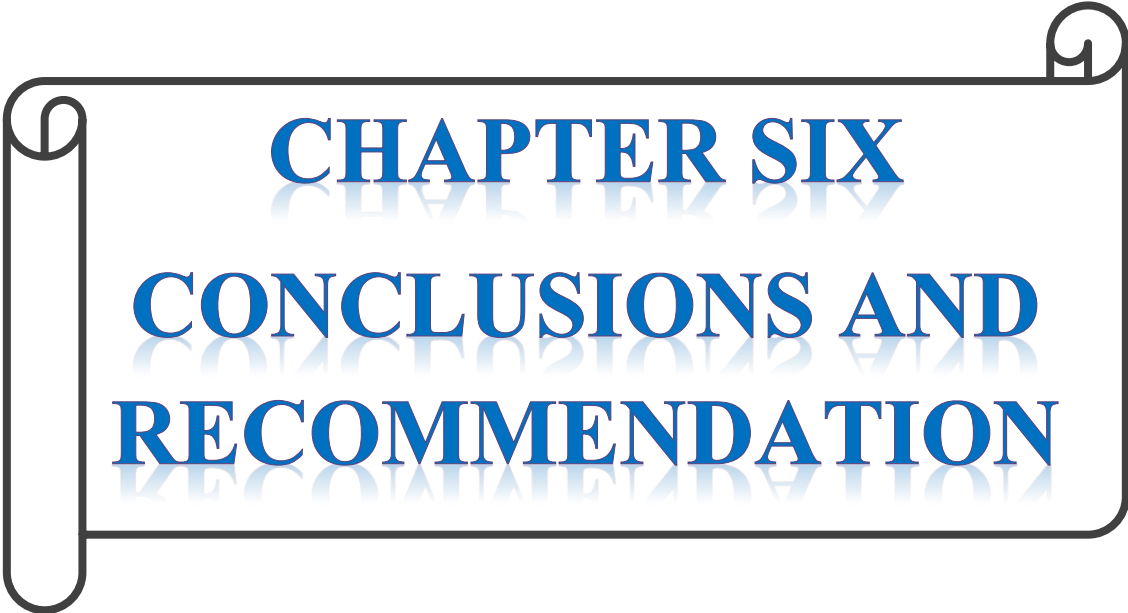


Figure (5.43):Hardness of Fracture Areas Due to Notch Position When the Notch Depth is (2) mm and the Applied Load is 150 N



CHAPTER SIX
CONCLUSIONS AND
RECOMMENDATION

Chapter Six

Conclusions and Recommendations

6.1 Conclusions

The most important conclusions and remarks obtained in this thesis are summarized in this chapter. Furthermore, some recommendations for future research work are mentioned as well. The following conclusions are obtained from this work:

- 1- There are two different effects of notches concerning to their position. The first one is decreasing the fatigue life, while the second one is increasing the fatigue life, and the fatigue life has been increased experimentally by the ratio more than (75) % and numerically by the ratio more than (73) %.
- 2- Can expect the S/N curve of the notched specimens according to the S/N curve of smooth specimens (based on the fracture stress developed at the notch tip).
- 3- IR camera is a good instrument to investigate problems incorporating failure due to stress concentration over the designed limit.
- 4- Using numerical methods (ANSYS) gives a good visualization similar to the experimental results, so the ANSYS program can be used to study the effects of notch on fatigue life.
- 5- Shifting the notch position results in maximum fatigue life.
- 6- Hardness of fracture surface and area of sudden fracture region of notch region is decreased due to notch shifting.

6.2 Recommendations

The recommendations for future work are sorted as follows:

- 1- Studying the effects of double notches.
- 2- Studying the effect of notch location for other notch shapes.
- 3- Studying the effect of Nano surface hardening on fatigue life of notched specimens.



REFERENCES

References

- 1- Ralph I. Stephens, et. al, "*Metal Fatigue in Engineering*", Second Edition, Aweiley- Interscience Publication, John Wiley and Sons Inc., pp. 5, 69-84, (2001).
- 2- Nestor Perez, "*Fracture Mechanics*", Kluwer Academic Publishers, pp. 199-201, (2004).
- 3- Richard G. Budyhas and J. Keith Nisbett, "*Shigley's Mechanical Engineering Design*", Tenth Edition, Mc Graw-Hill Education, pp. 274-303, (2015).
- 4- William F. Hosford, "*mechanical Behavior of Materials*", Cambridge University Press, pp. 281-283, (2005).
- 5- M. A. Bolten W., "*Engineering Materials Technology*", Second Edition, Newnes, pp. 32, 133, (1993).
- 6- J. Schijve, "*Fatigue of Structures and Materials*", Second Edition, Springer, pp. 16, (2009).
- 7- J. A. Collins, "*Failure of Materials in Mechanical Design, Analysis, Prediction, Prevention*", John Wiley and Sons Inc., (1981).
- 8- Warren C. Young and Richard G. Budynas, "*Roark's Formulas for Stress and Strain*", Seven Edition, Mc Graw-Hill, pp. 770-780, (2002).
- 9- G. Pluinage, "*Fracture and Fatigue Emanating from Stress Concentration*", Kluwer Academic Publishers, pp. 1-7, (2004).
- 10- Marc Meyers and Krishan Chawla, "*Mechanical Behavior of Materials*", Second Edition, Cambridge University Press, pp.161,715, (2009).
- 11- C.S.Yen and T.J.Dolan," A Critical Review of the Criteria for Notch – Sensitivity in Fatigue of Metals" University of Illinois at Urbana Champaign Library Large –Scale Digitization Project, pp. 29, (2007).
- 12- Theodore Nicholas, "*High Cycle Fatigue*", A Mechanics of Materials Perspective, pp. 27,213, (2006).

- 13- Guruswami Ravichandran et. al., "On The Conversion of Plastic Work in to Heat During High-Strain-Rate Deformation", American Institute of Physics, Volume 7, Issue 2, pp. 557-562, (2002).
- 14- A. Rabiei, A. G. Evans, and J.W.Hutchinson, "Heat Generation during the Fatigue of a Cellular Al Alloy", Metallurgical and Materials Transaction, Volume 31A, pp. 1129-1136, (2000).
- 15- N. Kadi, "Notch effect in High Cycle Fatigue", NATO Science Series Volume 11, Issue 2, pp. 207-220, (2001).
- 16- A. Fatemi, Z. Zeng, and A. Plaseied, "Fatigue Behavior and Life Predictions of Notched Specimens Made of QT and Forged Micro Alloyed Steels", International Journal of Fatigue, Elsevier, Volume 26, Issue 5, pp. 663-672, (2004).
- 17- Michele Ciavarella and Giovanni Meneghetti, "On fatigue limit in the presence of notches: classical vs. recent unified formulations", International Journal of Fatigue, Volume 26, Issue 3, pp. 289-298, (2004).
- 18- Borivoj Sustarsic, Bojan Sencic, and Boris Arzensek, Philippe Jodin, "The Notch Effect on the Fatigue Strength of 51CrV4Mo Spring Steel", Original scientific article, Materials and Technology, Volume 41, Issue 01, pp. 29-34, (2007).
- 19- Y. Verreman, H. Guo, "Short cracks at notches and fatigue life prediction under mode I and mode III loadings", Nordam Group, Tulsa, OK, USA, pp. 1-10, (2009).
- 20- Dragi Stamenkovic and Katarina Maksimovic, "Fatigue Life Estimation of Notched Structural Components", Journal of Mechanical Engineering, Volume 56, Issue 12, pp. 846-852, (2010).
- 21- XU Jian-xin, et. al., "The effect of hole shape on fatigue life of bolted connectors", International Conference on Transportation, Mechanical, and Electrical Engineering (TMEE), pp. 1957-1960, (2011).

- 22- N.A, Alang, et. al., "Effect of Surface Roughness on Fatigue Life of Notched Carbon Steel", International Journal of Engineering of Technology (IJENS), Volume 11, No. 01, pp. 160-163, (2011).
- 23- Masao Sakane, et. al., "Notch Effect on Multiaxial Low Cycle Fatigue", International Journal of Fatigue, Volume 33, Issue 8, pp. 959-968, (2011).
- 24- Goanta Viorel, et al., "The Variation of the Vickers Micro – Hardness in the Vicinity of the Fracture Surface at Static Loading", Journal of Engineering Studies and Research, Volume 17, No. 3, pp. 30-39, (2011).
- 25- Nasim Daemi & Gholam Hossein Majzoubi, "Experimental and Theoretical Investigation on Notched Specimens Life Under Bending Loading", World Academy of Science, Engineering and Technology, Volume 5, No. 8, pp. 1639-1643, (2011).
- 26- Deepan Marudachalam & R.Krishnaraj, "Optimization of shaft design under fatigue loading using Goodman method", International Journal of Scientific & Engineering Research Volume 2, Issue 8, pp. 1-8, (2011).
- 27- Bikash Joadder, et. al., "Fatigue Failure of Notched Specimen -A Strain-Life Approach ", Materials Sciences and Applications, Volume 2, Issue 2, pp. 1730-1740, (2011).
- 28- Caroline Hyll, et. al., "Analysis of the Plastic and Elastic Energy during the Deformation and rupture of Paper Sample Using Thermography", Nordic Pulp and Paper Research Journal, Volume 27, No. 2, pp.329-334, (2012).
- 29- G. Meneghetti and S. Masaggia, "Estimation of the fatigue limit of components made of Austempered Ductile Iron weakened by V-shaped notches", World Foundry Congress, Volume 3, pp. 1-9, (2012).
- 30- Reda I. Elghnam, "Experimental and Numerical Investigation of Heat Transfer from Rotating Horizontal Cylinder Rotating in Still Air Round its own Horizontal Axes, International Journal of Thermal Technologies, Volume 3, No. 2, pp.23-31, (2013).

- 31- Qasim Bader, " Effect of V Shape Notch Location on Fatigue Life in Steel Beam Made of Carbon Steel Alloys with Different Content of Carbon ", International Journal of Mechanical and Production Engineering Research and Development (IJMPERD), Volume 4, Issue 4, pp. 69-78, (2014).
- 32- Bruce Boardman, "Fatigue Resistance of Steels", ASM Handbook, Volume 1, pp.673-688, (1990).
- 33- ASM, "*Handbook of Mechanical Testing*", Tenth Edition, volume 8, (1981).
- 34- Walter D. Pilkey, Deborah F. Pilkey, "*Peterson's Stress Concentration Factors*", Third Edition, John Wiley & Sons, Inc., pp.4, 165-197, (2008).
- 35- Noa- Aki Noda and Yasushi Takase, "Stress Concentration Formula Useful for All Notch Shape in a Round Bar (Comparison between Torsion, Tension and Bending)" International Journal of Fatigue, Volume 28, pp. 151-163, (2006).
- 36- Saeed Moaveni, "*Finite Element Analysis Theory and Application with ANSYS*", Prentice – Hall, Inc., pp. 1, (1999).
- 37- Raymond Browell and Al Hancq, "Calculating and Displaying Fatigue Results", ANSYS, Inc., pp.7-9, (2006).
- 38- Luay S. AL- Ansari, "Calculating of Natural Frequency of Stepping Cantilever Beam", International Journal of Mechanical and Mechatronics Engineering, Volume 12, No. 5, pp. 59-68, (2012).
- 39- Luay S. AL- Ansari, "Calculating Static Deflection and Natural Frequency of Stepping Cantilever Beam Using Modified Rayleigh Method", International Journal of Mechanical and Production Engineering Research and Development, Volume 3, Issue 4, pp. 113-124, (2013).
- 40- J. P. Holman, "*Heat Transfer*", Tenth Edition, Mc Graw-Hill, pp. 1-16, (2010).



APPENDICES

A. 1. Material Grade Certification

الشركة العامة للفحص والتأهيل الهندسي S.I.E.R
قسم البحث والتطوير (شعبة المواصفات) R.D.S

الجهة المستفيدة : جامعة كربلاء كلية الهندسة
أمر العمل : 2017/80
التاريخ : 2017/ 1 /25
نوع النموذج : قضيب فولاذي

Certificate

Sample	Type of material
قضيب فولاذي (Ø= 14 mm)	المعدن يقع ضمن النوعية St37-2

الملاحظات :
المطابقة من حيث الخواص المفحوصة فقط



الشركة العامة للفحص والتأهيل الهندسي
قسم البحث والتطوير
R.D.S
S.I.E.R
نجاة كاظم

١/٢٥

/س مسؤول شعبة المواصفات
زينب طالب

اعداد

بان مكرم

A. 2. Chemical Composition Test results Certification

الشركة العامة للفحص والتأهيل الهندسي
قسم المختبرات والفحص الهندسي. Lab. & E. I. Dep.

الجهة المستفيدة : جامعة كربلاء – كلية الهندسة
امر العمل : 2017 /80
التاريخ : 2017 / 1 /25
نوع النموذج : قضيب فولاذي

Certificate

- Chemical composition:

Sample	C%	Si%	Mn%	P%	S%	Cr%	Mo%	Ni%	Al%	Cu%	Fe%
قضيب فولاذي Ø=14mm	0.187	0.281	0.636	0.0041	0.021	0.122	0.011	0.091	0.020	0.136	Bal.

الملاحظات:
- النتيجة تخص النموذج المفحوص فقط .
- تم الفحص بدرجة حرارة (20.3°C) ونسبة الرطوبة (35 %).




٢. ميان هادي سلمان
 رئيس قسم المختبرات والفحص الهندسي

٣. علي خير الله
 الفاحص

LI-1 Issue 6 (Jan 14)

B.1 Heat Indication

This part of theoretical work deals with heat that is generated as a result of the fatigue testing process until the fracture. Due to plastic deformation, the temperature of the specimen increases in the fractured region (see section 1.6). At the beginning, there are many assumptions must be used to reduce the complicity in calculating the temperature change due to plastic deformation. These assumptions will be mentioned later in this part of work. Figure (B.1) demonstrate the control volume, where the heat is generated or plastic deformation happens until the fracture. The heat balance at this region can be written as:

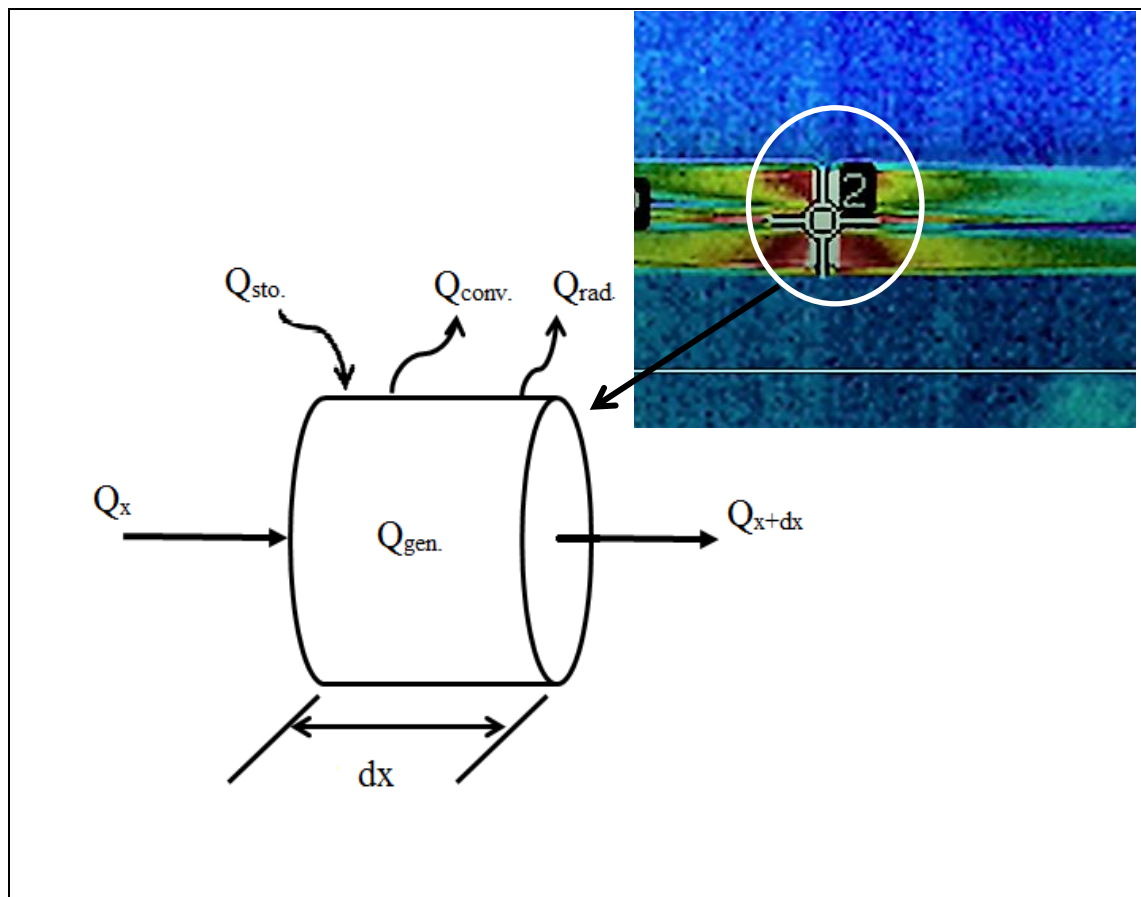


Figure (B.1): Control Volume of Deformed Region

$$Q_x + Q_{\text{gen.}} = Q_{x+dx} + Q_{\text{sto.}} + Q_{\text{conv.}} + Q_{\text{rad.}} \quad \dots \text{ (B.1)}$$

The components of the heat balance are;

1- Q_x = Heat Input.

2- $Q_{\text{gen.}}$ = Heat Generation.

3- Q_{x+dx} = Heat Output.

4- $Q_{\text{sto.}}$ = Heat Stored and it can be calculated by:

$$Q_{\text{sto.}} = q_{\text{sto.}} * \Delta V = \rho C \Delta V \frac{dT}{dt} \quad \dots \text{ (B.2)}$$

Where;

ρ = Material Density = (7800 Kg/m³).

C = Specific Heat. (490 J/Kg. K) (For carbon steel).

ΔV = Volume

5- $Q_{\text{conv.}}$ = Heat Convection and it can be calculated by:

$$Q_{\text{conv.}} = h A (T_s - T_{\text{amb.}}) \quad \text{(Newton's Law of cooling)} \quad \dots \text{ (B.3)}$$

Where;

h = Heat Convection Coefficient that can be calculated from the following relation[40].

$$h = \frac{\text{Nu} * K}{dx} \quad \dots \text{ (B.4)}$$

Where;

K = Thermal Conductivity of Air at max. Temp. 35° C = 0.0267(W/(m.K))

Nu = Nusselt number and it calculated from below relation [30]:

$$\text{Nu} = 0.022 * \text{Re}^{0.821} \quad \dots \text{ (B.5)}$$

Where:

Re = Reynolds number and it was calculated from below equation [30]:

$$\text{Re} = \frac{\omega * d^2}{2 * \nu} \quad \dots \text{ (B.6)}$$

Where;

ω = is the angular velocity and equals 2800 rpm= 293.215 rad/sec.

d = is the diameter of specimen and equals (0.008 m).

ν = Kinematic viscosity of air that temp. = 16.505*10⁻⁶ (m²/s) [40].

A = Area of Contact.

T_s = Surface Temperature.

$T_{\text{amb.}}$ = Ambient Temperature (Air Temperature).

6- $Q_{\text{rad.}}$ = Heat Radiation and it can be calculated by:

$$Q_{\text{rad.}} = \sigma A (T_S^4 - T_{\text{amb.}}^4) \quad \dots (B.7)$$

Where;

$$\sigma = \text{Stefan Boltzman Constant} = 5.669 * 10^{-8} \text{ W/m}^2 \cdot \text{K}^4 \cdot$$

A = Area of Radiation.

T_s = Surface Temperature.

$T_{\text{amb.}}$ = Ambient Temperature (Air Temperature).

In order to simplify equation (B.9), the following assumptions were made:

$$(a) Q_x \approx Q_{x+dx} \text{ (dx is very small)} \quad \dots (B.8)$$

If dx is very small, the heat transfer in x-coordinate is very small.

- (b) The heat transfer in r-coordinate is very large (i.e. the temperature of element reaches to steady state temperature as fast as possible).

Therefore, equation (B.) becomes:

$$Q_{\text{gen.}} = q_{\text{gen.}} * \Delta V = \rho C \Delta V \frac{dT}{dt} + h A (T_s - T_{\text{amb.}}) + \sigma A (T_S^4 - T_{\text{amb.}}^4) \dots (B.9)$$

Equation (B.9) is an empirical equation depends on some experiments which represented by the figure (B.1).

The heat generation can be calculated for this work using Eq. (B.9) after calculating $(\frac{dT}{dt})$. The value of Q_{gen} can be calculated as:

- (1) The temperature - time curve of fatigue specimen must be measured using IR camera (see Figure (B.2)).

$$T(t) = 0.0034 * t + 312.72$$

- (2) The equation, described the temperature as a function of time, must found by using curve fitting and the function will be derivative with respect to time.

Where, $(\frac{dT}{dt})$ represent the rate of change of temperature of specimen, and its value as bellow:

$$\frac{dT}{dt} = 0.0034$$

- (3) Calculating Q_{gen} at any time.

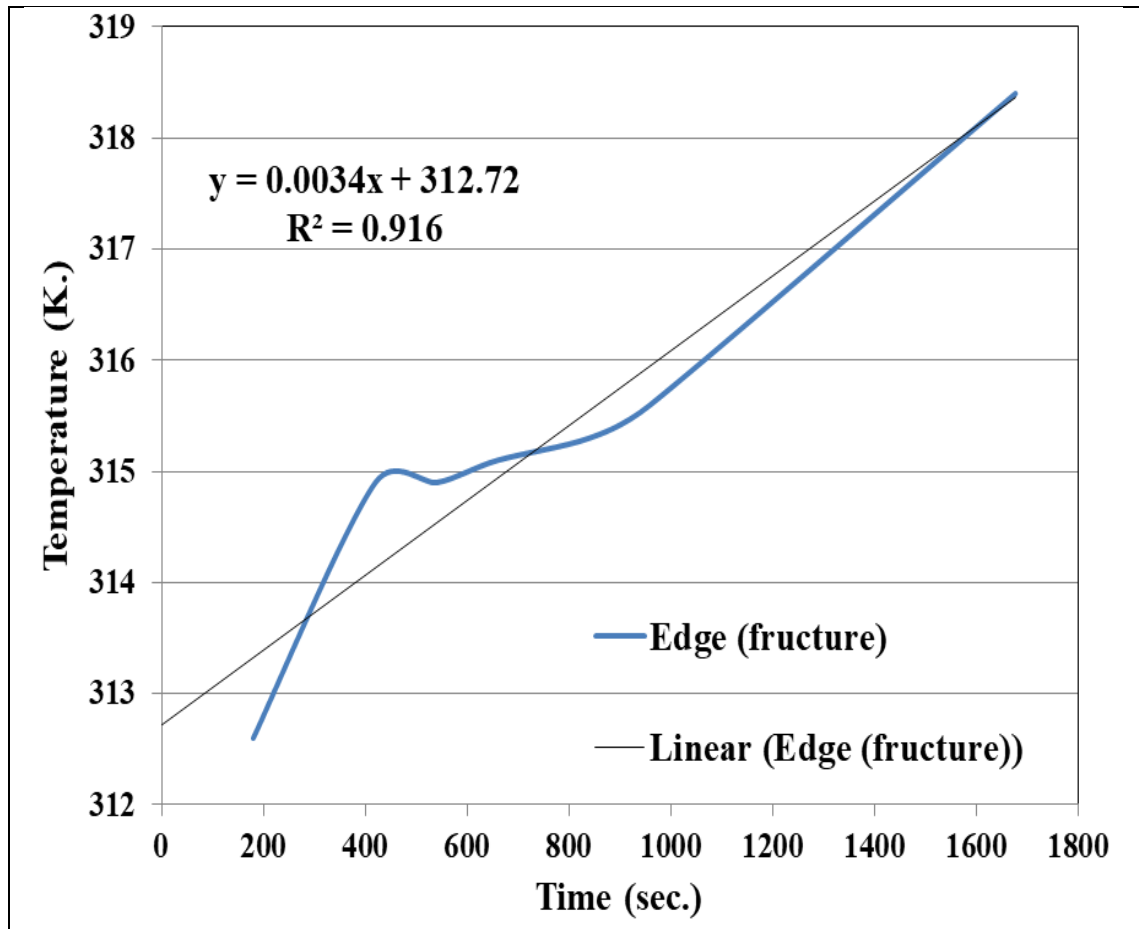


Figure (B.2): Temperature Varying With Time at Edge (Position of Fracture) During Fatigue Test

For more simplifying:

(c) The Heat Convection part can be neglected.

(d) The Heat Radiation can be neglected.

So Eq. (B.17) becomes as bellow;

$$Q_{\text{gen.}} = Q_{\text{sto.}} \quad \dots \text{(B.10)}$$

$$q_{\text{gen.}} * \Delta V = q_{\text{sto.}} * \Delta V$$

$$q_{\text{gen.}} * \Delta V = \rho C \Delta V \frac{dT}{dt}$$

$$q_{\text{gen.}} = \rho C \frac{dT}{dt} \quad (\text{W/m}^3) \quad \dots \text{(B.11)}$$

So, equation (3.9) (or equation (3.11)) can be used to calculate the heat generation due to plastic deformation at any fracture point during fatigue test.

B.2 Heat Indication Results

Figures (B.3) and (B.4) show the pictures of thermal camera for temperature distribution along the specimen and temperature change during the fatigue test. Also, Figures (B-6) to (B.8) show the temperature change at critical points (edge and notch points) during the fatigue life, where the following points can be found:

- 1- At specific notch position, thermal behavior is similar for all cases. For example, at notch position (40) mm for the cases (V1-100N, V1-150N, V1.5-100N, V1.5-150N), the same thermal behavior is observed.
- 2- Maximum amount of heat generation occurs in fracture position because of concentrating the stress and strain at this region.
- 3- Heat generation is promoted with increasing the strain rate. This can be seen during the fracture occurrence, where the temperature variation curve slope is increased.
- 4- The rate of temperature change at the edge point is increased gradually due to shifting the notch away from the edge as a result of increasing the strain at the edge position.
- 5- In the cases before transforming the crack from the notch to edge position, it is observed that the thermal behavior is similar at both the edge and notch points. This is because the stresses at these points are almost equal.
- 6- The thermal behavior change (Temperature Increasing at Notch and Edge Points during Fatigue Test) for case (V1-60-100N) has not been measured because its process duration was too long, so the IR camera is not able to record during such a long time.

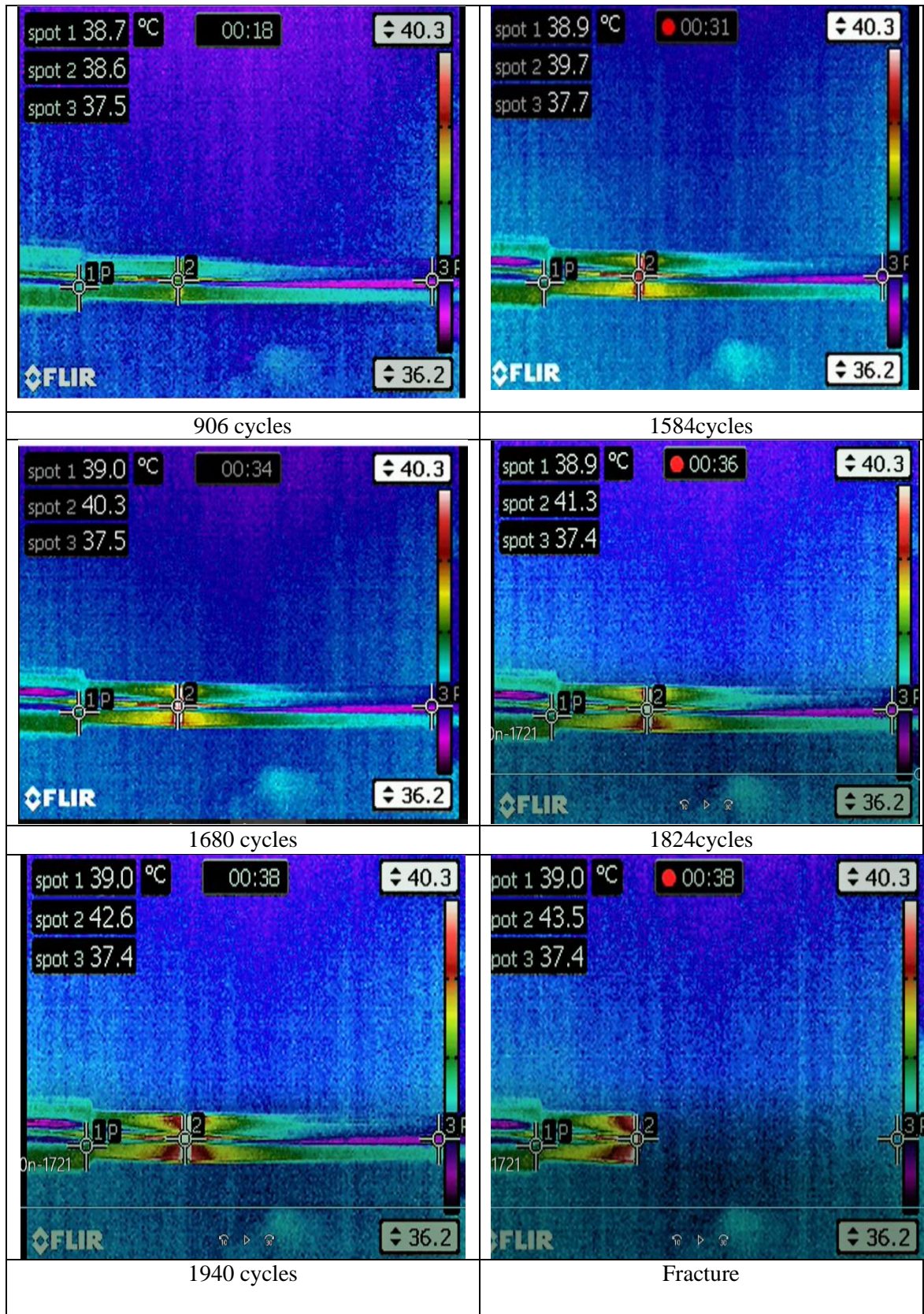


Figure (B.3): Temperature Distribution Measured by IR. Camera Consequently During Fatigue Test of V1-20-150N

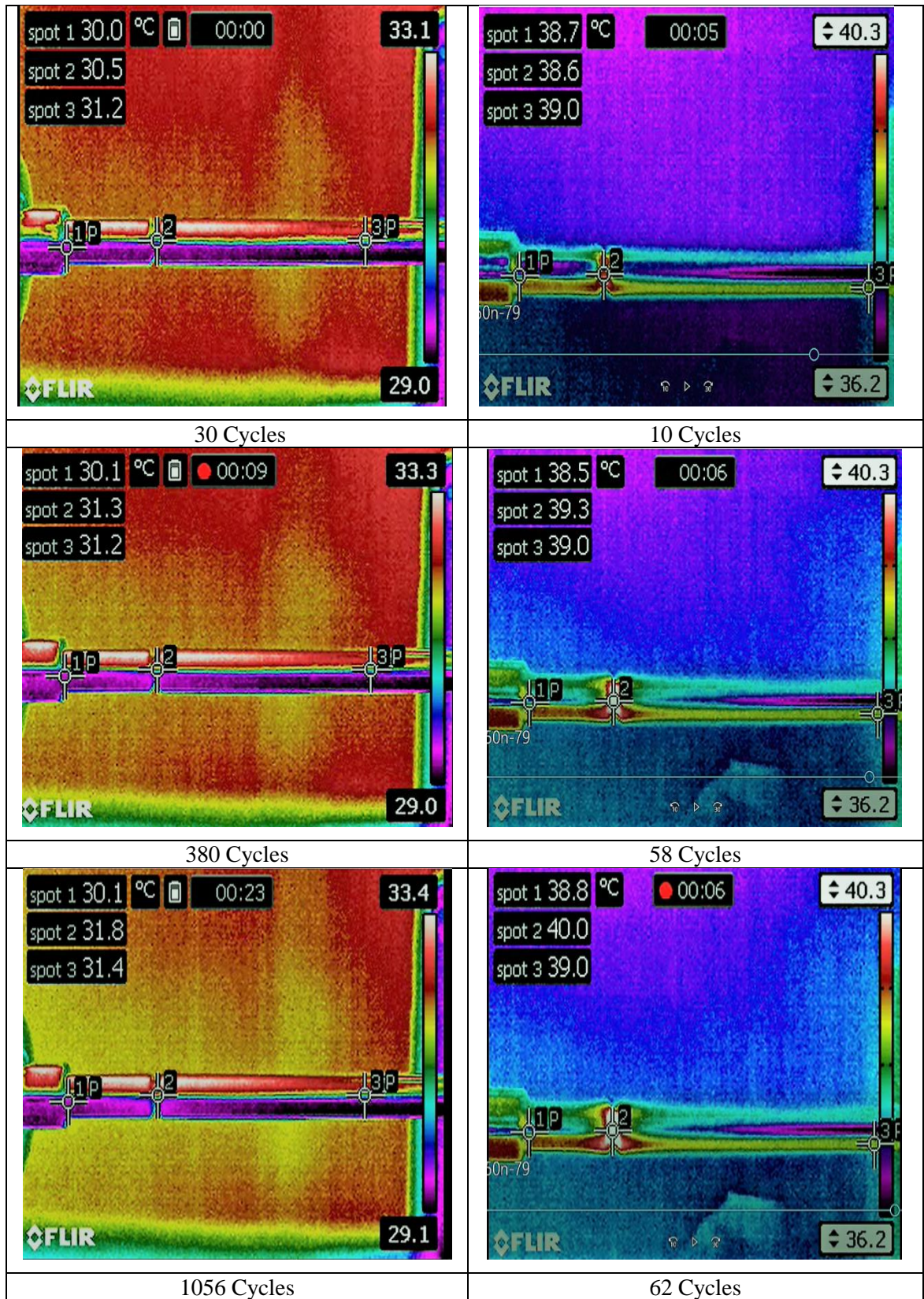


Figure (B.4): Temperature Distribution Measured by IR. Camera During Fatigue Test of V1.5—20-100N and V1.5-20-150N

<p>1392 Cycles</p>	<p>65 Cycles</p>
<p>1525 Cycles</p>	<p>70 Cycles</p>
<p>Fracture</p>	<p>Fracture</p>
<p>V1.5—20-100N</p>	<p>V1.5—20-150N</p>
<p>Contd.</p>	

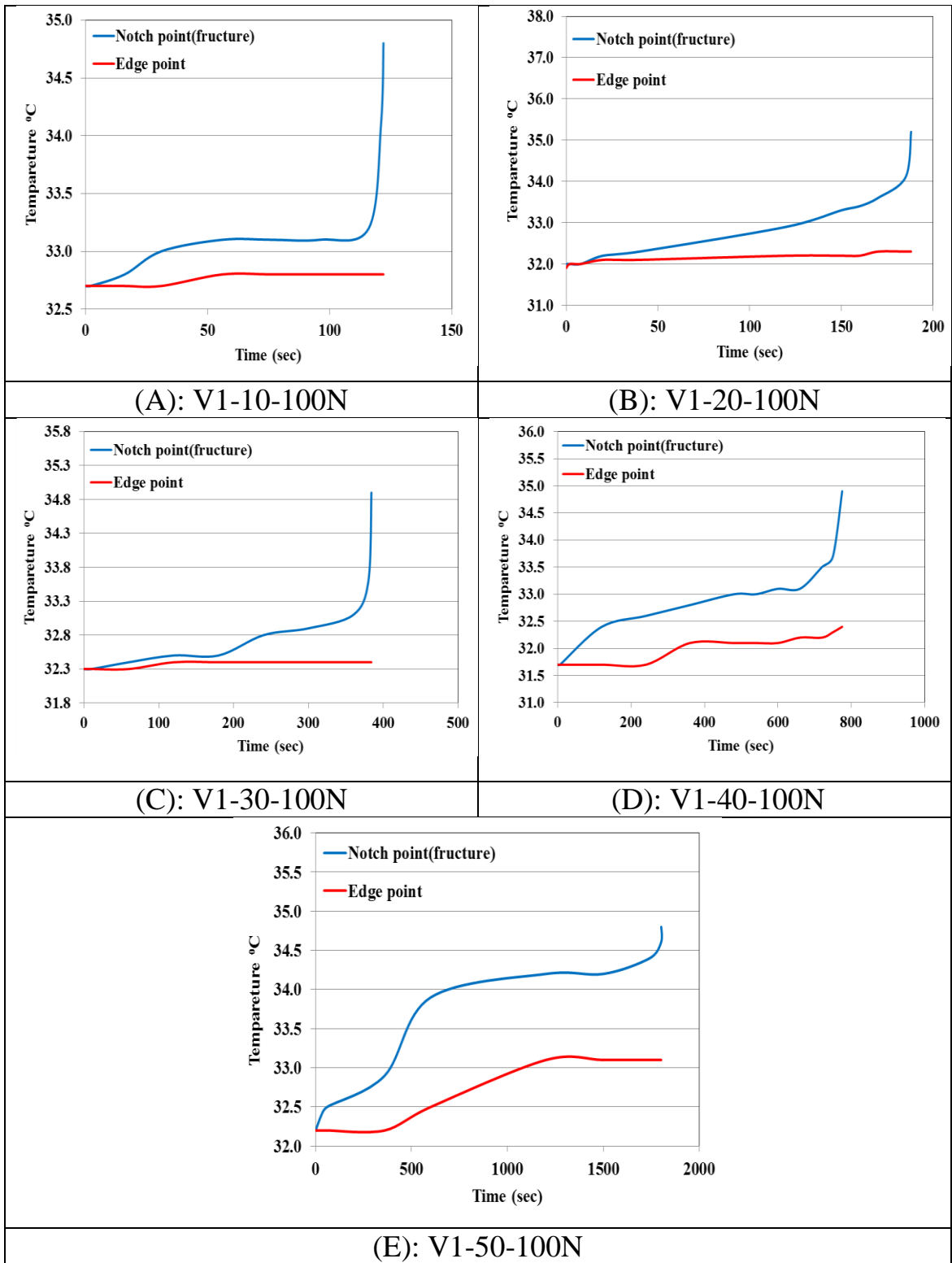


Figure (B.5): Temperature Increasing of Notch and Edge Points During Fatigue Test on V1-100N

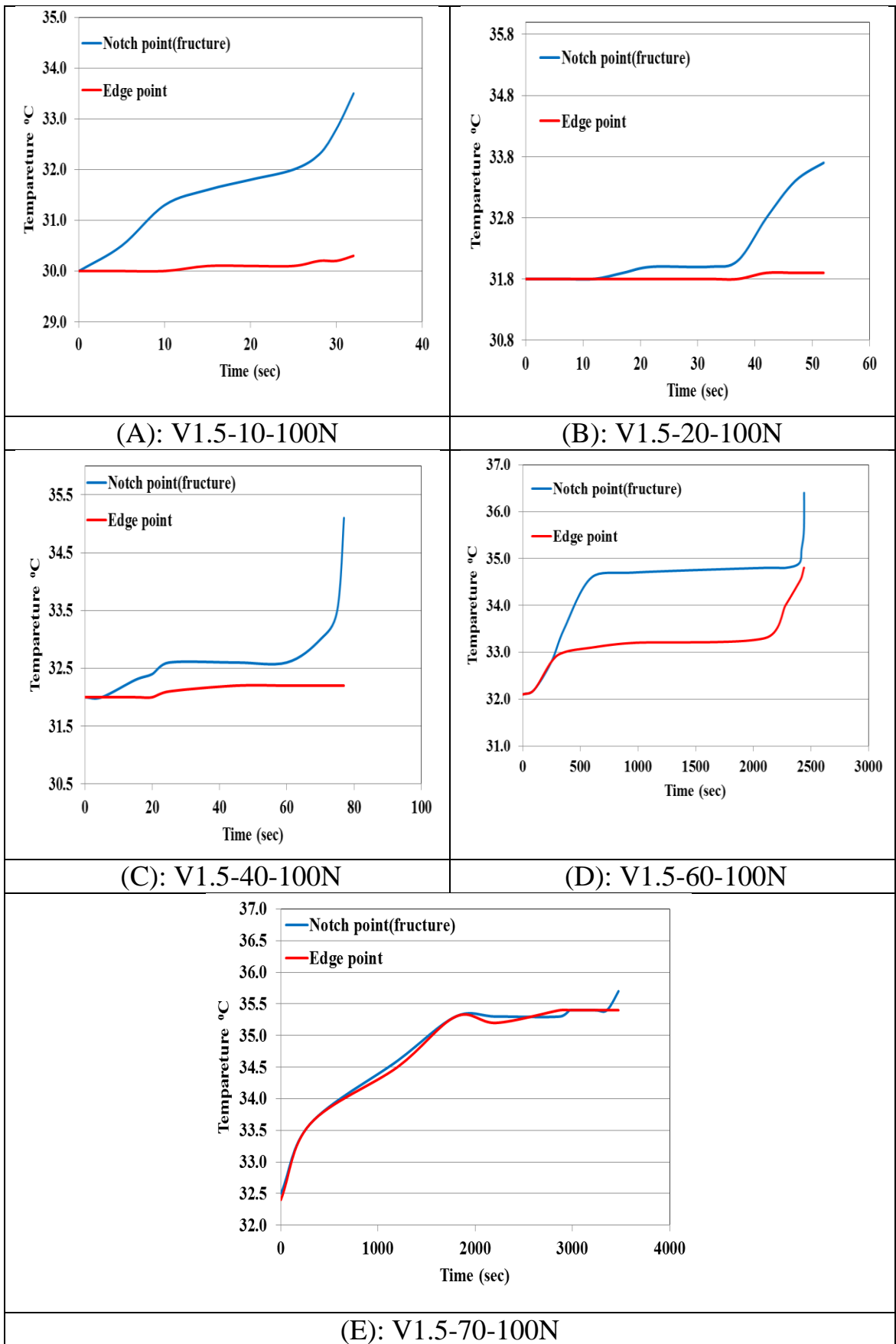


Figure (B.6): Temperature Increasing of Notch and Edge Points During Fatigue Test on V1.5-100N

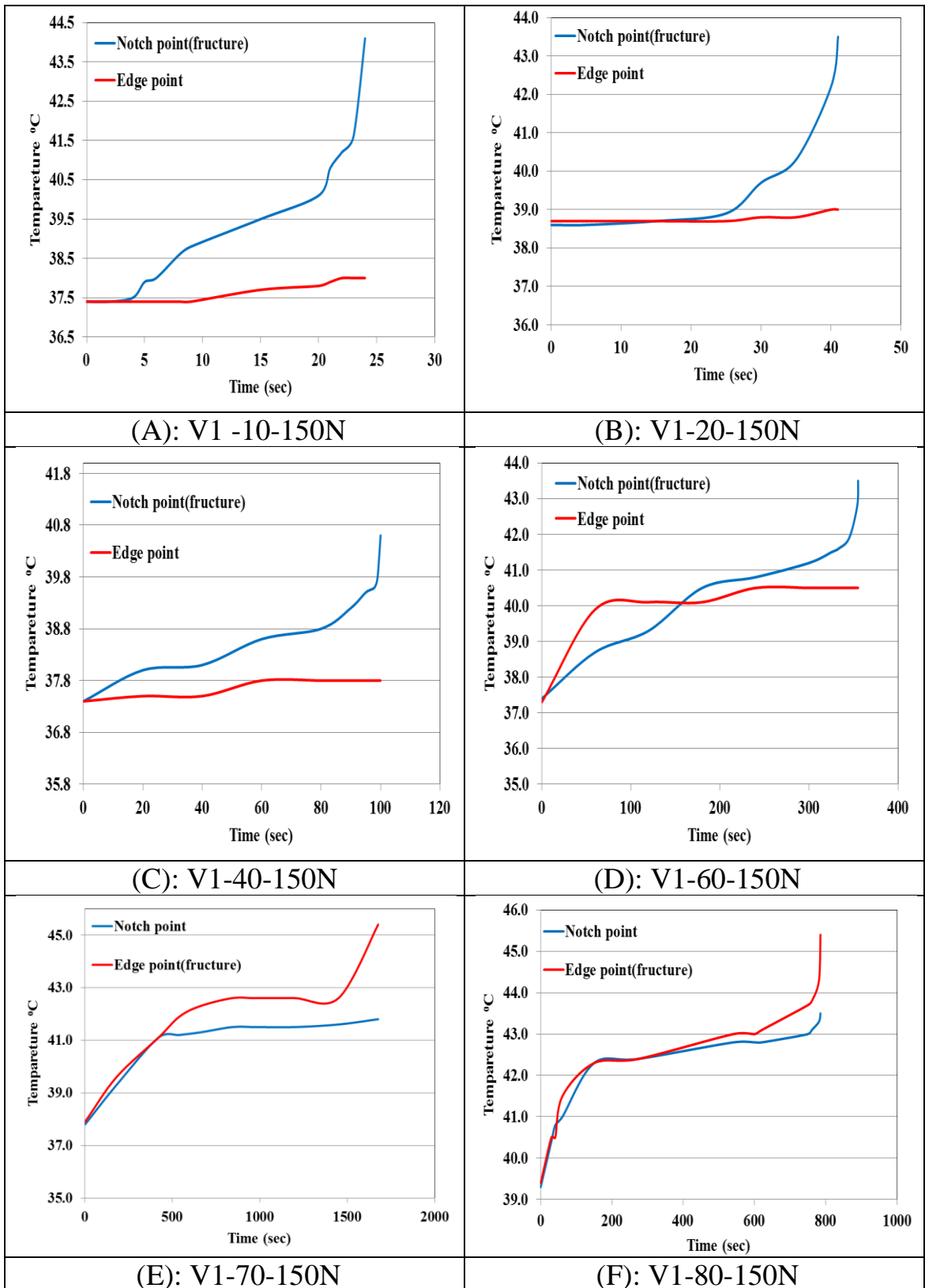


Figure (B.7): Temperature Increasing of Notch and Edge Points During Fatigue Test on V1-150N

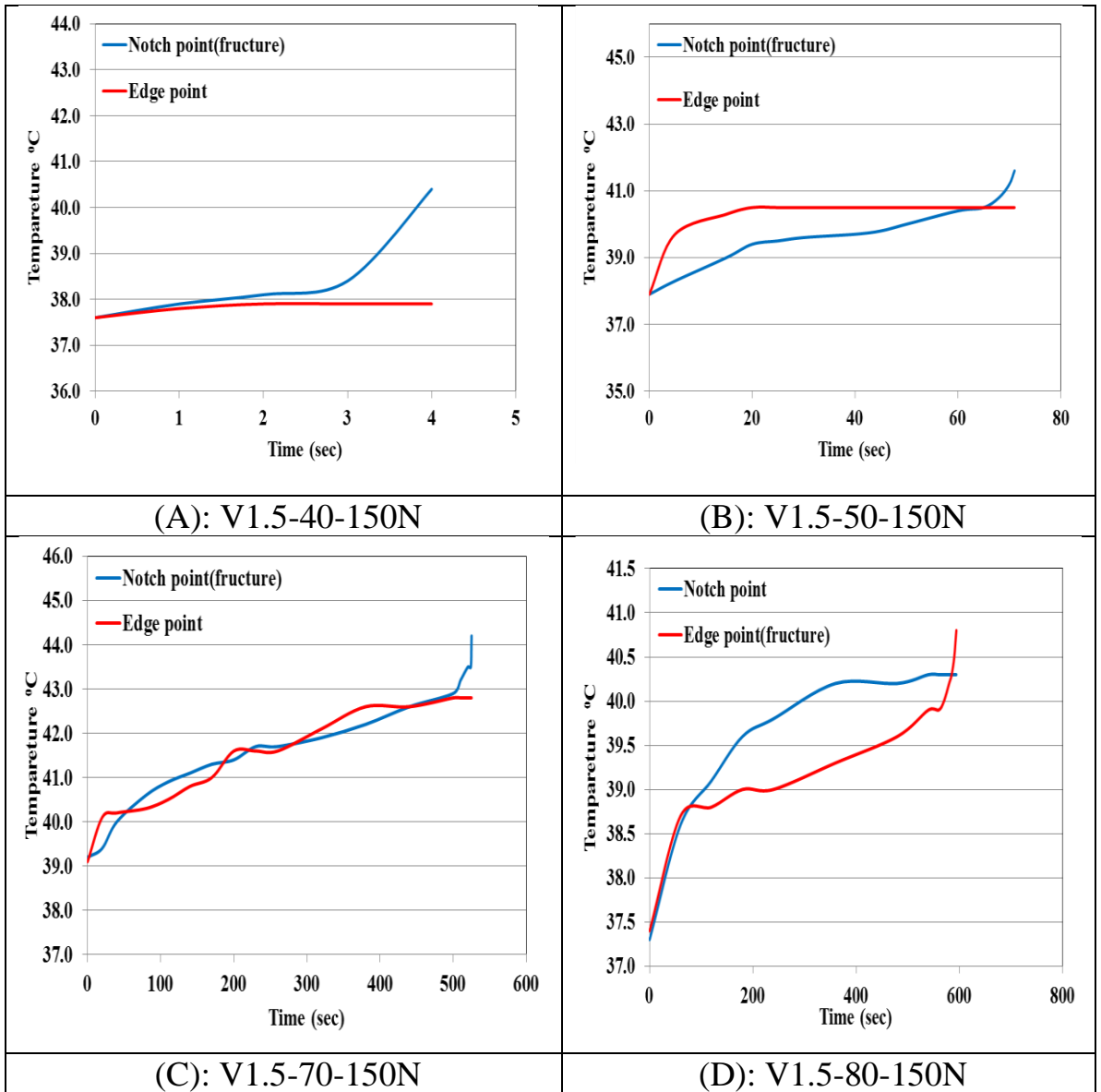


Figure (B.8): Temperature Increasing of Notch and Edge Points During Fatigue Test on V1.5-150N

الخلاصة

العمل الحالي هو دراسة تأثيرات موقع وعمق الشق كذلك مقدار الحمل المسلط على عمر الكلال و السلوك الحراري لعينات الذراع الناتئ الدوار المصنوعه من فولاذ واطئ الكاربون (ST37-2) من خلال تسليط حمل انعكاسي كامل ومعدل اجهاد يساوي صفر. فضلا عن ذلك، فان تغير في درجة الحرارة في عينات الاختبار خصوصا في نقاط محددة (الحافة و الشق) خلال اختبار الكلال قيس بواسطة كامرا الاشعة تحت الحمراء. وفي موضوع ذي صلة تمت دراسة تأثير العوامل اعلاة على مساحة سطح الكسر المفاجئ كذلك الصلادة في نقطتين على مساحة الكسر (نقطة على منطقة نمو الشق و نقطه على منطقة الكسر المفاجئ). عدديا، تم الحصول على النموذج الخاص بطريقة (FINITE ELEMENT) باستخدام برنامج (- ANSYS WORKBENCH 15.0) و الذي في بياناته يستند على المخطط العملي لل (S/N). من النتائج، موقع الشق يمكن ان يغير موقع الكسر من موقع الشق الى موقع الحافة. كذلك عمر الكلال ازداد الى اقصى قيمه بواسطة التزحيف للشق وصولا الى موقع مناسب بنسبة عمليه اكثر من (٧٥) % و عدديا (٧٣) %. من ناحية اخرى انتقال الشق بعيدا عن موقع الحافة انتج تناقص في مساحة الكسر المفاجئ و صلادة سطح الكسر لغايه لغايه نقطة الانقلاب، و اظهرت المقارنات بين النتائج العملية و العدديه تشابه في السلوك، حيث ان نموذج ال (ANSYS) الذي يستند على منحنى ال (S/N) العملي اعطى تنبؤا جيد لعمر الكلال. اعطى تغير درجة الحرارة عند نقاط مختلفة على العينات تنبؤا جيدا لموقع الكسر قبل حدوثه.



جمهورية العراق
وزارة التعليم العالي والبحث العلمي
جامعة كربلاء- كلية الهندسة
قسم الهندسة الميكانيكية

دراسة تأثير عمق و موقع الشق على خواص الكلال

رسالة مقدمة الى كلية الهندسة - جامعة كربلاء كجزء من متطلبات نيل درجة ماجستير علوم في
الهندسة الميكانيكية - ميكانيك تطبيقي

من قبل

أيث حسين محمد

بكالوريوس ٢٠٠٨

بإشراف

الاستاذ المساعد الدكتور لؤي صادق الانصاري

المدرس الدكتور محمد وهاب الجبوري

March

2017

جمادي الثاني

1438